Flow Regime Prediction via Froude Number Calculation in a Rock-Bedded Stream

By

Michael J. Meyers

A thesis submitted to
The Department of Earth Sciences, Brock University
in partial fulfillment of the requirements
for the degree Master of Science

March, 2010
Brock University
St. Catharines, Ontario

Abstract

Mathematical predictions of flow conditions along a steep gradient rock bedded stream are examined. Stream gage discharge data and Manning's Equation are used to calculate alternative velocities, and subsequently Froude Numbers, assuming varying values of velocity coefficient, full depth or depth adjusted for vertical flow separation. Comparison of the results with photos show that Froude Numbers calculated from velocities derived from Manning's Equation, assuming a velocity coefficient of 1.30 and full depth, most accurately predict flow conditions, when supercritical flow is defined as Froude Number values above 0.84. Calculated Froude Number values between 0.8 and 1.1 correlate well with observed transitional flow, defined as the first appearance of small diagonal waves. Transitions from subcritical through transitional to clearly supercritical flow are predictable. Froude Number contour maps reveal a sinuous rise and fall of values reminiscent of pool and riffle energy distribution.

Acknowledgements

Thank you to Dr. Keith J. Tinkler for his enthusiastic embrace, guidance and refinement of an initially amorphous idea into the present study. The degree of freedom he provided to explore unanticipated results is greatly appreciated.

Thank you to Dr. Richard J. Cheel, Ms. Diane Gadoury and Ms. Lorraine Sciamonte for their additional guidance and administrative advocacy at Brock University.

Thank you to Mr. Richard H. White for his surveying help, intellectual stimulation and generally whimsical outlook.

Thank you to Mr. Robert Stanton and Mr. John Hoffman for their patient help with seemingly endless computer questions.

Thank you to Mr. Ken Ahlstrom and the rest of the river guides for their instruction, patience, support and companionship.

Thank you to Mr. James W. Scatterday for his example of healthy academic skepticism.

Thank you to Mr. David C. Mathewson for his example of professional excellence.

Thank you to Ms. Wendilorion Morgan and Dr. Amanda J. Meyers for their scholastic empathy, humor and unconditional love.

And, most of all, thank you to Ms. Laurie Kay Hine Meyers.

Table of Contents

Tables

Figures

Appendices

Symbols

Variables are set in italics to identify their particular use in the present study.

A, A_c, A_c = area of cross section occupied by water

A_r, $A_r = A_t/A_c$ dimensionless ratio, percentage of total area filled by water in each panel

A_t, $A_t = yb_i$ interval (panel) area occupied by water, calculated in square feet

b, b_n = channel width, in feet

b_i = interval width

C = wave velocity

d = depth of faster moving water in separated flow

E = Specific Energy

$E_h = y+v_h\text{^}2/2g$ Specific Energy, with velocity from discharge data

$E_m = y+v_m\text{^}2/2g$ Specific Energy, with velocity from Manning's Equation

E_n = interval elevation, determined from cross section of streambed topography, in feet

Fr = Froude Number

$Fr_h = v_h/(gy/\alpha)\text{^}0.5$ Original Froude Number, velocity from discharge data at full depth

$Fr_{ha} = v_h/(gy_a/\alpha)\text{^}0.5$ Original Froude Number, velocity from discharge data at adjusted depth

$F_{hs} = v_h/(gy)\text{^}0.5$ Simplified Froude Number, velocity from discharge data

$Fr_m = v_m/(gy/\alpha)\text{^}0.5$ Original Froude Number, velocity from Manning's Equation at full depth

$Fr_{ma} = v_m/(gy_a/\alpha)^{0.5}$ Original Froude Number, velocity from Manning's Eq., adjusted depth

$F_{ms} = v_h/(gy)^{0.5}$ Simplified Froude Number, with velocity from Manning's Equation

$F_{pan} = v_{pan}/(gy)^{0.5}$ Panel (Modified) Froude Number

g, g = acceleration due to gravity, 32 feet per second per second in the present study

h = velocity head

n, n = Manning's resistance coefficient, set at 0.025 in the present study; also identifies the cross section panel

P = wetted perimeter of cross section

Q = discharge

Q = discharge at USGS stream gage, measured in cubic feet per second

$Q_{cal} = (\sum q_n)b_i$ calculated discharge

$Q_n = QA_r$ discharge in interval (panel), in cubic feet per second

q = discharge per unit width

$q = Q/b_n$ discharge per unit (channel) width, calculated in square feet per second

q_n = discharge at panel n

$q_{pan} = Q_n/b_i$ discharge in panel divided by panel width, in square feet per second

R = hydraulic mean radius

S = longitudinal slope

$S = (WE_u\text{-}WE_d)/200$ dimensionless water surface slope

U = velocity difference between faster and slower moving water

v = stream velocity

v_c = critical water velocity

v_c , v_c = *((g)y$_c$))^0.5* critical velocity, calculated in feet per second

v_h = *q/y* water velocity, from discharge data, calculated in feet per second

v_h/v_c = dimensionless ratio of velocity to critical velocity

v_m= *(1.49)(y^0.67)(s^0.5)/n* velocity from Manning's Equation, in feet per second

v_{me} = mean velocity of entire water column

v_{pan} = q_{pan}/y water velocity from discharge per panel, calculated in feet per second

WE = water elevation, measured at water's edge in feet

WE_d = water edge elevation at the downgradient cross section

WE_u = water edge elevation at the upgradient cross section

y = water depth

y, y_n = *WE-E$_n$* water depth at each interval (panel), calculated in feet

y_a = 0.66 y adjusted depth

y_c , y_c *y$_c$=(q^2/g)^0.33* critical depth, calculated in feet

y/y_c = dimensionless ratio of depth to critical depth

α = velocity coefficient, set at 1.15 or 1.30 in the present study

$\sum q_n$ = summation of discharge values of each panel

Stream Level / Discharge Conversion Table

Stream Level (feet above datum)	Discharge cubic feet per second	Discharge Cubic meters per second
2.76	970	27.16
3.26	1430	40.04
4.19	2670	74.76
4.7	3470	97.16
5.18	4310	120.68
6.34	6780	189.84
6.99	8430	236.04

1. Introduction and Background

1.1 General Context

Water flows through open channels in one of three regimes of flow, known as subcritical, critical and supercritical. The flow regimes are mathematically defined by the Froude Number as a function of velocity and depth under ideal conditions of uniform flow through a regular rectangular channel. However, such conditions very rarely, if ever, occur in natural channels. This thesis examines the spatial distribution of flow conditions along a steep gradient irregular rock bedded stream at several different discharge rates. At low flow, streambed geometry and direct measurement of water velocity and depth are possible across partly exposed beds of soft, flat lying shale, cut by joints into easily erodible plates and a progressively dominant thalweg, bordered by abrupt ledges. However, higher flows breed rougher conditions that culminate in vicious diagonal waves at supercritical flow, six foot tall river-wide hydraulic jumps and similarly sized standing wave trains that render direct measurements impossible. Therefore, the study offers mathematical predictions of flow conditions with the original and two variations of the Froude Equation, based on streambed geometry, discharge data from a nearby stream gage and direct measurement of water edge locations at progressively higher flows. The results are compared with photos of the study reach taken at the time of water edge location measurement.

1.1.1 Previous Work

Sir Isaac Newton's Second Law of Motion,

$$\text{Force (F)} = \text{Mass (m)} \times \text{Acceleration (a)}$$

provides the basis for subsequent equations to describe fluid flow through open channels. Henderson (1966) and other standard texts develop the pertinent equations that culminate in the Froude Number, defined as the non-dimensional representation of the ratio of inertial forces to gravitational forces. In open channel flow, the Froude Number is represented as the ratio of stream velocity to wave velocity.

$$Fr = v/C = v/(gy)^{0.5}$$

Where Fr = Froude Number

v = stream velocity

C = wave velocity

g = acceleration due to gravity

y = water depth

Under ideal conditions of uniform flow and no friction, Froude Numbers less than unity define subcritical flow in open channels. Subcritical flow allows a wave propagated by a disturbance to flow to migrate upstream as a calm to choppy water surface. Conversely, Froude Numbers greater than unity define supercritical flow, in which a propagated wave is swept downstream and appears as a diagonal wave across all or part of the channel. Froude Numbers near or equal to unity define critical flow, in which a train of standing waves remain fixed in position within the channel.

Previous work on the subject has included mathematical modeling under ideal conditions, flume experiments or descriptions of observed phenomena in the field. Benton (1954) postulated that hydraulic jumps can occur if a supercritical layer overlies a subcritical layer under conditions of vertical flow separation. Kennedy (1963) showed that sediment on the bed could result in critical flow conditions at Froude Numbers as low as 0.84. Schoellhamer (1982) used a computer model to calculate subdivision Froude Numbers for variable flow regimes across a single section. Cheel (1990) estimated that in-phase bed waves resulted from flows at a minimum Froude Number of 0.84. Triests (1992) modeled a historic dam failure and concluded that supercritical flow could not be maintained for distances greater than 0.1 miles, except in high gradient, smooth, uniform solid bedrock channels. Tinkler (1997a) distinguished between Froude Numbers calculated from average flow depth, width and velocity across a single section and Froude Numbers calculated from accurate values of depth, width and velocity measured within narrow panels in a small bedrock stream. Richardson and Carling (2006) found that subcritical flow approaches critical flow as discharge increases in a straight, trapezoidal bedrock channel. Valle and Pasternack (2006) found that supercritical Froude Numbers decreased as discharge increased at a natural hydraulic jump in a bedrock channel.

Most of the referenced studies used mean average velocity to calculate Froude Numbers and/or limited analysis to single cross sections or stream features. Tinkler (1997a) subdivided a cross section and measured velocities at individual panels, then back-calculated Manning's roughness values for a range of slopes and depths. The present

study utilizes streambed geometry, measured discharge data and Manning's Equation to calculate velocities, and ultimately a range of Froude Numbers from thirteen variations of the Froude Equation, at individual panels within nine cross sections along an 800 foot reach through seven discharge levels over two orders of magnitude. Photos of each cross section at each water level are used to compare the accuracies of the different calculation methods to predict subcritical, critical and supercritical flow at individual panels and throughout an entire reach of a steep gradient, bedrock stream.

1.2 Thesis Goal and Objectives

The goal of this thesis is to test the capability of the Froude Equation to predict the state of flow at specific points and throughout a reach in an irregular rockbed stream through several levels of discharge. The specific objectives to achieve this goal are:

1) to determine the streambed geometry of the study reach and establish benchmarks at cross sections every 100 feet, with each section subdivided into 10 foot wide panels;

2) to directly measure the location and elevation of the water's edge at each cross section, and photographically record the actual stream conditions, during progressively higher discharge events;

3) to record the discharge at each event as measured at a United States Geological Survey stream gage located approximately 2000 feet downstream of the study reach;

4) to calculate water velocities at each panel at each water level via three methods:

   i) assume constant discharge per unit width (original Froude Equation assumption);

   ii) calculate percentage discharge per panel (Panel Froude Equation);

   iii) use Manning's Equation with known slope and depth;

5) to calculate the Froude Numbers at each panel at each water level via several methods;

6) to compare the calculation results with the photos of the cross sections to determine calculation method accuracies.

The hypothesis is that the Froude Equation is useful for prediction of flow conditions in an irregular, rock bedded stream, provided that appropriate velocity, water surface slope and depth factors are considered.

1.3 Study Context

1.3.1 Study Area

The study area lies along Cattaraugus Creek, 1800 to 900 feet upstream of the railroad bridge in the Village of Gowanda, New York, USA (Figure 1). Cattaraugus Creek forms the boundary between Cattaraugus and Erie counties at this location. From its headwaters, the stream flows westward through agricultural lands, on glacial lacustrine clays overlain by fluvial deposits and outwash sand and gravels, and through four rockbed gorges en route to discharge into Lake Erie at Sunset Bay. The study area begins approximately 6500 feet downstream of the mouth of Zoar Valley Gorge. Immediately downstream of the study area, the streambed of Cattaraugus Creek changes from bedrock to alluvial deposits of the glacially filled Conewango Valley.

United States Geological Survey Stream Gage 04213500 is located on the right bank of the stream at latitude 42 degrees, 27 minutes, 50 seconds, longitude 78 degrees, 56 minutes, 7 seconds, approximately 2900 feet downstream of the study area (Figure 2). The drainage area at the stream gage is 436 square miles.

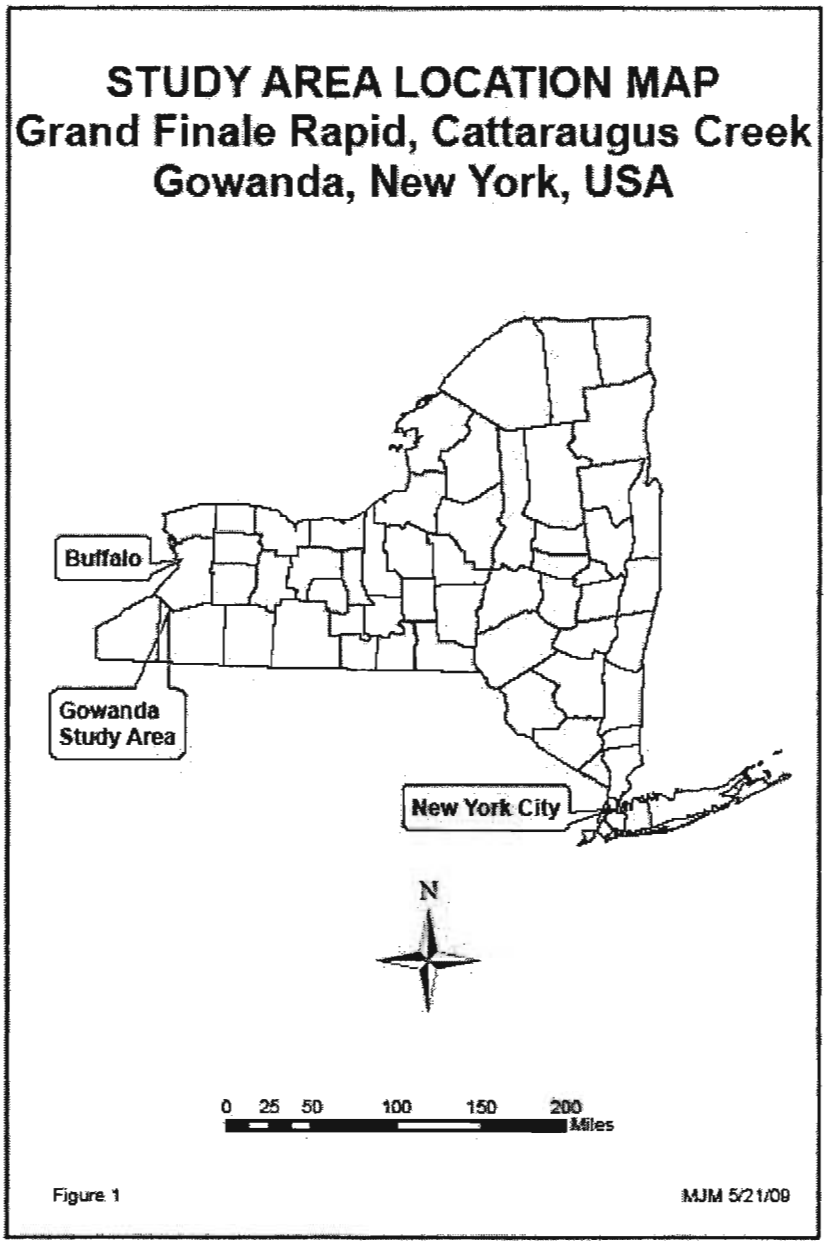

Figure 1. Study Area Location Map

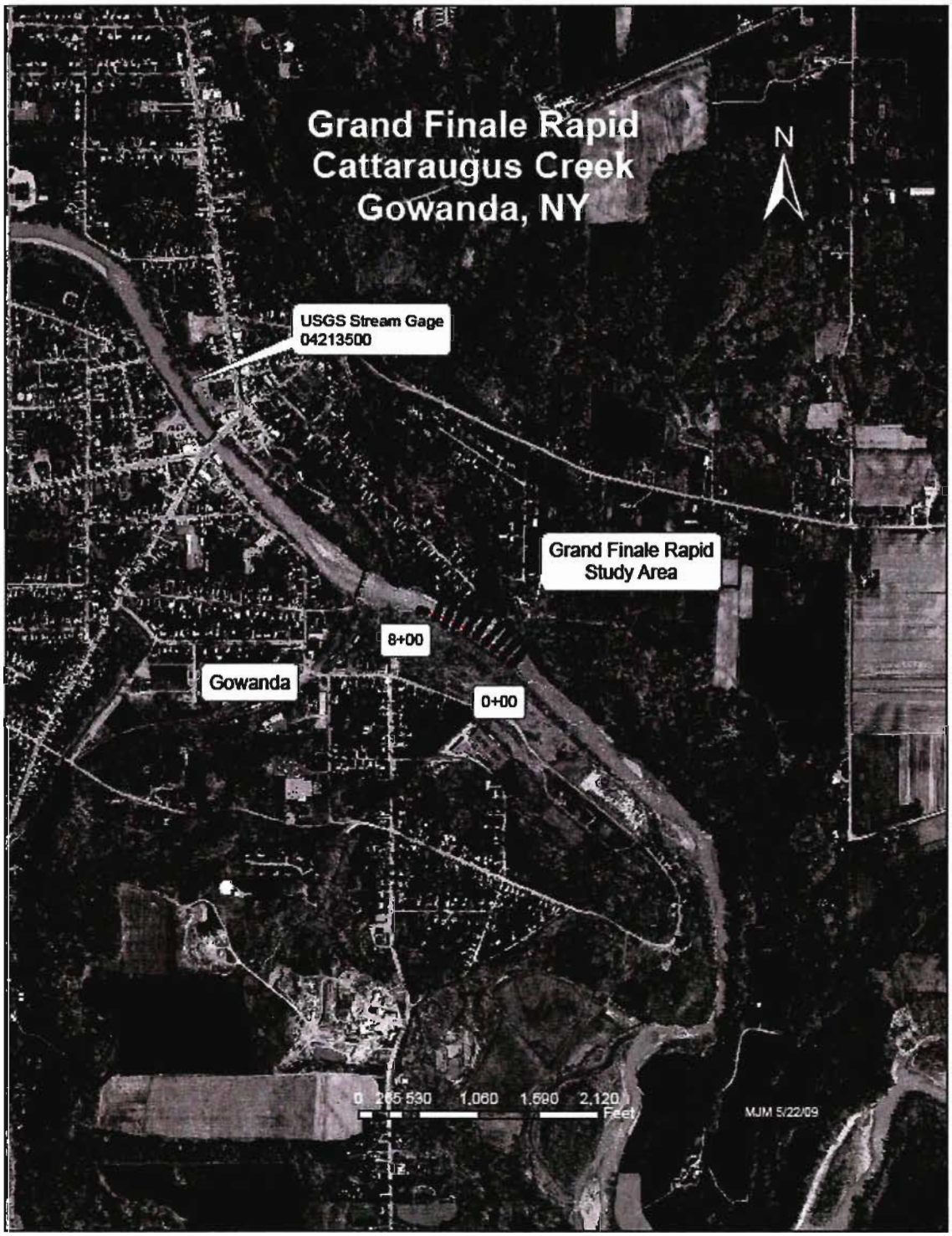

Figure 2. Grand Finale Rapid Study Area

The study area streambed is weak shale bedrock of the Gowanda Member of the Late Devonian Canadaway Formation. The thalweg tends to follow a strong northwest-trending joint set, periodically cut by northeast- and east-trending joints. The thalweg gradient is 0.010. Within the streambed, additional discontinuous minor channels parallel the thalweg throughout the study area. The left bank is a vertical concrete wall, broken along a 60 foot long segment. The right bank is a bedrock and talus slope beneath a vertical outcrop of shale with rare thin siltstone beds.

In the upper sections of the study area (Figure 3), the streambed is carved with multiple deeper grooves that coalesce into a secondary pool and a single thalweg, separated by in situ plates, a pattern previously recognized by Blank (1958) and Shepherd and Schumm (1974). The pool terminates as the streambed then passes through a middle section (Figure 4) dominated by river-wide continuous in situ plates cut by a thalweg and incipient deeper grooves that again coalesce into a secondary pool that terminates. The single thalweg progressively widens to become a dominant pool, bordered by ledges, at the downstream end of the study reach (Figure 5). The cross sections are labeled consecutively, measured in feet from the upstream end of the study reach

Cross Section 0+00

Cross Section 1+00

Cross Section 2+00

Figure 3. Upper section of study reach. Water flows from right to left. Multiple channels, separated by dry in situ plates of shale, coalesce downstream into a pool near the right descending bank.

Cross Section 3+00

Cross Section 4+00

Cross Section 5+00

Figure 4. Middle section of study reach. Water flows from right to left. Incipient multiple channels coalesce downstream and terminate in a secondary pool along the right bank. A single thalweg grows near the left bank (bottom of photos).

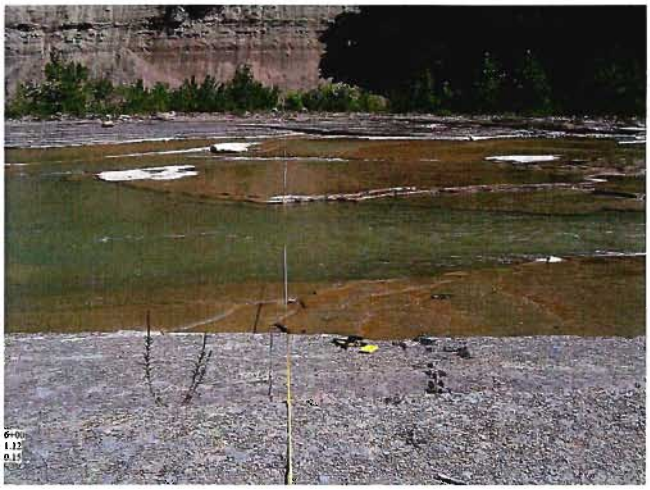

Cross Section 6+00

Cross Section 7+00 (water flows left to right)

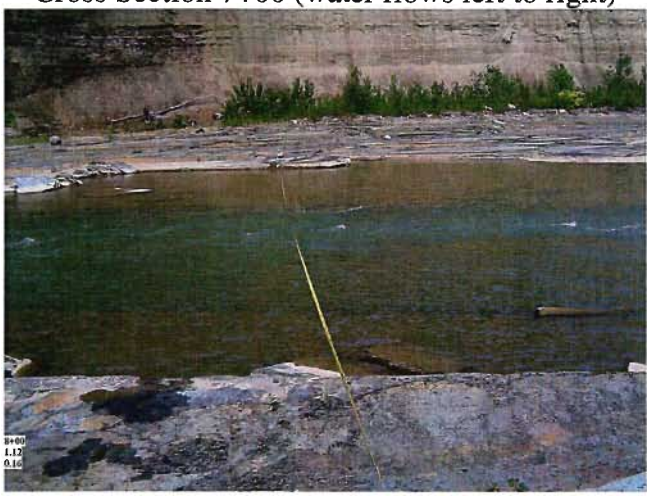

Cross Section 8+00

Figure 5. Lower section of study reach. Water flows from right to left, except as noted. A single thalweg opens downstream into a widening pool, bordered by bedrock ledges.

1.3.2 Regional Geology

The study area lies at the edge of the Allegheny Plateau physiographic province in western New York. Late Devonian sediments of the prograding Catskill Delta were eroded to a peneplain surface, uplifted, eroded into a maturely dissected plateau and repeatedly glacially modified, most recently during Late Wisconsinan time (Tesmer, 1975). Glacial meltwater channels and stream diversions incised several rockbed gorges in the Cattaraugus Creek drainage basin. Human encroachment into the left bank floodplain has straightened the stream immediately above and along the study area.

1.3.2.1 Stratigraphy

The study area streambed crosses weak shale at the type locality of the Gowanda Member of the Late Devonian Canadaway Formation. Tesmer (1975) describes the Gowanda Shale Member as follows:

"The Gowanda consists of interbedded medium light gray to grayish-black shales, silty shales and thin to thick-bedded ripple-marked light gray siltstones. Also present are many zones of calcareous concretions and septaria of various shapes, ranging from small nodules to about three feet in diameter. Some concretionary zones can be traced for short distances."

Rarely, plant fossils can be found within the study area, probably washed into the depositional basin from the easterly upland.

1.3.2.2 Structural History

Previous field investigations in the vicinity of Zoar Valley Gorge (Van Tyne, et al., 1980, Beinkafner, 1983, Jacobi, et al., 1999, Meyers, 1999) have revealed five distinct fracture trends: N (35-10 degrees), NE (20-40 degrees), ENE (60-70 degrees), E (80-110 degrees) and NW (310-330 degrees). In summary, E, ENE and NE features exert significant influence on streambed orientation until truncated by a strong NW fracture zone as Cattaraugus Creek leaves the gorge to occupy the pre-glacial Allegheny River Valley. Structural influence on pre- and post-glacial stream orientation has been recognized in nearby Ontario, Canada by Eyles and Scheidegger (1995) and Eyles, et al. (1997), among others, and in Texas, USA by Blank (1970).

The thalweg follows the NW fracture zone through the study area.

1.3.2.3 Glacial History

Prior to glaciation, the ancestral Allegheny River Valley flowed northwesterly past Gowanda, NY and into the Erie lowlands (Carll, 1880). Cattaraugus Creek did not exist. Instead, Tertiary north-flowing stream valleys drained the region.

Multiple episodes of glacial advances progressively dammed the valleys to divert drainage southward into the present day Allegheny-Ohio-Mississippi River system.

Pro-glacial lakes filled the moraine- and/or ice-dammed pre-glacial Tertiary north-flowing valleys. Progressively lower outlets were exposed as the ice receded, draining the lakes and cutting four gorges through the former interfluves to form Cattaraugus Creek (Tesmer, 1975). The study area is immediately upstream of the rockbed/alluvial bed contact in Cattaraugus Creek that marks the edge of the pre-glacial ancestral Allegheny River Valley.

1.3.2.4 Human Influences on Channel Formation

A vertical concrete wall forms the left bank of Cattaraugus Creek at high water levels for several hundred feet upstream and continues through the 800 foot length of the study area. A former factory site and landfill lie on the landward side of the wall, prohibiting natural channel formation in the alluvial, lacustrine and outwash sediments of the filled edge of the ancestral Allegheny River Valley. Thus channelized, Cattaraugus Creek concentrates flow in the northwest-trending fracture zone of weakened shale. Annual discharge is sufficient to remove cliff debris generated from the right bank outcrop of weak Gowanda Shale.

A naturally occurring bedrock-floored reach of Cattaraugus Creek that exhibits similar flow conditions throughout the same discharge levels as analyzed in the present study exists in the left channel at Refrigerator Island Rapid in Zoar Valley Gorge. Appendix I contains photos of the study area and the Refrigerator Island reach at low and high water levels for comparison.

1.3.3 Mathematical Basis for the Present Study

Flowing water visibly expresses energy distribution predicted by mathematical equations. The present study compares several such equations with observations recorded via photos. The key equations used in the present study solve for the Froude Number, Specific Energy, critical depth and critical velocity. This section summarizes the pertinent equations.

1.3.3.1 Froude Equation

In open channel flow, the Froude Number is represented as the ratio of stream velocity to wave velocity.

$$Fr = v/C = v/(gy)^{0.5}$$

Where Fr = Froude Number

v = stream velocity

C = wave velocity

g = acceleration due to gravity

y = water depth

Water flows in one of three visible regimes of flow, defined as subcritical, critical and supercritical (Figure 6). Under ideal conditions of uniform flow, subcritical flow occurs when $v<(gy)^{0.5}$, so $Fr<1.0$. Subcritical flow is visually identified by relatively deep, slow moving water, as normally observed in natural channels. Critical flow occurs when

v=(gy)^0.5, so Fr=1.0. Critical flow is visually identified by trains of standing waves. Supercritical flow occurs when v>(gy)^0.5, so Fr>1.0. Supercritical flow is visually identified by relatively shallow, fast moving water, sometimes cut by diagonal waves.

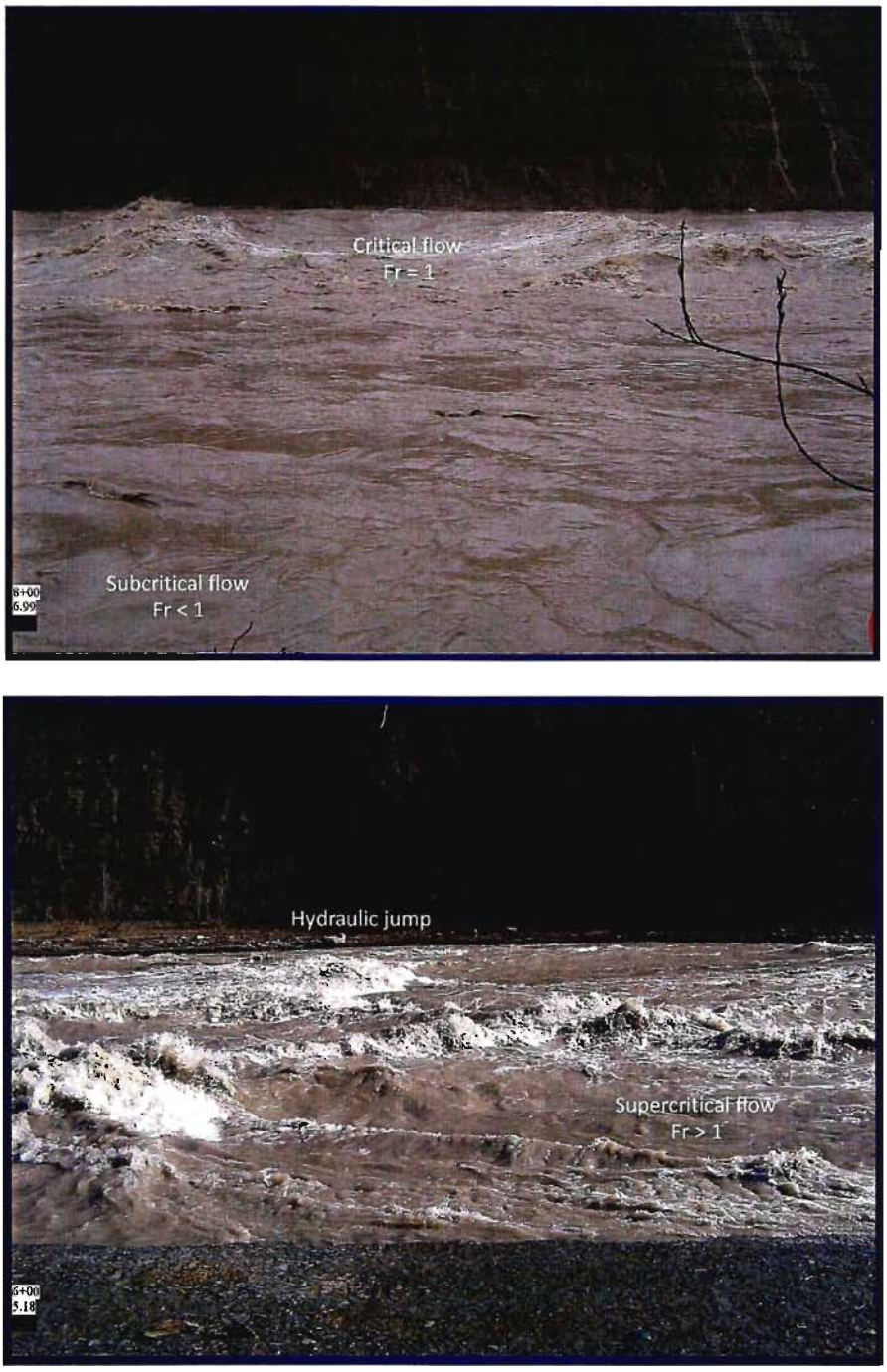

Figure 6. Flow regimes. Upper photo shows subcritical flow and critical flow. Lower photo shows supercritical flow and a hydraulic jump.

1.3.3.2 Specific Energy Equation

Henderson (1966) defines Specific Energy as the energy referred to the channel bed as the datum, such that

$$E = y + v^2/2g,$$

where E = Specific Energy.

Assuming uniform flow and constant discharge across the entire section, discharge through a cross section is defined as

$$Q = vA$$

where Q = discharge

v = mean velocity at right angles to the cross section

A = area of cross section occupied by water.

Subsequently,

$$q = Q/b = vy$$

where q = discharge per unit width

b = water surface width of cross section.

Re-arranging terms,

$$v = q/y,$$

so, by substitution into the Specific Energy Equation,

$$E = y + q^2/2gy^2.$$

Assuming a rectangular cross section and constant q,

$$(E - y)y^2 = q^2/2g = \text{constant}.$$

The above quadratic equation defines a parabola whose solution usually yields two possible realistic depths y for given E and q. The greater and lesser depths represent subcritical or supercritical flow, respectively. Specific energy is at a minimum at critical flow (Henderson, 1966) and yields a singular result at the tangent parallel to the y axis of the parabola described by the quadratic equation.

The present study calculates Specific Energy values with stream velocity values from measured discharge data and Manning's Equation, respectively, and then compares graphs of the results with the ideal graph derived from the quadratic equation described above. The comparison serves as a check on the validity of the two velocity calculation methods and as an indirect check on the validity of the various Froude Number calculation methods. The basic relationship between Specific Energy and the Froude Number holds for a non-rectangular section (Henderson, 1966) and thus is valid for the study area.

1.3.3.3 Critical Depth and Critical Velocity

Henderson (1966) defines critical velocity as the velocity with which a long wave of low amplitude propagates itself in water of depth y.

At critical flow,

$$v_c^2 = gy_c$$

$$y_c = (q^2/g)^{0.33}$$

where v_c = critical water velocity

y_c = critical water depth.

Solving for v_c yields

$$v_c = (gy_c)^{0.5}$$

where v_c = critical velocity of water at a given depth and discharge.

The present study calculates critical velocity and critical depth values with stream velocity values from measured discharge data and Manning's Equation, respectively, then compares the results to evaluate the validity of the different velocity calculation methods and as an indirect check on the validity of the various Froude Number calculation methods.

1.3.3.4 Summary of Study Variations

Velocity was calculated either from discharge data or from Manning's Equation to compare calculation method accuracies (Section 1.3.3.5). The velocity coefficient was varied from 1.0 to 1.30 to consider non-uniform flow due to bed roughness (Section 2.2.3.1.2). Water depth was varied from the full depth to 0.66 full depth to consider vertical flow separation (Section 1.3.3.6).

The following variations of the Froude Equation were examined in this study.

Name	Equation	Origin of Velocity Value	Velocity Coefficient	Depth
Simplified Froude Number	$F_{hs}= v_h/ (gy)^{0.5}$	discharge data	1	full
Manning's *v* Simplified Froude Number	$F_{ms}= v_m/(gy)^{0.5}$	Manning's Equation	1	full
Original Froude Number	$F_h=v_h/ (gy/1.15)^{0.5}$	discharge data	1.15	full
Manning's *v* Original Froude Number	$F_m=v_m/ (gy/1.15)^{0.5}$	Manning's Equation	1.15	full
Original Froude Number	$F_h=v_h/ (gy/1.30)^{0.5}$	discharge data	1.3	full
Manning's *v* Original Froude Number	$F_m=v_m/ (gy/1.30)^{0.5}$	Manning's Equation	1.3	full
Panel Froude Number	$F_{pan}= v/(gy)^{0.5}$	discharge data/panel	1	full
Depth Adjusted Simplified Froude Number	$F_{hsa}= v_h/ (gy_a)^{0.5}$	discharge data	1	0.66*y*
Depth Adjusted Manning's *v* Simplified Froude Number	$F_{msa}= v_m/(gy_a)0.5$	Manning's Equation	1	0.66*y*
Depth Adjusted Original Froude Number	$F_{ha}=v_h/ (gy_a/1.15)^{0.5}$	discharge data	1.15	0.66*y*
Depth Adjusted Manning's *v* Original Froude Number	$F_{ma}=v_m/ (gy_a/1.15)^{0.5}$	Manning's Equation	1.15	0.66*y*
Depth Adjusted Original Froude Number	$F_{ha}=v_h/ (gy_a/1.30)^{0.5}$	discharge data	1.3	0.66*y*
Depth Adjusted Manning's *v* Original Froude Number	$F_{ma}=v_m/ (gy_a/1.30)^{0.5}$	Manning's Equation	1.3	0.66*y*

Table 1 Summary of Froude Equation Variations

1.3.3.5 Calculation of Velocity Within Each Panel

While the Specific Energy Equation and Froude Equation are mathematically valid for the present study, calculation of velocity within each 10 foot wide stream panel becomes problematic in non-rectangular sections. Solving v = Q/A, as discussed in Section 1.3.3.1 above, yields an average mean velocity across an entire section. Observations of natural channels show that subcritical, critical and supercritical flow can occur simultaneously along the same section, with obviously different velocities in each state of flow, rendering the assumption of constant velocity across the section invalid.

Nevertheless, many workers use mean average velocity to calculate Froude Numbers (Schoellhamer, 1982; Schoellhamer, et al., 1985; Jimenez and Chaudhry, 1988; Sarma, et al., 1991; Ohtsu and Yasuda, 1991; Beffa, 1996; Meselhe, et al., 1997; Causon, et al., 1999; Guo, 1999; Chanson, 2006; Richardson and Carling, 2006; Valle and Pasternack, 2006; Carollo, et al., 2007; Catella, et al., 2008; Turowski, et al., 2008a; Turowski, et al., 2008b). In addition, HEC-2 and HEC-RAS, two widely used programs produced by the United States Army Corps of Engineers Hydraulic Engineering Center to analyze open channel flows, also use mean average velocity to calculate Froude Numbers (HEC-2 Water Surface Profiles User's Manual September 1990: Revised September, 1991; HEC-RAS River Analysis System Hydraulic Reference Manual Version 4.0 March 2008). It should be noted that Schoellhamer (1982), Schoellhamer, et al. (1985), HEC-2 and HEC-RAS subdivide cross sectional flow into main channel and overbank flow. Furthermore, Richardson and Carling (2006) state:

"Mean velocities estimated from the discharge and the cross-sectional area of the whole channel are unrealistically low."

1.3.3.5.1 Calculation of "Henderson's v"

As an alternative, calculation of velocity at each panel from discharge data, for the set of equations labeled "Original Froude Number with Henderson's v", occurs as follows. "Henderson's v" is so named because the derivation of the equations can be found in Henderson (1966), as well as other hydraulics texts, and to differentiate this set of equations from a subsequent set of equations, described later, that utilizes velocity values derived from Manning's Equation.

To calculate velocity at each panel from discharge data,

$$Q = vA$$

where Q = discharge

v = mean velocity at right angles to the cross section

A = area of cross section occupied by water.

For the purpose of this study,

$$q = Q/b = vA/b = vy_n$$

where q = discharge per unit width

b = water surface width of cross section

y_n = water depth at each interval (panel)

$$v = q/y_n$$

Velocity is now a function of water depth at each panel. However, the basic assumption that discharge q is constant across the section is not valid for a non-rectangular section. Furthermore, if $v = q/y_n$, then velocity would vary inversely with depth, an invalid condition. Nonetheless, the calculations were run to ascertain the accuracy of the ideal Froude Number when compared with digital photographs of the cross sections at each water level.

1.3.3.5.2 Calculation of "Panel v"

To avoid the assumption of constant unit discharge q across the section, the percentage of discharge per individual panel area was calculated as follows. The resultant set of calculations was labeled "Panel Froude Number".

To calculate the percentage of discharge per individual panel area,

$$A_r = A_t/A_c$$

where A_r = area ratio

A_t = area of interval

A_c = area of cross section occupied by water.

$$Q_n = QA_r$$

where Q_n = discharge in interval,

so

$$q_{pan} = Q_n/b_i = v_{pan}y$$

where q_{pan} = discharge per panel width as calculated from Q_n

b_i = interval width,

so,

$$v_{pan} = q_{pan} / y$$

for each panel. However, subsequent calculations result in constant velocity values across the entire section, an invalid assumption as discussed in Section 1.3.3.4.

1.3.3.5.3 Calculation of "Manning's v"

To avoid the invalid assumptions of constant discharge or constant velocity across the entire section, another alternative calculation of velocity at each panel comes from the well-known Manning's Equation.

$$v = 1.486(R^{0.67})(S^{0.5})/n$$

where R = hydraulic mean radius

S = longitudinal slope

n = Manning's resistance coefficient (valued at 0.025 for clean, straight channels, from Henderson, 1966).

$$R = A_c / P$$

where A_c = area of cross section occupied by water

P = wetted perimeter of cross section.

In wide channels where the width exceeds 20 times the depth (Tinkler, 1982), the wetted perimeter P approximates the surface width of the stream b, so

$$R = A_c / P = A_c / b = y$$

where y = water depth,

yields results with minimal error.

As in Section 1.3.3.4.1 above, the general Manning's Equation yields an average mean velocity across the entire section. However, by substituting the water depth of each panel in this study, the Manning's Equation is solved to yield the mean velocity at each panel,

$$v_m = 1.49(y^{0.67})(S^{0.5})/n,$$

where v_m = velocity as calculated from Manning's Equation.

Section 4.4.3 discusses a method to check the validity of velocity use as calculated from Manning's Equation by comparison of calculated and measured discharges.

1.3.3.6 Adjusted Depth

Tinkler (1997a) suggests that faster moving water in the upper portion of a panel sometimes shears over slowing moving water near the streambed, generating separated flow, a view shared by Benton (1954). An upper region of near critical or critical flow could overlie a lower region of subcritical flow. Visible examples include standing waves in a deep pool at the base of a steep drop. Simple "at a station" calculations of velocities and resultant Froude Numbers at panels across the section would yield anomalously low results, based on water depth. To account for vertical flow separation in a panel, Tinkler (unpublished communication) argues that panels of critical flow are surrounded by regions of subcritical flow, possibly with flow reversed as lateral slackwaters, and underlying regions near the streambed. Since pressure varies inversely with velocity, water in the lateral regions of low velocity is forced beneath the faster moving water in the region of critical flow. To determine the depth of the faster moving water (Tinkler, unpublished communication),

$$U = (2gh)^{0.5}$$

where U = velocity difference between faster and slower moving water

h = velocity head.

Re-arranging terms,

$$h = U^2/2g$$

If the faster flow is surrounded by eddies with no mean velocity (worst case scenario), then

$$U = v = (2gh)^{0.5}$$

where v = mean velocity of the faster flow.

At critical flow,

$$U = v = (gd)^{0.5}$$

where d = depth of faster moving water.

By substitution,

$$h = U^2/2g = gd/2g = 0.5d$$

which results in a jet of faster moving water of depth d lifted by a wedge of water of depth 0.5 d, such that

$$y = d + 0.5\ d = 1.5\ d$$

where y = water depth.

Re-arranging terms,

$$d = 0.66\ y$$

As the velocity of the water surrounding the jet increases, the difference between U and velocity head, h, decreases, resulting in increased values of the depth of the faster moving water, d. Thus, the value of d = 0.66 y represents the minimum depth of the jet of fast

moving water. Similarly, Richardson and Carling (2006) recognized that near critical flow decoupled to create central plug flow flanked by dead zones of low velocity flow. However, their work suggested that vertical flow separation was not necessary to achieve critical flow conditions.

A separate set of calculations were performed that substituted 0.66 y for water depth y. Although critical flow was assumed in the above equations, substitution of 0.66 y for y was made for all calculations to determine the overall accuracy of the substitution for all states of flow. Limited substitution for near critical flows only, or substitution of values other than 0.66, may result in increased calculation accuracy.

1.3.3.7 Ancillary Calculations

To check the results of this study with theoretical results under ideal conditions, three additional sets of calculations were performed. At each panel at each water level for each method of determining velocity, critical depth y_c and critical velocity v_c were calculated as per Section 1.3.3.2 above and divided by the actual and adjusted water depth and calculated velocity, respectively. After determination of the most accurate Froude Number calculation method, the results of the ancillary calculations at two water levels were plotted against the associated Froude Numbers. The resultant graphs were then compared with idealized graphs. Furthermore, the calculated values of specific energy were also plotted against the associated Froude Numbers.

2. Experimental Method

The study reach was surveyed using the traditional cross section approach. Benchmarks were established at each cross section. Geologic features of the study reach streambed were mapped. Water edge location and elevation were measured at each cross section at several different water levels. Discharge data as measured at the USGS stream gage downstream of the study reach was telephonically collected at the time of water edge measurement. Water surface features at each cross section were photographically recorded at the time of each water edge measurement.

The collected streambed survey data were used to create streambed cross sections. The streambed was divided into 10 foot wide panels at each cross section. The average elevation of the streambed in each panel was determined. The water elevation at each cross section at each water level was used to determine water depth at each panel. Discharge, water depth and water surface slope were used to calculate water velocity and Froude Number at each panel. The calculated Froude Numbers were compared with the photographs to determine the accuracy of the calculations' predictions of subcritical, critical and supercritical flow in an irregular channel with non-uniform flow.

2.1 Experimental Design

2.1.1 Data Collection

2.1.1.1 Cross Section Data Collection

The study reach streambed was topographically surveyed with a Spectra LL600 laser level, Brunton compass and 300 foot long nylon tape. A benchmark with an arbitrary elevation of 100.00 feet was established at the base of the left bank vertical concrete wall at Cross Section 0+00, directly beneath a four inch diameter metal pipe that extends through the wall. The elevation of the bottom of the pipe was measured at the time of benchmark establishment to be 106.00. This proved to be fortuitous because subsequent high water washed away the original benchmark.

The bearing of Cross Section 0+00 was chosen to cross Cattaraugus Creek perpendicular to the current flow. A baseline point was chosen along the strike of Cross Section 0+00 and assigned a horizontal position of 0.00. The vertical elevation relative to the benchmark was recorded. A 1.0 inch diameter hole was drilled 0.5 inches deep at the baseline point to mark its location. A nylon tape was stretched from the baseline point across the stream and secured in vegetation on strike with the cross section bearing. At water's edge, slope breaks, thalweg, other channel bottoms, vegetation line and other points of interest, the horizontal distance from the baseline and vertical elevation relative to the benchmark were recorded. The tape was then extended from the baseline point to

the left bank vertical wall. At slope breaks, vegetation line, and at the benchmark at the base of the wall, the horizontal distance from the baseline and vertical elevation relative to the benchmark were recorded. The horizontal distances from the baseline point in the direction of the wall were recorded as negative numbers. The base of the pipe above the benchmark was painted metallic gold for identification. The base of the pipe now serves as the benchmark for Cross Section 0+00 for future investigations.

The survey procedure was repeated at 100.00 foot intervals downstream for 800 feet. Two inch diameter benchmarks were painted metallic gold on the concrete wall above the intersection of each cross section and the base of the wall along the left bank. The elevations of the benchmarks were recorded.

It should be noted that the streambed survey occurred prior to final design of the present study. Cross Sections 0+00 through 4+00 concentrate on the locations of the thalweg, other channel bottoms, water's edge and vegetation line, with few other streambed details. Cross Sections 5+00 through 8+00 contain much more detail with regard to extent of inter-channel high areas and slope breaks.

2.1.1.2 Geologic Data Collection

The bedrock geology of the study reach was mapped at the time of the topographic survey and rechecked during low water level. Location and bearing of joints were particularly noted.

2.1.1.3 Streamflow Data Collection

Water edge location data were collected at desired discharge levels with a MDL Laser Ace 300 laser rangefinder and Brunton compass. Discharge at the USGS stream gage was recorded by calling the gage at (716)532-0626 when on location at Cross Section 0+00. The Brunton compass was used to locate each cross section relative to the benchmark. The laser rangefinder was used to establish the horizontal and vertical location of the intersection of the water's edge and each cross section relative to the benchmark. Digital photographs of the water surface features at each cross section were recorded immediately after each measurement. Upon completion of the survey at each discharge event, the USGS stream gage discharge data was again recorded to determine any discharge rate changes during the survey.

2.2 Calculations

The primary calculations in this study determined water depth, channel width, water surface slope and water velocity. The results were used in several variations of the Froude Equation. Ancillary calculations included critical velocity, critical depth and specific energy. Variables are set in italics from this point forward to identify their particular use in the present study.

2.2.1 Primary Calculations

2.2.1.1 Water depth (y)

Water depth (y) of each panel at each water level was determined by subtracting the panel (interval) bed elevation (E_n) from the water elevation (WE), or

$$y=WE-E_n$$

2.2.1.2 Channel Width (b_n)

Channel width (b_n) at each cross section at each water level was determined from the intersection of the water surface with the streambed as measured from each cross section.

2.2.1.3 Velocity from Discharge Data (v_h)

Velocity (v_h) was determined using the discharge data as recorded from the USGS stream gage as follows:

Discharge (Q) = [Discharge per unit channel width (q)][Channel width (b_n)], or

$$Q = (q)(b_n)$$

Therefore, $$q=Q/b_n$$

As defined in Henderson (1966),

water velocity (v_h)= Discharge per unit channel width (q)/ Water depth (y), or

$$v_h=q/y$$

2.2.1.4 Velocity from Manning's Equation (v_m)

An alternative method to determine velocity (v_m), using Manning's Equation, follows:

$$v_m=(1.49)(y\text{^}0.67)(s\text{^}0.5)/n$$

where roughness $n=0.025$ and slope s is calculated by subtracting the water edge elevation at the upgradient cross section (WE_u) from the water edge elevation at the downgradient cross section (WE_d), then dividing the remainder by the distance between the upstream and downstream cross sections, $s=(WE_u-WE_d)/200$.

2.2.2 Cross Section Constructions

The topographic survey data for each cross section were entered into a mapping program called PC Survey. A plan map and cross sections 0+00 through 8+00 of the streambed were generated (Appendix 1). Each cross section was divided into ten foot wide panels. The average streambed elevation in each panel was visually determined and recorded.

A series of water surface elevation plan maps and cross sections were similarly constructed for each recorded discharge event. PC Survey then calculated the area occupied by water at each cross section at each water level (Appendix 2). Width of the channel occupied by water was also determined by measuring the distances between the intersections of the water elevations and the streambed at each cross section at each water level.

2.2.3 Spreadsheet Constructions

Excel spreadsheets were created for each cross section to perform several series of calculations that culminated in a variety of Froude Numbers for each panel for each discharge event. The spreadsheets are included in digital Appendix III.

2.2.3.1 Original Froude Equation Spreadsheets

2.2.3.1.1 Simplified Froude Equation Spreadsheets

The Simplified Froude Equation, as presented in Henderson (1966), is

$$F_{hs}=v_h/(gy)^{0.5}.$$

The variables are defined below.

Each spreadsheet contains the following columns:

Interval (n): identifies the cross section panel n

Discharge (Q) cfs: discharge at USGS stream gage, measured in cubic feet per second

Water Elevation (WE) ft: water elevation, measured at water's edge in feet

Interval Elevation (E_n) ft: interval elevation, determined from cross section of streambed topography, calculated in feet

Water Depth (y) ft.: water depth $y=WE-E_n$, calculated in feet

Channel Width (b_n) ft: channel width, determined from intersection of water elevation with streambed , calculated in feet

Acceleration due to gravity (g) ft/sec/sec: acceleration due to gravity, set at 32 feet per second per second

$q=Q/b_n$ ft^2/sec: discharge per unit channel width, calculated in square feet per second

Velocity (v_h) ft/sec: water velocity $v_h=q/y$, defined in Henderson (1966), calculated in feet per second

Critical Depth (y_c) ft: critical depth $y_c=(q^2/g)^0.33$, defined in Henderson (1966), calculated in feet

Critical Velocity (v_c) ft/sec: critical velocity $v_c=((g)y_c))^0.5$, defined in Henderson (1966), calculated in feet per second

Simplified Froude Number (F_s): Froude Number $F_{hs}=v_h/(gy)^0.5$, defined in Henderson (1966)

Specific Energy (E): Specific Energy $E=y+v_h^2/2g$, defined in Henderson (1966)

Depth/Critical Depth (y/y_c): dimensionless ratio of depth to critical depth

Velocity/Critical Velocity (v_h/v_c): dimensionless ratio of velocity to critical velocity

After entry of discharge and water elevation data for each cross section at each water level, the spreadsheets performed the calculations. The findings are discussed in Section 4.1.1.1.

2.2.3.1.2 Original Froude Equation Spreadsheets with Velocity Coefficients

To account for non-uniform flow due to bed roughness, the spreadsheets were revised to include velocity coefficients into the Original Froude Equation, i.e.

$$Fr_h = v_h/(gy/\alpha)^{0.5}$$

where α = velocity coefficient.

The velocity coefficient, α, corrects the underestimation of kinetic energy when velocity varies throughout the water column.

$$\alpha = \int v^3 dA / v_{me}^3 A$$

where $v^3 dA$ = mean velocity (cubed) of an element of area in a water column

v_{me} = mean velocity of entire water column

Values of $\alpha = 1.15$ as average values for regular channels, spillways and flumes and $\alpha = 1.30$ as average values for natural streams and torrents were chosen from Chow (1959).

In addition, the Specific Energy equation was also revised,

$$E = y + \alpha v_h^2/2g$$

The findings of the revised calculations are discussed in Sections 4.1.1.2 and 4.1.1.3, respectively.

2.2.3.2 Panel Froude Equation Spreadsheets

The Original Froude Equation is based on constant discharge per unit width of stream channel occupied by water ($q=Q/b_n$). Velocity varies simply with water depth ($v_h=q/y$), as does Froude Number ($Fr_h=v_h/(gy)$^0.5). In an attempt to more accurately calculate the influence of discharge distribution on the Froude Number, this study proposes to calculate the percentage of discharge passing through each panel at each water level.

Each modified spreadsheet contains the following columns:

Interval (n): identifies the cross section panel

Discharge (Q) cfs: discharge at USGS stream gage, measured in cubic feet per second

Channel Area (A_c) ft^2: area of channel occupied by water, calculated by PC Survey in square feet

Water Elevation (WE) ft: water elevation, measured at water's edge in feet

Interval Elevation (E_n) ft: interval elevation, determined from cross section of streambed topography, calculated in feet

Water Depth (y) ft.: water depth $y=WE-E_n$, calculated in feet

Interval Width (b_i) ft: panel width, in feet

Interval Area (A_i) ft^2: panel area occupied by water $A_i=yb_i$, calculated in square feet

Area Ratio (A_r): dimensionless ratio, defines percentage of total area occupied by water in each panel $A_r=A_i/A_c$

Acceleration due to gravity (g) ft/sec/sec: acceleration due to gravity, set at 32 feet per second per second

Discharge in Interval (Q_n) cfs: discharge in panel $Q_n=QA_r$, in cubic feet per second

q_{pan} ft^2/sec: discharge in panel divided by panel width $q_{pan}=Q_n/b_i$, calculated in square feet per second

Velocity (v_{pan}) ft/sec: water velocity $v_{pan}=q_{pan}/y$, calculated in feet per second

Critical Depth (y_c) ft: critical depth $y_c=(q_{pan} ^2/g)^0.33$, defined in Henderson (1966), calculated in feet

Critical Velocity (v_c) ft/sec: critical velocity $v_c=((g)y_c))^0.5$, defined in Henderson (1966), calculated in feet per second

Panel Froude Number (F_{pan}): Froude Number $F_{pan}= v_{pan} /(gy)^0.5$

Specific Energy (E): Specific Energy $E=y+ v_{pan} ^2/2g$, defined in Henderson (1966)

Depth/Critical Depth (y/y_c): dimensionless ratio of depth to critical depth

Velocity/Critical Velocity (v_{pan} /v_c): dimensionless ratio of velocity to critical velocity

After entry of discharge and water elevation data for each cross section at each water level, the spreadsheets performed the calculations. The findings are discussed in Section 4.1.2.

2.2.3.3 Simplified and Original Froude Equations with Velocity Calculated from Manning's Equation

For comparison purposes, the Simplified and Original Froude Equation results were recalculated with velocity values derived from Manning's Equation. The following columns were added to the spreadsheets.

Slope *S*: dimensionless water surface slope calculated by subtracting the water edge elevation at the upgradient cross section *(WE_u)* from the water edge elevation at the downgradient cross section *(WE_d)*, then dividing the remainder by the distance between the upstream and downstream cross sections, *$S=(WE_u-WE_d)/200$.*

Velocity (v_m): velocity derived from Manning's Equation $v_m=(1.49)(y\text{^}0.67)(s\text{^}0.5)/n$ where $n=0.025$, in feet per second

The new velocity values (v_m) were substituted into the equations to calculate Froude Number, Specific Energy and Velocity/Critical Velocity for the Simplified and Original Froude Equations. The findings of the recalculations are discussed in Sections 4.1.3.

2.2.3.4 Adjusted Depth Calculations

Tinkler (1997) suggests that a flowing water column vertically segregates such that the upper portion may exhibit critical flow with simultaneous subcritical flow in the lower portion. Since direct measurement of velocities throughout the water column in each panel at each water level was impossible in this field study, the water depths at each panel were mathematically adjusted to 0.66 times the depth calculated by subtracting the interval elevation (E_n) from the water elevation (*WE*). The calculations were then re-run for the Original Froude Equations with velocity from Henderson (1966) and from Manning's Equation, respectively. The findings are discussed in Section 4.1.4.

3. Results

Calculation results for the different methods of determining the Froude Number are found in Appendix III. The results are grouped by cross section, with increasing water levels.

3.1 Raw Data and Basic Calculations

Appendix III contains an example of the raw data and subsequent calculations, divided into three sets. The first set contains calculations for the Simplified Froude Equation and the Original Froude Equation with $\alpha = 1.15$ and $\alpha = 1.30$, respectively, all with velocities derived from Henderson (1966) and from Manning's Equation, respectively. The second set contains revised calculations for the Simplified Froude Equation and the Original Froude Equation with $\alpha = 1.15$ and $\alpha = 1.30$, respectively, all with velocities derived from Henderson (1966) and from Manning's Equation, respectively, but with water depths adjusted to 0.66 y. The third set contains calculations for the Panel Froude Equation, which is based on the percentage of discharge passing through each panel at each water level. The complete set of calculation results are found in digital Appendix III.

3.2 Cross Section Photos With Froude Numbers

Digital Appendix III also contains photos of each cross section at each water level, displayed above the Froude Number calculations derived by each method in the study.

The photos are grouped by cross section, with increasing water level. Each cross section interval (panel) is classified as subcritical, critical or supercritical flow, with a description of the interval's water surface features.

3.3 Accuracy of Calculations

The calculated Froude Numbers were classified as subcritical flow when Fr < 0.84, critical flow when 0.84<= Fr <= 1.00 and supercritical flow when Fr > 1.00, then compared with the cross section interval classifications from the photos.

Figure 7 displays a bar graph to summarize the accuracy of the various calculation methods as determined by visual comparison of the resultant Froude Numbers and the photos taken at the time of water level measurement. Accuracy in this study is defined as the percentage of correctly calculated Froude Numbers, based on visual observation. Various visible features noted during the streambed survey, such as boulders, shelves, channels, etc., were used at each cross section at low water to identify individual panels. At higher water levels, the responses of the water surface to the features were used to identify individual panels.

Figure 8 displays line graphs to show the average accuracies of the various calculation methods as functions of water level, using actual and adjusted water depths, respectively. The Panel Froude Number results appear on each graph as a reference for comparison purposes.

Figure 9 displays line graphs to show the average accuracies of the various calculation methods at each cross section, using actual and adjusted water depths, respectively. The Panel Froude Number results appear on each graph as a reference for comparison purposes, even though the assumption of constant velocity renders the calculations invalid.

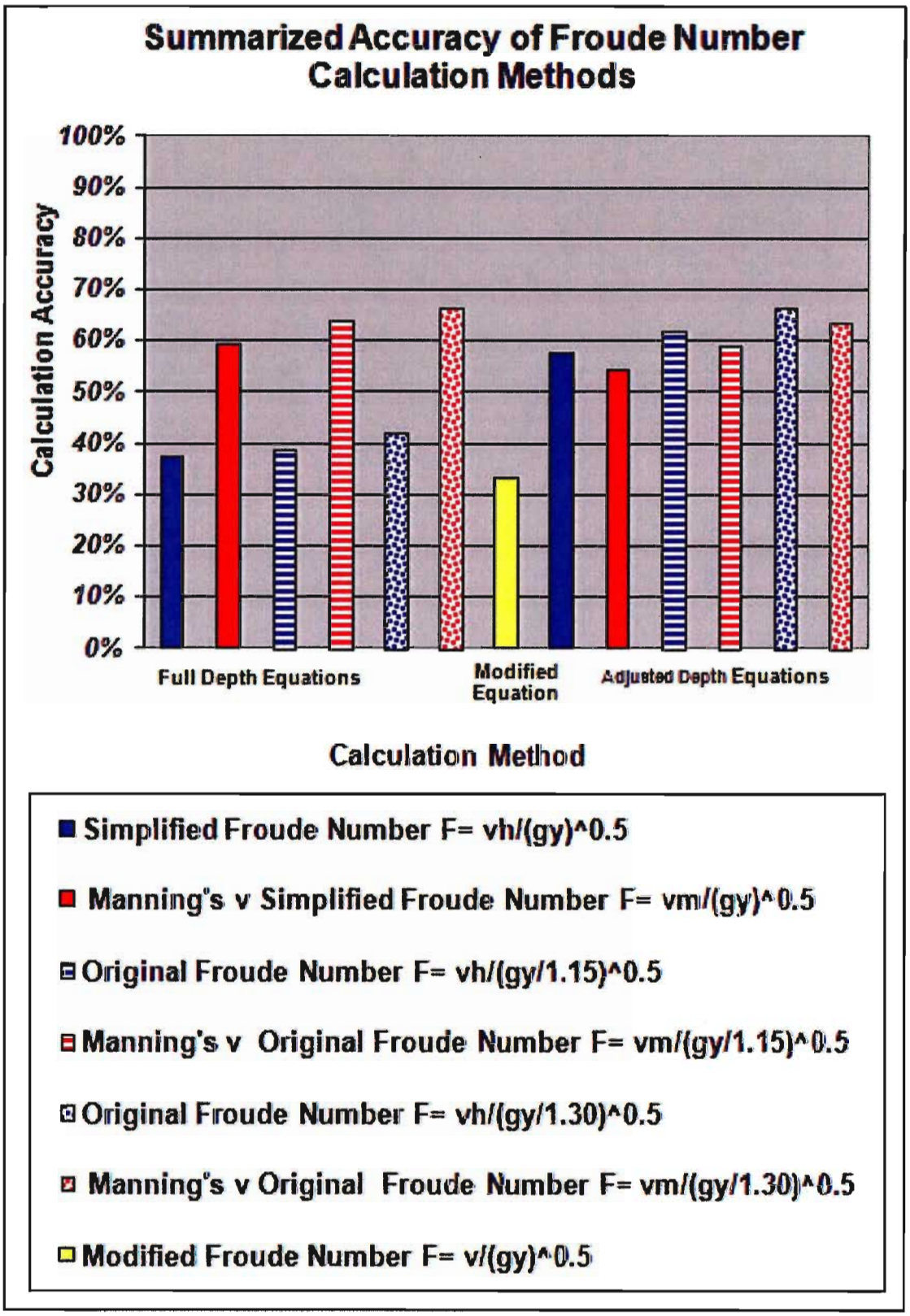

Figure 7. Summarized Accuracy of Froude Number Calculation Methods

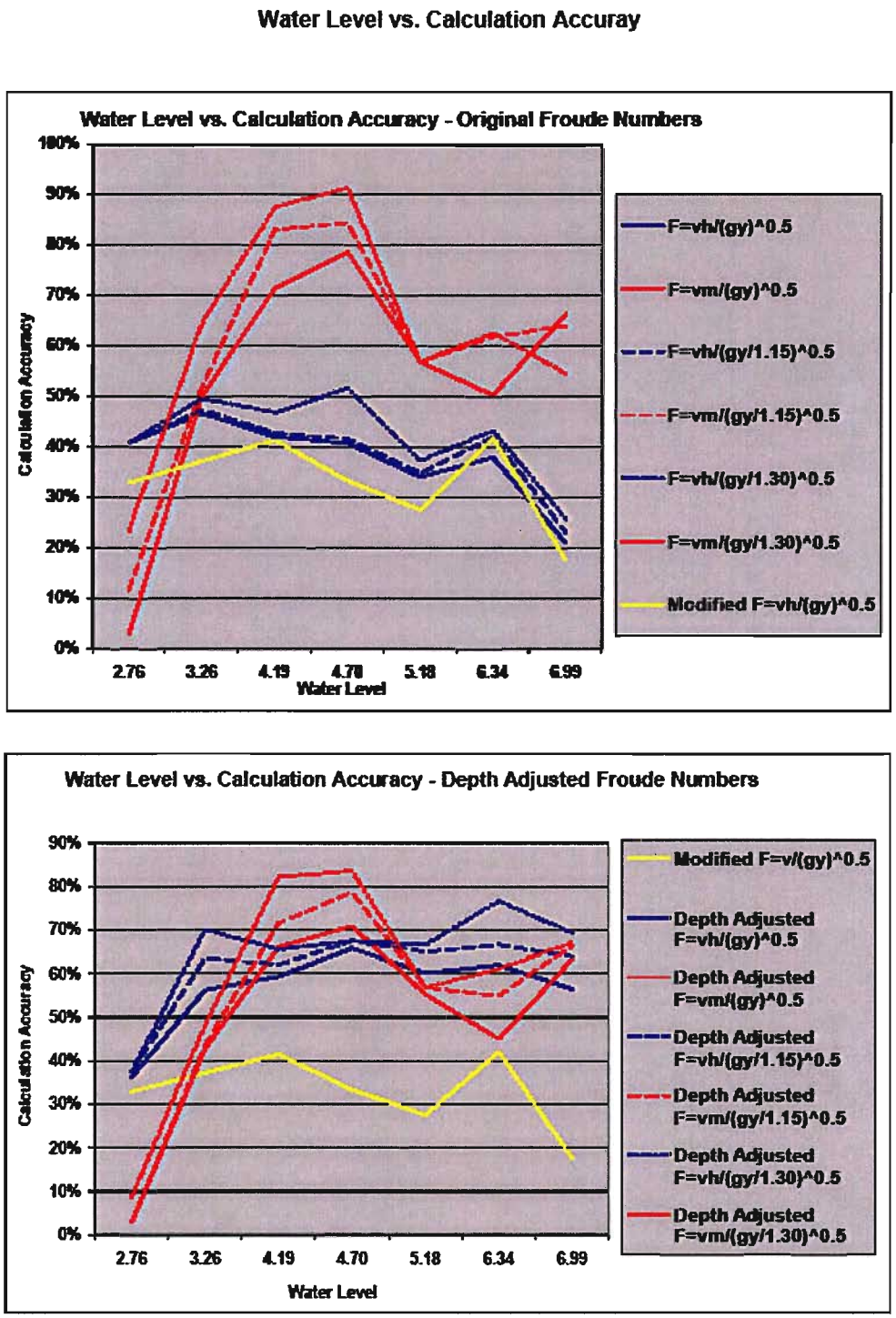

Figure 8. Water Level v. Calculation Accuracy

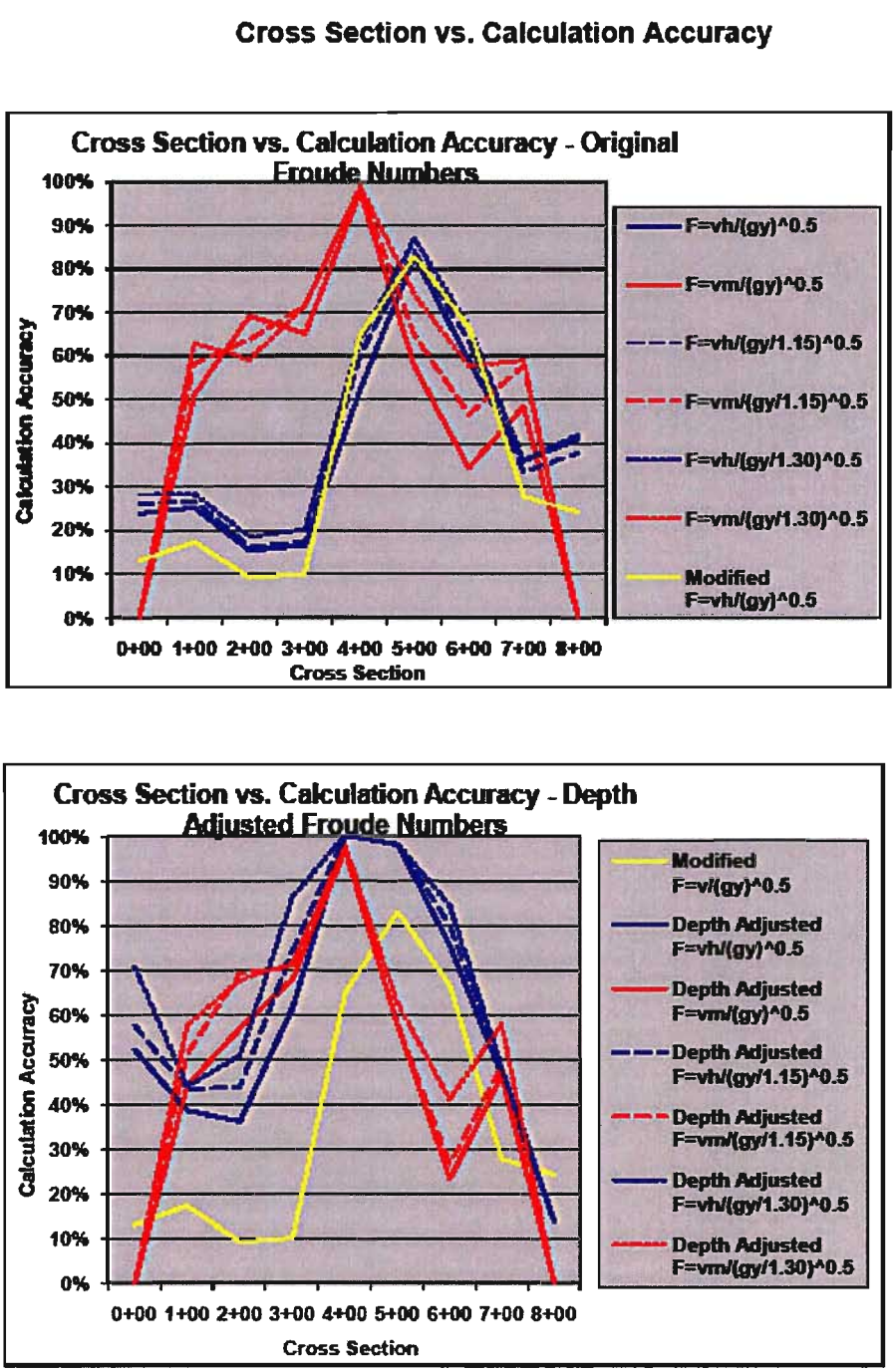

Figure 9. Cross Section v. Calculation Accuracy

4. Discussion

4.1 Comparison of Results with Photos

Comparison of the results of the various calculation methods with the photos reveals fair to poor accuracy (Figures 7 through 9).

At 68%, the most accurate method was the Original Froude Equation, with a velocity coefficient of $\alpha = 1.30$ and velocity derived from Manning's Equation,

$$Fr_m = v_m / (gy/1.30)^{\wedge}0.5.$$

At 33%, the least accurate method was the Panel Froude Equation, with velocity as a function of the percentage of discharge passing through each panel,

$$Fr_{pan} = v_{pan} / (gy)^{\wedge}0.5.$$

.

4.2 Comparison of Results with Photos After Revising Flow State Classifications

After review of the results discussed in Section 4.1 above and re-examination of the photos, the flow regime classifications were revised. Subcritical flow remained for Fr<0.84. However, critical flow, as defined by a train of standing waves, was very rarely observed in the photos. Supercritical flow, as defined by the first appearance of diagonal waves, was much more commonly observed at Fr values that exceeded 0.84. Therefore, the flow regimes were re-classified as critical flow when Fr = 0.84 and supercritical flow when Fr > 0.84. Richardson and Carling (2006) report that the first appearance of non-

breaking standing waves in their bedrock study channel occurred at Froude Numbers approximating 0.7, and that 90% of the channel was occupied by standing waves at Froude Numbers approximating 0.8.

The accuracy of the revised results increased dramatically. Comparison of the results of the various calculation methods with the photos reveals excellent to poor accuracy (Figures 10 through 12).

At 94%, the most accurate method was the Original Froude Equation, with a velocity coefficient of $\alpha = 1.30$ and velocity derived from Manning's Equation,

$$Fr_m = v_m/(gy/1.30)^{0.5}.$$

At 43%, the least accurate method was the Panel Froude Equation, with velocity as a function of the percentage of discharge passing through each panel,

$$Fr_{pan} = v_{pan}/(gy)^{0.5}.$$

4.2.1 Original Froude Equation Accuracy

4.2.1.1 Simplified Froude Equation

The revised overall accuracy of the Simplified Froude Equation,

$$F_{hs} = v_h/(gy)^{0.5}$$

was 42%. The most accurate revised result by water level was 56% at water level 2.76. The least accurate revised result by water level was 24% at water level 6.99. The most

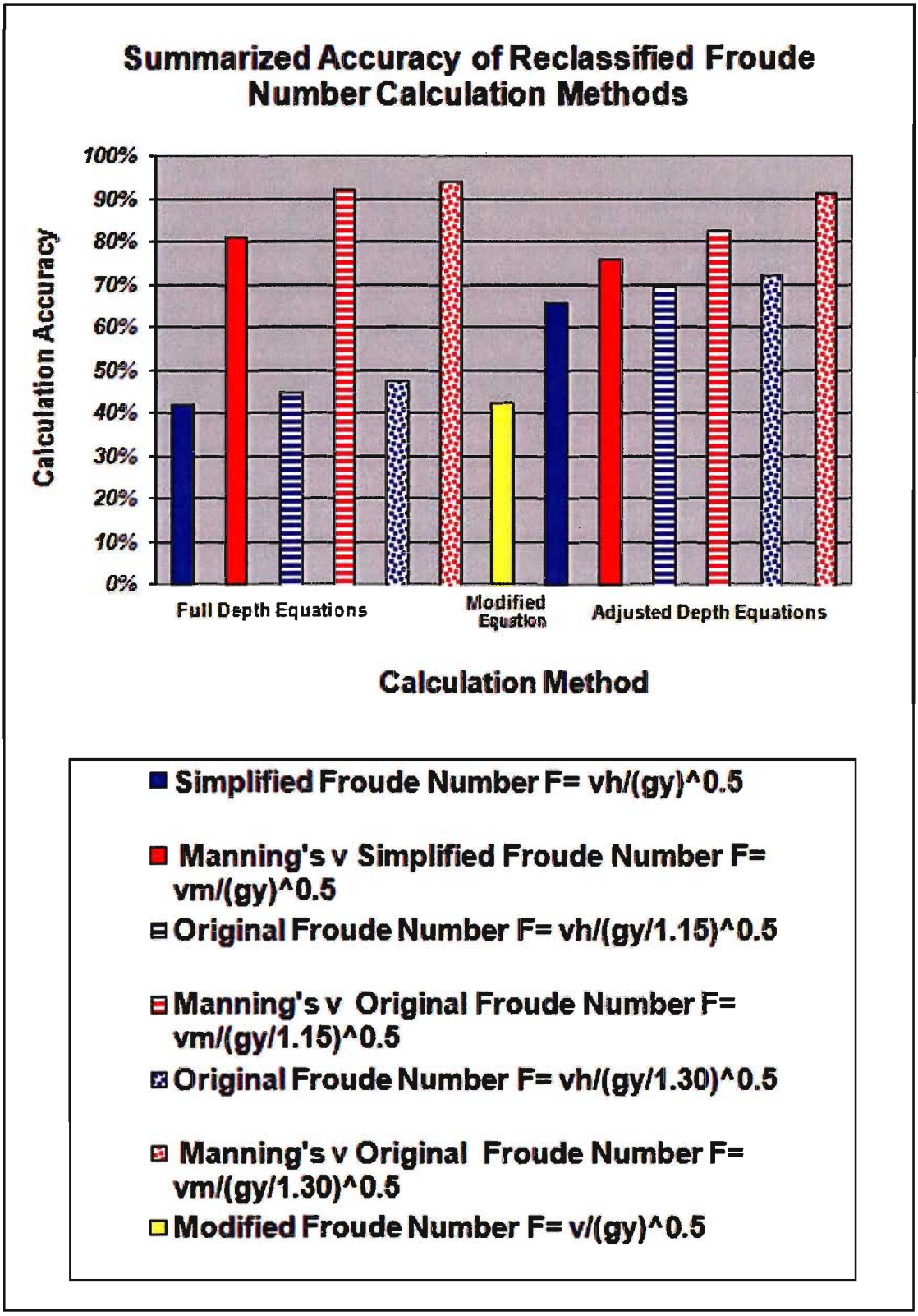

Figure 10. Summarized Accuracy of Reclassified Froude Number Calculation Methods

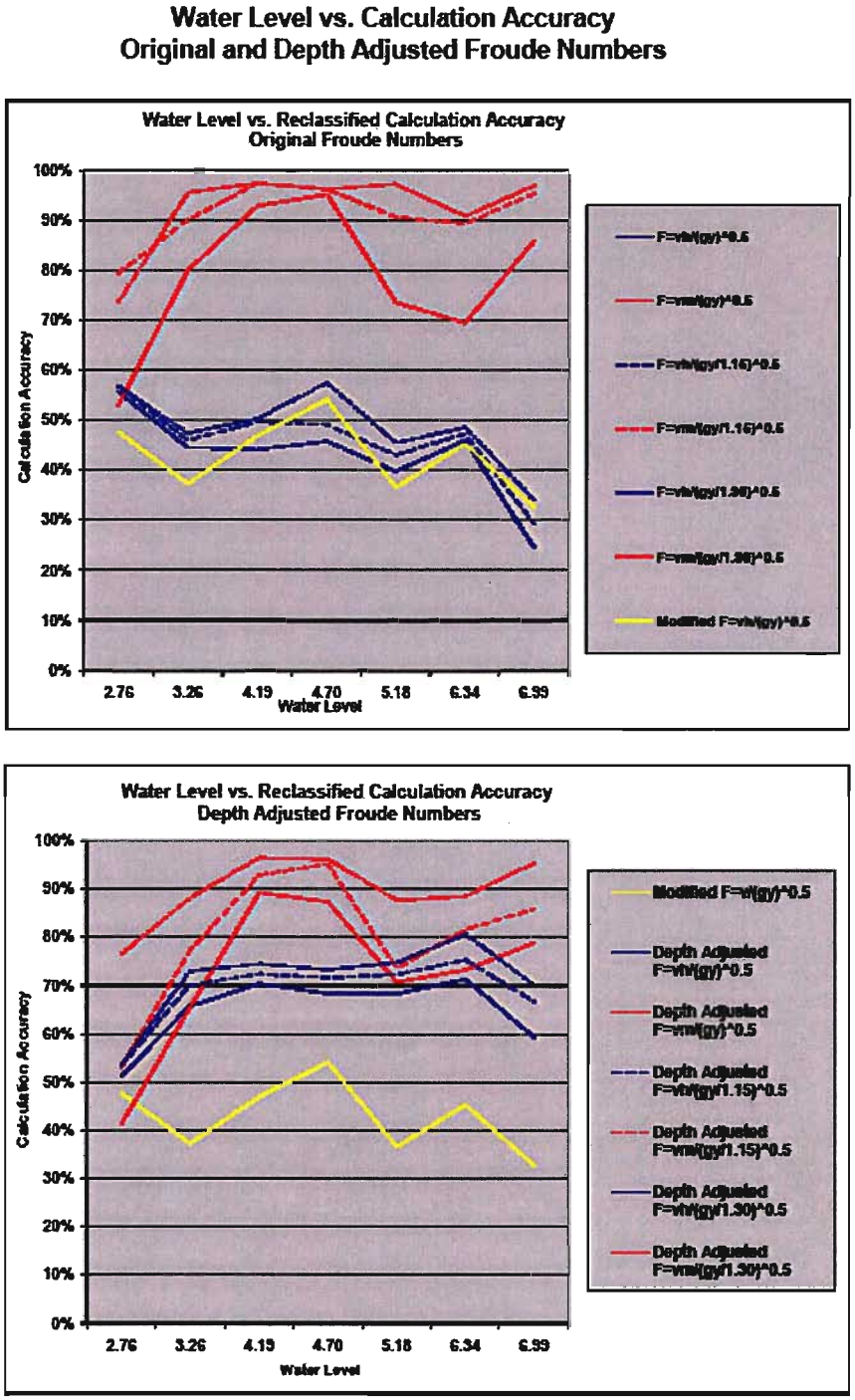

Figure 11. Water Level v. Reclassified Calculation Accuracy

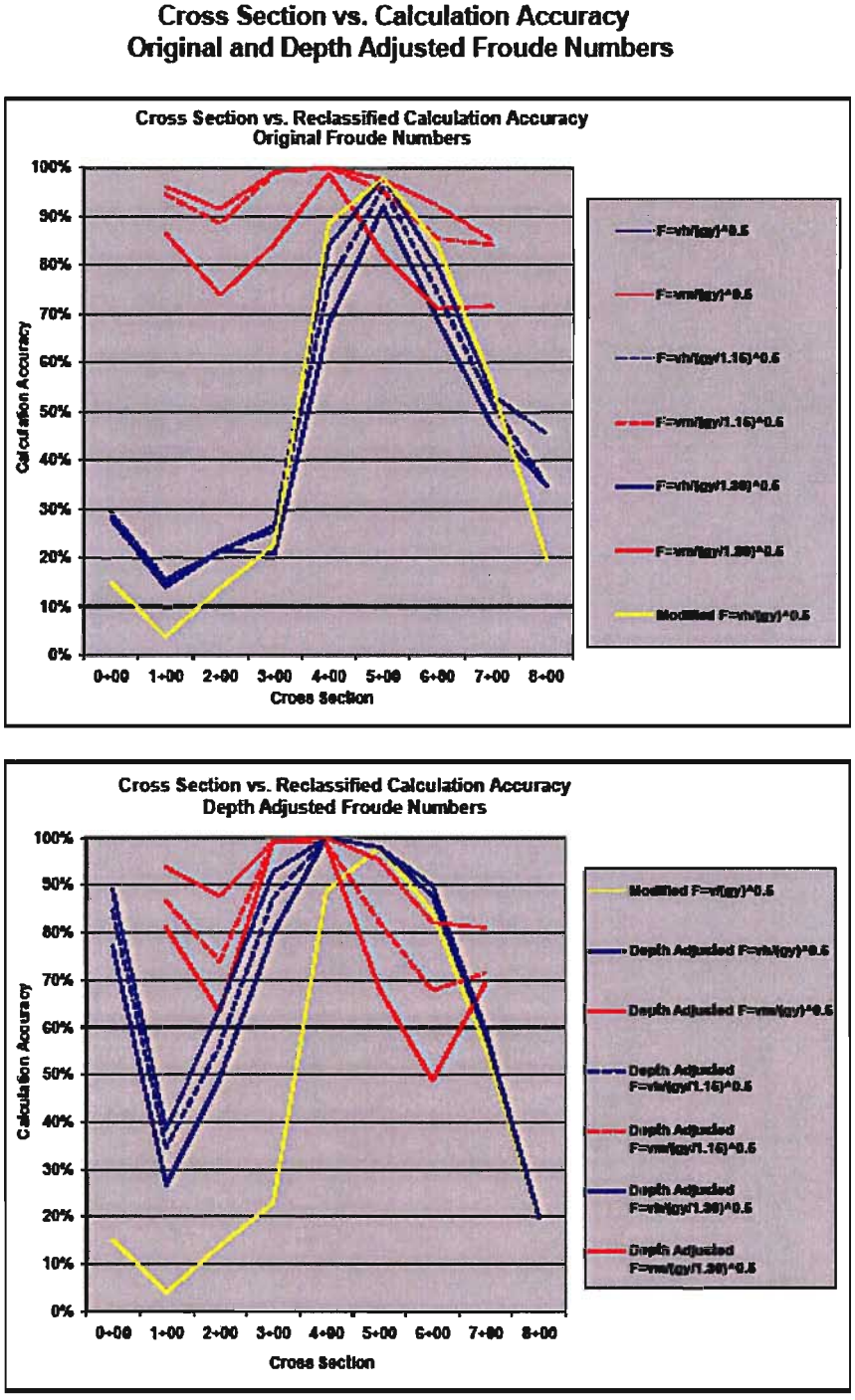

Figure 12. Cross Section v. Reclassified Calculation Accuracy

accurate revised result by cross section was 92% at cross section 5+00. The least accurate revised result by cross section was 14% at cross section 1+00.

4.2.1.2 Original Froude Equation with $\alpha = 1.15$

The revised overall accuracy of the Original Froude Equation with $\alpha = 1.15$,

$$Fr_h = v_h/(gy/1.15)^{0.5}$$

was 45%. The most accurate revised result by water level was 57% at water level 2.76. The least accurate revised result by water level was 29% at water level 6.99. The most accurate revised result by cross section was 96% at cross section 5+00. The least accurate revised result by cross section was 15% at cross section 1+00.

4.2.1.3 Original Froude Equation with $\alpha = 1.30$

The revised overall accuracy of the Original Froude Equation with $\alpha = 1.30$,

$$Fr_h = v_h/(gy/1.30)^{0.5}$$

was 48%. The most accurate revised result by water level was 58% at water level 4.70. The least accurate revised result by water level was 34% at water level 6.99. The most accurate revised result by cross section was 98% at cross section 5+00. The least accurate revised result by cross section was 16% at cross section 1+00.

4.2.2 Panel Froude Equation Accuracy

The revised overall accuracy of the Panel Froude Equation,

$$Fr_{pan} = v_{pan} /(gy)\text{^}0.5$$

was 43%. The most accurate revised result by water level was 54% at water level 4.70. The least accurate revised result by water level was 33% at water level 6.99. The most accurate revised result by cross section was 98% at cross section 5+00. The least accurate revised result by cross section was 4% at cross section 1+00.

4.2.3 Original Froude Equation Accuracy with v from Manning's Equation

4.2.3.1 Simplified Froude Equation with v from Manning's Equation

The revised overall accuracy of the Simplified Froude Equation with v from Manning's Equation,

$$F_{ms} = v_m /(gy)\text{^}0.5$$

was 81%. The most accurate revised result by water level was 95% at water level 4.70. The least accurate revised result by water level was 53% at water level 2.76. The most accurate revised result by cross section was 99% at cross section 4+00. The least accurate revised result by cross section was 71% at cross section 6+00.

4.2.3.2 Original Froude Equation with α =1.15 with v from Manning's Equation

The revised overall accuracy of the Original Froude Equation with α =1.15 with v from Manning's Equation,

$$F_m=v_m/(gy/1.15)^{0.5}$$

was 92%. The most accurate revised result by water level was 97% at water level 4.19. The least accurate revised result by water level was 79% at water level 2.76. The most accurate revised result by cross section was 100% at cross section 4+00. The least accurate revised result by cross section was 84% at cross section 7+00.

4.2.3.3 Original Froude Equation with α =1.30 with v from Manning's Equation

The revised overall accuracy of the Original Froude Equation with α =1.30 with v from Manning's Equation,

$$F_m=v_m/(gy/1.30)^{0.5}$$

was 94%. The most accurate revised result by water level was 97% at water levels 5.18 and 6.99. The least accurate revised result by water level was 74% at water level 2.76. The most accurate revised result by cross section was 100% at cross section 4+00. The least accurate revised result by cross section was 85% at cross section 7+00.

4.2.4 Adjustment for 0.66y

4.2.4.1 Adjusted Simplified Froude Equation

The revised overall accuracy of the Adjusted Simplified Froude Equation,

$$F_{hsa}=v_{ha}/(gy_a)^{0.5}$$

was 66%. The most accurate revised result by water level was 71% at water level 6.34. The least accurate revised result by water level was 51% at water level 2.76. The most accurate revised result by cross section was 100% at cross section 4+00. The least accurate revised result by cross section was 20% at cross section 8+00.

4.2.4.2 Adjusted Original Froude Equation with $\alpha = 1.15$

The revised overall accuracy of the Original Froude Equation with $\alpha = 1.15$,

$$Fr_{ha}=v_{ha}/(gy_a/1.15)^{0.5}$$

was 70%. The most accurate revised result by water level was 75% at water level 6.34. The least accurate revised result by water level was 53% at water level 2.76. The most accurate revised result by cross section was 100% at cross section 4+00. The least accurate revised result by cross section was 20% at cross section 8+00.

4.2.4.3 Adjusted Original Froude Equation with $\alpha = 1.30$

The revised overall accuracy of the Original Froude Equation with $\alpha = 1.30$,

$$Fr_{ha}=v_{ha}/(gy_a/1.30)^{0.5}$$

was 72%. The most accurate revised result by water level was 81% at water level 6.34. The least accurate revised result by water level was 53% at water level 2.76. The most accurate revised result by cross section was 100% at cross section 4+00. The least accurate revised result by cross section was 20% at cross section 8+00.

4.2.4.4 Adjusted Simplified Froude Equation with v from Manning's Equation

The revised overall accuracy of the Adjusted Simplified Froude Equation with v from Manning's Equation,

$$F_{msa}=v_{ma}/(gy_a)^{0.5}$$

was 76%. The most accurate revised result by water level was 89% at water level 4.19. The least accurate revised result by water level was 41% at water level 2.76. The most accurate revised result by cross section was 99% at cross sections 3+00 and 4+00. The least accurate revised result by cross section was 49% at cross section 6+00.

4.2.4.5 Adjusted Original Froude Equation with α =1.15 with v from Manning's Equation

The overall accuracy of the Original Froude Equation with α = 1.15 with v from Manning's Equation,

$$Fr_{ma}=v_{ma}/(gy_a/1.15)^{0.5}$$

was 83%. The most accurate result by water level was 95% at water level 4.70. The least accurate result by water level was 53% at water level 2.76. The most accurate result by cross section was 99% at cross sections 3+00 and 4+00. The least accurate result by cross section was 68% at cross section 6+00.

4.2.4.6 Adjusted Original Froude Equation with α =1.30 with v from Manning's Equation

The revised overall accuracy of the Original Froude Equation with α = 1.30 with v from Manning's Equation,

$$Fr_{ma}=v_{ma}/(gy_a/1.30)\text{^}0.5$$

was 91%. The most accurate revised result by water level was 97% at water levels 4.19, 5.18 and 6.99. The least accurate revised result by water level was 76% at water level 2.76. The most accurate revised result by cross section was 100% at cross section 4+00. The least accurate revised result by cross section was 81% at cross section 7+00.

4.3 Ancillary Calculations: Comparison of Results with Ideal Graphs

Based on overall accuracy of the varying calculation methods, calculations with data from water level 4.70, and the velocity coefficient set at α=1.30, were plotted in a series of graphs and compared with ideal results as illustrated in http://nptel.iitm.ac.in/courses/IIT-MADRAS/Hydraulics/pdfs/Unit8/8_1 (Figure 13). The results are shown for water level 4.70 in Figures 14 through 19, respectively, and

Figure below shows the variation of the specific energy as a function of depth when the discharge per unit width changes. when q increases the corresponding critical depths increase and the positive and negative limbs of the function move away from the origin. The opposite applies when q decreases. When q=0 the critical depth is equal to zero, the sub critical depth equals $E/\cos\theta$ and the supercritical depth (and the negative root) are equal to zero.

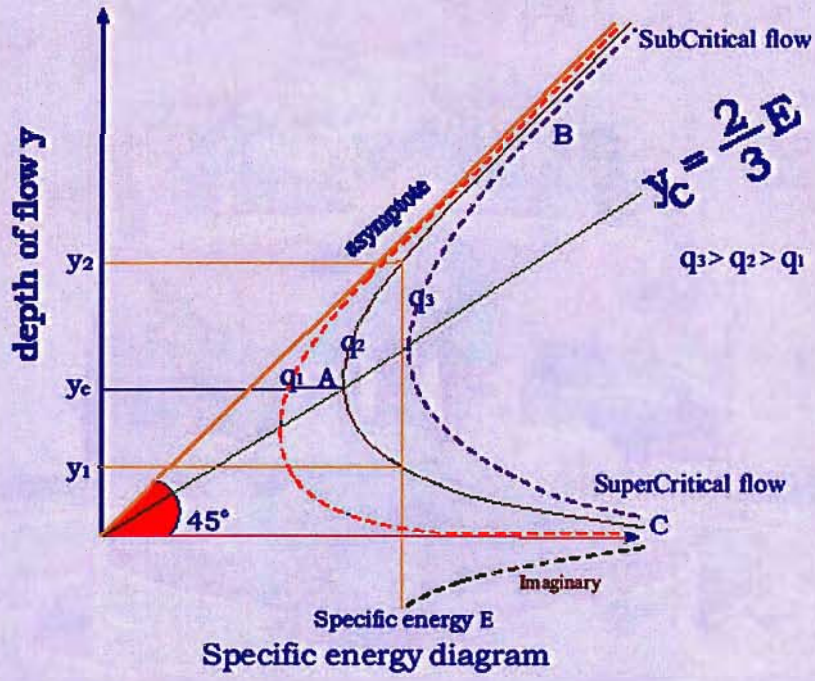

Specific energy diagram

The Specific energy curve is confined between two asymptotes namely y = E and y = 0. The first asymptote is at 45° with respect to abscissa. However, if the effect of the bed slope of the channel is considered the angel will be different from 45°.

For a given Q, specific energy curve has two limbs BA and AC.

Line BA represents Sub critical flow

Line AC represents Super critical flow

C represents Critical flow.

Figure 13. Specific Energy vs. Depth, from http://nptel.iitm.ac.in/courses/IIT-MADRAS/Hydraulics/pdfs/Unit8/8_1

discussed below. In Figures 14 through 19, the upper graph displays calculations with velocity derived from discharge data, v_h; the second graph displays calculations with velocity derived from Manning's Equation, v_m. In Figures 16 through 19, the third graph displays calculations with velocity derived from Manning's Equation, v_m, and revised with an alternative method of calculating discharge in each panel, as discussed in Section 4.3.4 below.

4.3.1 Specific Energy E v. Froude Number Fr

Regardless of depth, calculations with velocity derived from discharge, v_h, produce graphs (Figures 14 and 15) that closely mirror the ideal graph of Specific Energy E v. Depth y, found in Henderson (1966) and in http://nptel.iitm.ac.in/courses/IIT-MADRAS/Hydraulics/pdfs/Unit8/8_1.pdf, reproduced in Figure 13. As shown in Section 1.3.3.2 above, derivation of the Specific Energy Equation

$$E = y + v^2/2g$$

is based on the assumption of constant discharge across the entire section. Similarly, constant discharge per unit width, q, across the section is assumed during calculation of velocity derived from discharge,

$$v_h = q/y$$

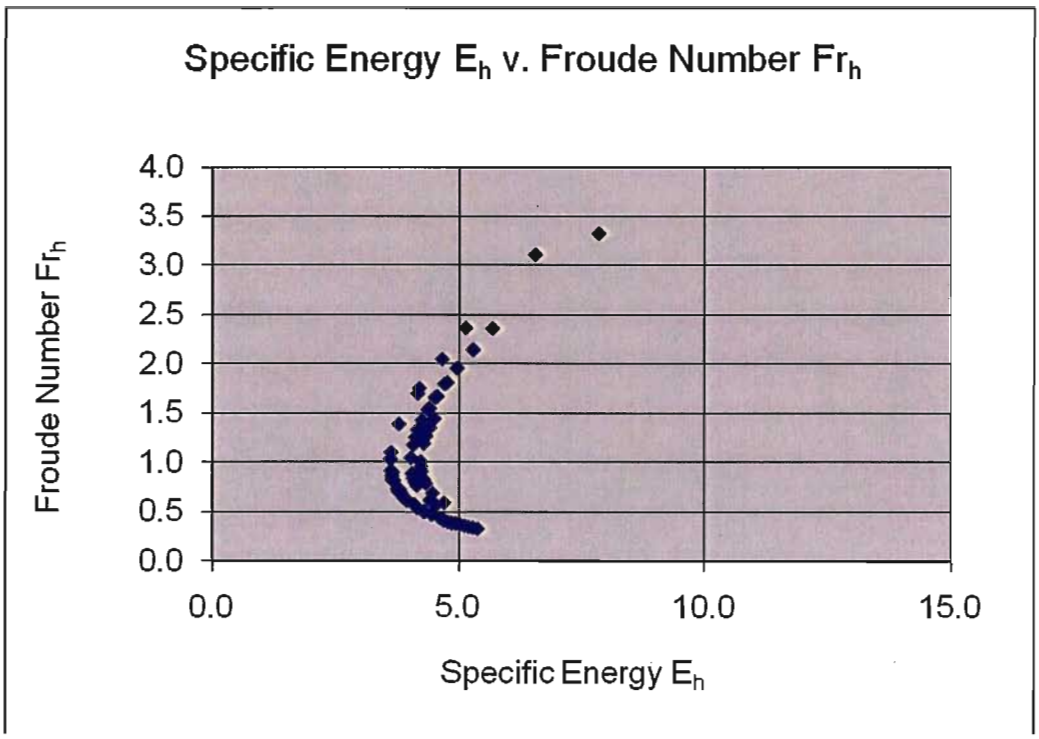

Velocity from discharge data

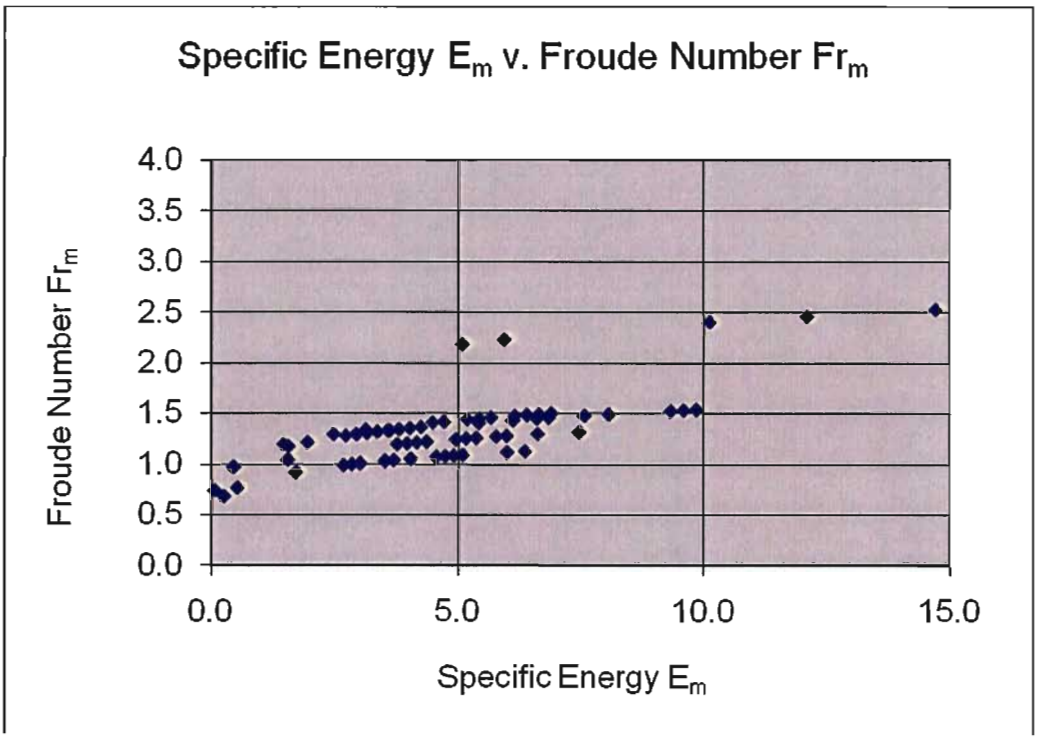

Velocity from Manning's Equation

Figure 14. Specific Energy v. Froude Number, full depth, water level 4.70

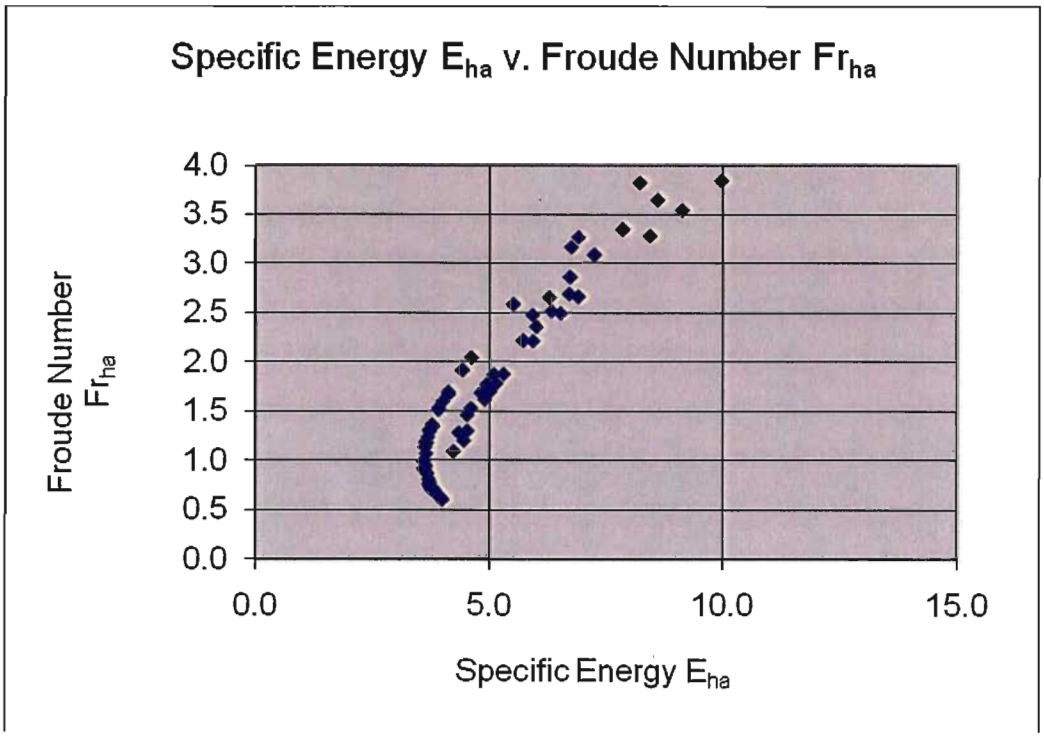

Velocity from discharge data

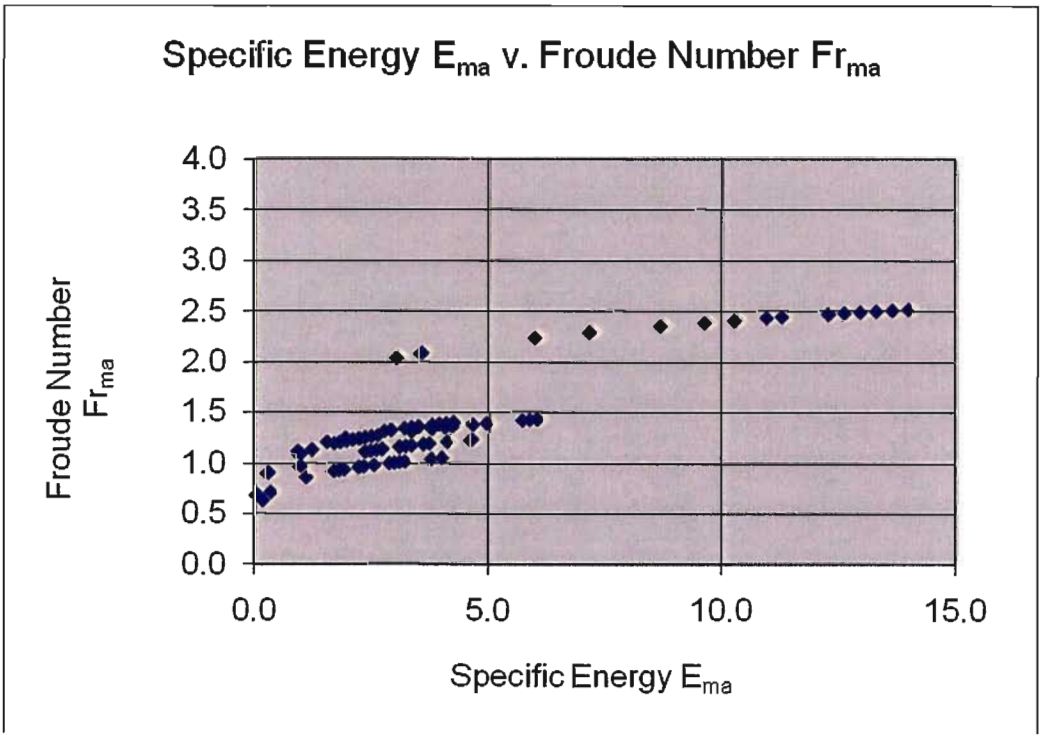

Velocity from Manning's Equation

Figure 15. Specific Energy v. Froude Number, adjusted depth, water level 4.70

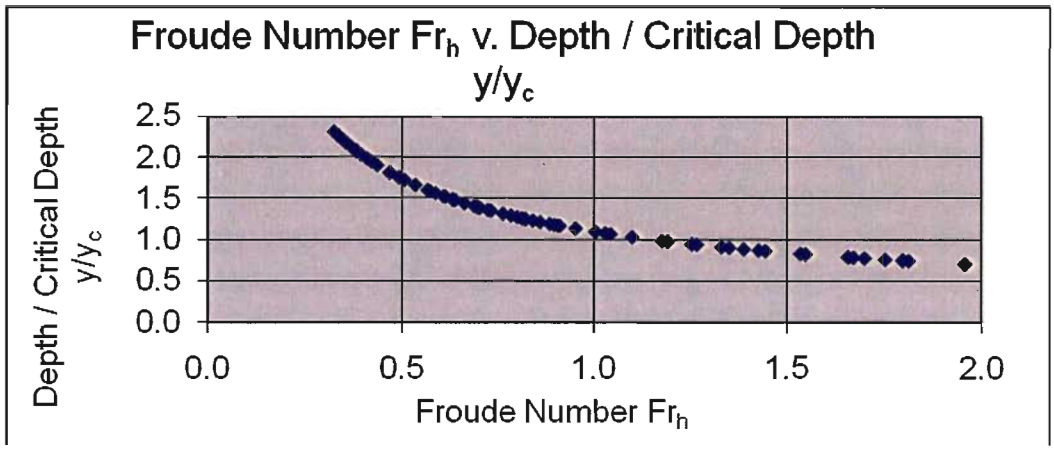

Velocity from discharge data

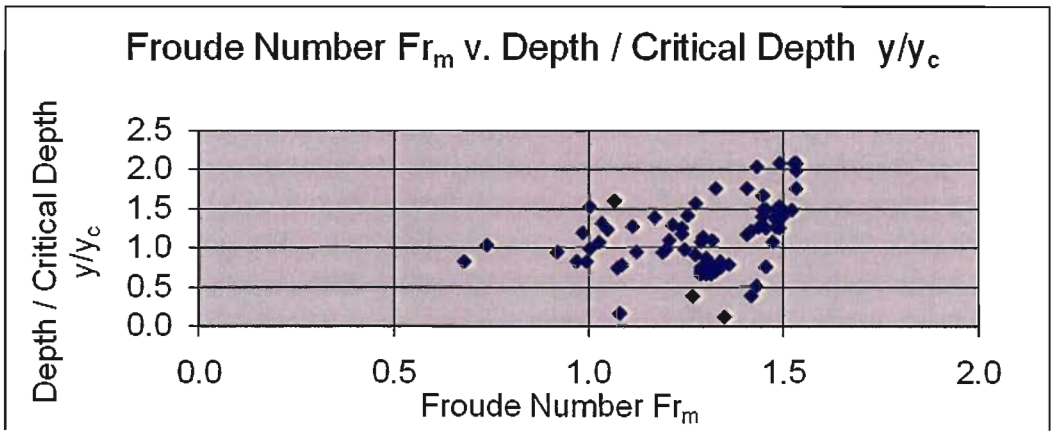

Velocity from Manning's Equation with $q=Q/b$

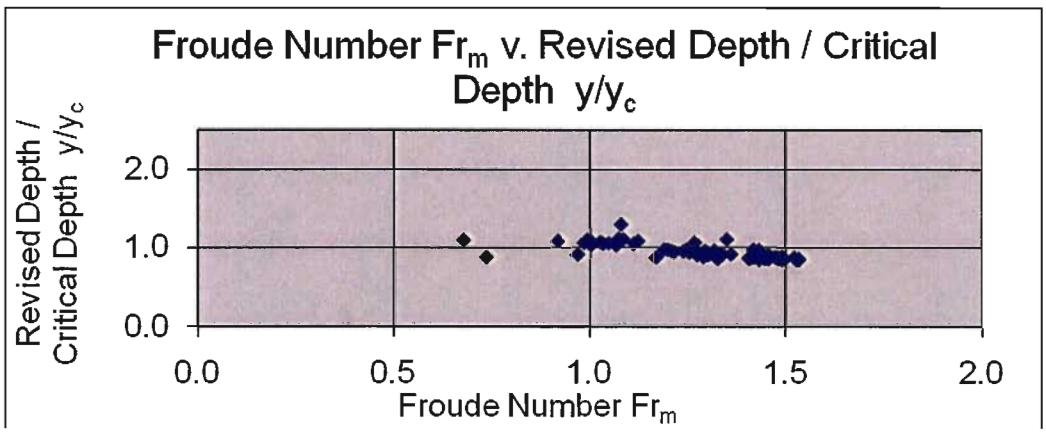

Velocity from Manning's Equation with $q=vy$

Figure 16. Froude Number v. Depth / Critical Depth, full depth, water level 4.70

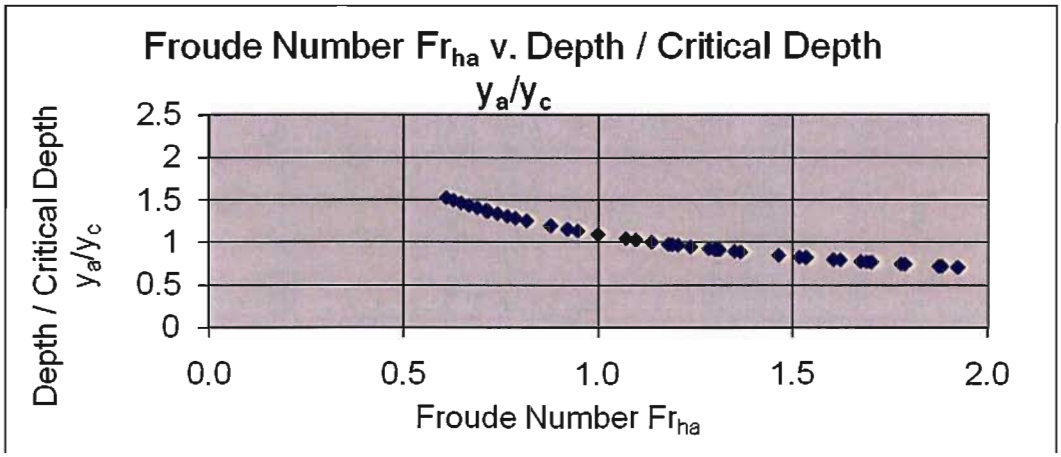

Velocity from discharge data

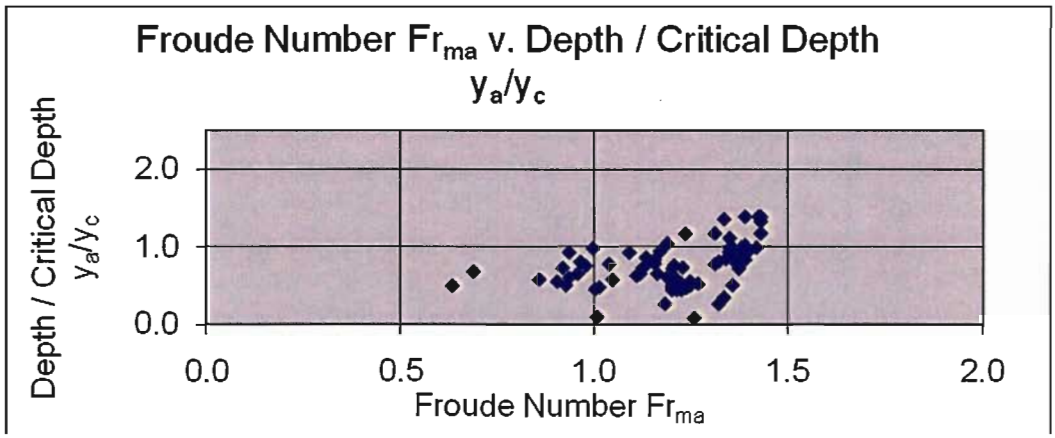

Velocity from Manning's Equation with $q=Q/b$

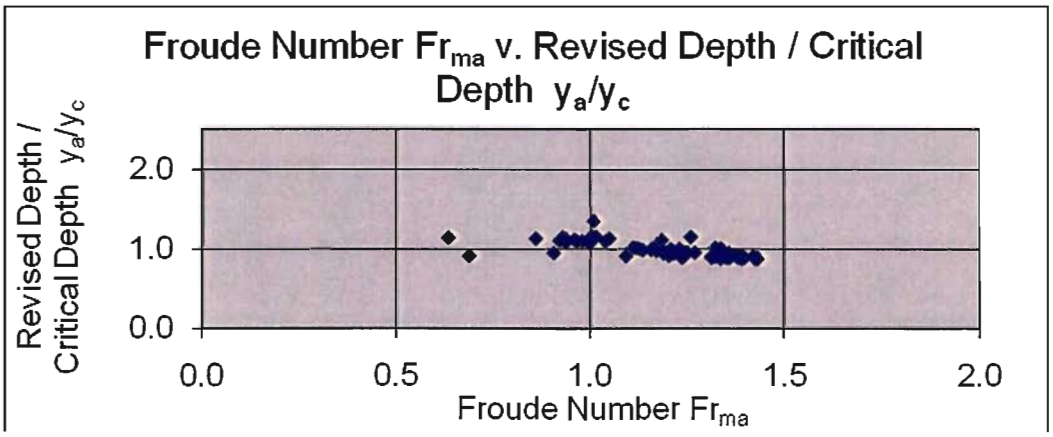

Velocity from Manning's Equation with $q=vy$

Figure 17. Froude Number v. Depth / Critical Depth, adjusted depth, water level 4.70

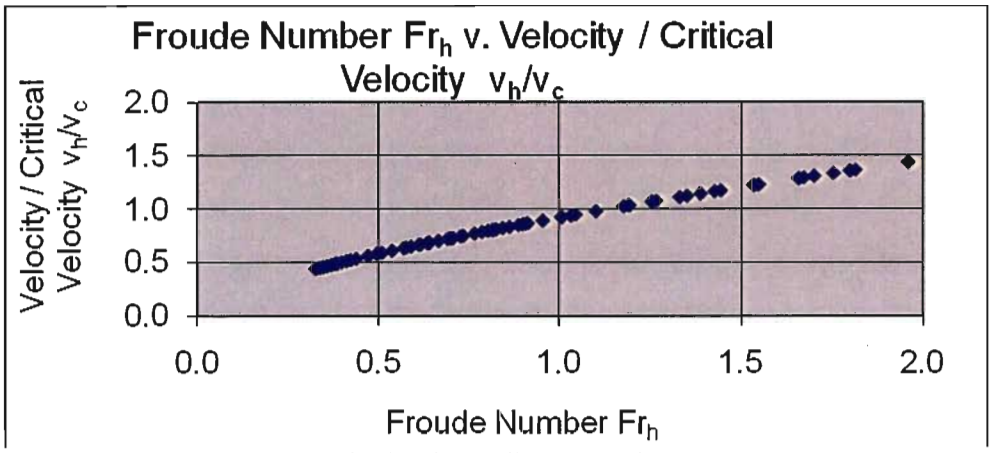

Velocity from discharge data

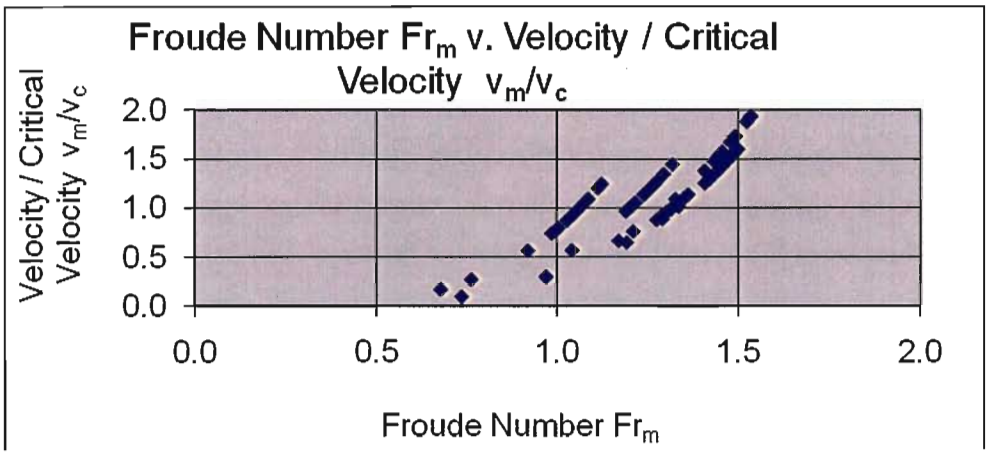

Velocity from Manning's Equation with $q=Q/b$

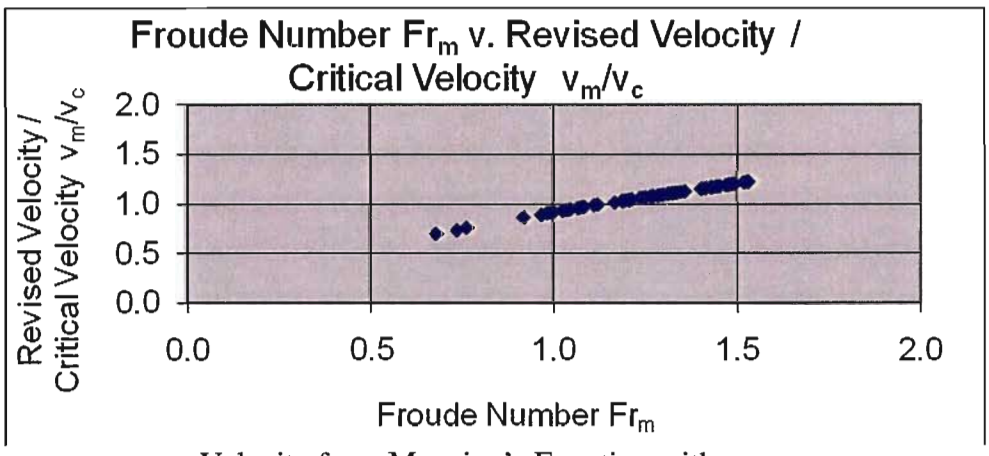

Velocity from Manning's Equation with $q=vy$

Figure 18. Froude Number v. Velocity / Critical Velocity, full depth, water level 4.70

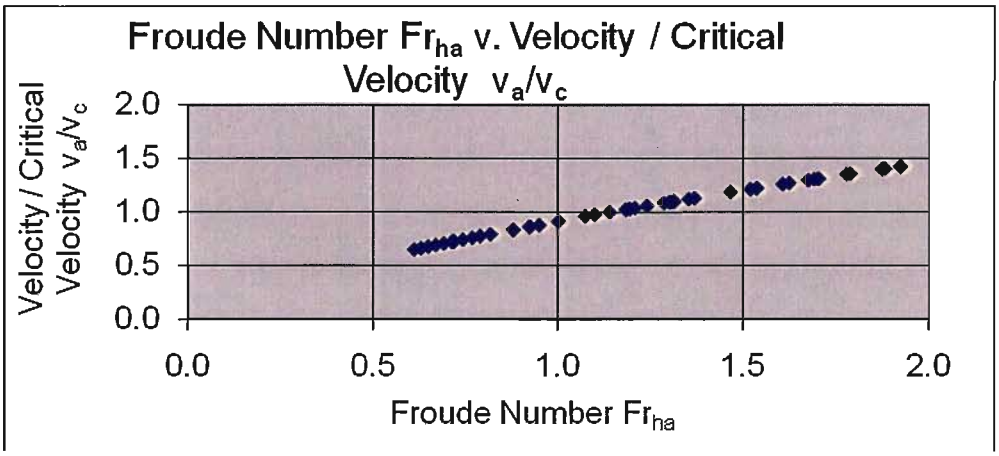

Velocity from discharge data

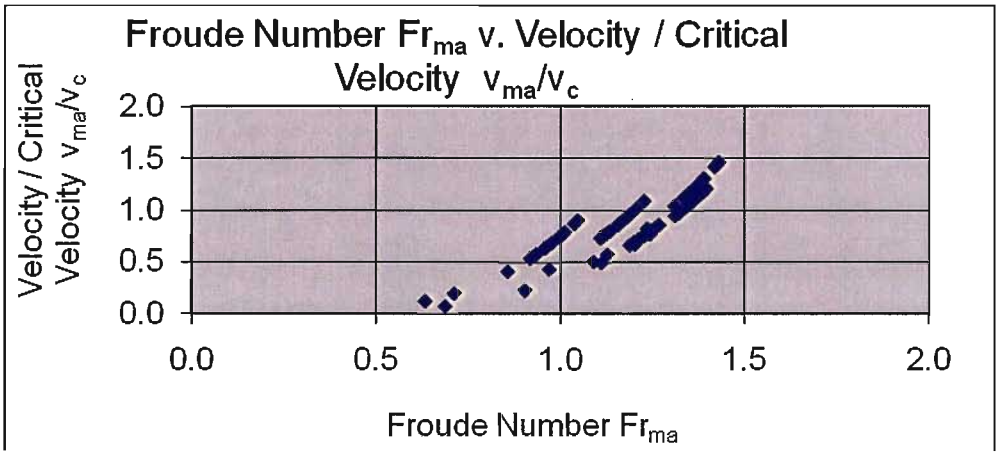

Velocity from Manning's Equation with $q=Q/b$

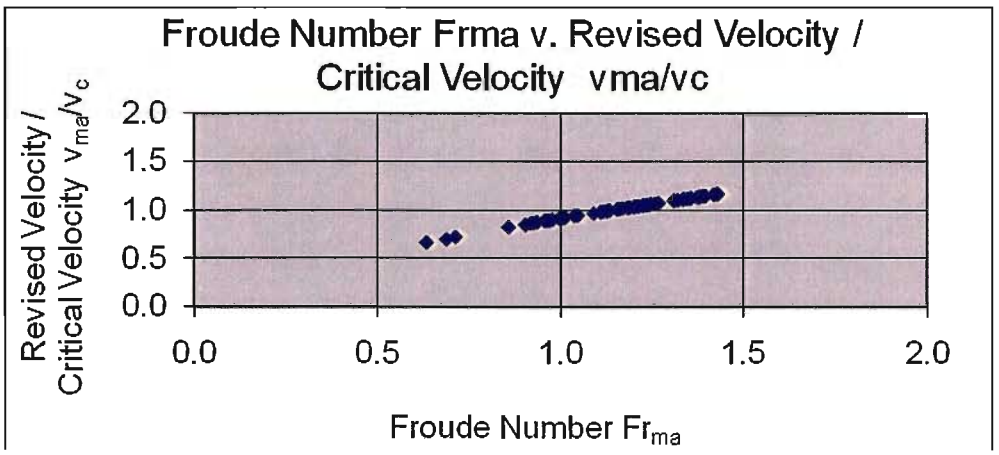

Velocity from Manning's Equation with $q=vy$

Figure 19. Froude Number v. Velocity/Critical Velocity, adjusted depth, water level 4.70

as shown in Section 1.3.3.5.1. To satisfy the assumption of constant discharge per unit width, calculated velocity must vary precisely with measured depth. Since Specific Energy E varies with the square of velocity, two values of Specific Energy E may be produced given a wide enough range of depth values. Although apparently mathematically consistent, the initial unrealistic assumption of constant discharge per unit width yields invalid predictions of flow conditions with fair accuracies of 58% at full depth to good accuracies of 73% at adjusted depth for water level 4.70 (Figure 11).

Regardless of depth, calculations with velocity derived from Manning's Equation, v_m, produce graphs that do not resemble the ideal graph found in http://nptel.iitm.ac.in/courses/IIT-MADRAS/Hydraulics/pdfs/Unit8/8_1.pdf. Without the limiting assumption of constant discharge per unit width, calculated velocity varies independently with depth, slope and bed roughness in Manning's Equation,

$$v_m = 1.49(y\text{^}0.67)(S\text{^}0.5)/n$$

as shown in Section 1.3.3.5.3 above. Freed from unrealistic assumptions, the resultant velocity and Froude Number values appear to yield valid predictions of flow conditions with excellent accuracies of 96% at full depth and 96% at the adjusted depth for water level 4.70 (Figure 11).

4.3.2 Froude Number Fr v. Depth / Critical Depth y/y_c

Regardless of depth, calculations with velocity derived from discharge, v_h, produce very similar graphs (Figures 16 and 17). As shown in Section 1.3.3.5 above, constant

discharge per unit width, q, across the section is assumed during calculation of velocity derived from discharge,

$$v_h = q/y$$

Similarly, the calculation of critical depth, y_c, also assumes constant discharge per unit width,

$$y_c = (q^2/g)^{0.33}$$

Since critical depth, y_c, remains constant across the section, the ratio y/y_c varies directly with the value of depth, y. However, velocity, v_h, varies inversely with depth, y. The value of the subsequently calculated Froude Number,

$$Fr_h = v_h/(gy/1.30)^{0.5}$$

also varies inversely with depth y. Therefore, an inverse linear relationship exists between Froude Number Fr_h and the ratio Depth / Critical Depth y/y_c, regardless of the use of the full or adjusted depth, as shown in Figures 16 and 17.

Although apparently mathematically consistent, the initial unrealistic assumption of constant discharge per unit width yields invalid results.

Regardless of depth, calculations with velocity derived from Manning's Equation, v_m, produce graphs that are meaningless (Figures 16 and 17). A Froude Number Fr_m calculated from the independently derived velocity cannot be logically compared with a critical depth value derived with the limiting assumption of constant discharge per unit width.

4.3.3 Froude Number *Fr* v. Velocity / Critical Velocity v/v_c

Regardless of depth, calculations with velocity derived from discharge, v_h, produce very similar graphs (Figures 18 and 19). As shown in Section 1.3.3.5 above, constant discharge per unit width, q, across the section is assumed during calculation of velocity derived from discharge,

$$v_h = q/y$$

Similarly, the calculation of critical depth, y_c, also assumes constant discharge per unit width,

$$y_c = (q\text{^}2/g)\text{^}0.33$$

Critical velocity, v_c, varies directly with critical depth, y_c,

$$v_c = (gy_c)\text{^}0.5$$

Since critical depth, y_c, and thus critical velocity, v_c, remain constant across the section, the ratio v/v_c varies directly with the value of velocity, v. The value of the subsequently calculated Froude Number,

$$Fr_h = v_h/(gy/1.30)\text{^}0.5$$

also varies directly with velocity v. Therefore, a direct linear relationship exists between Froude Number Fr_h and the ratio Velocity / Critical Velocity v/v_c, regardless of the use of the full or adjusted depth, as shown in Figures 18 and 19.

Although apparently mathematically consistent, the initial unrealistic assumption of constant discharge per unit width yields invalid results.

Regardless of depth, calculations with velocity derived from Manning's Equation, v_m, produce graphs that are meaningless (Figures 18 and 19). A Froude Number Fr_m calculated from the independently derived velocity cannot be logically compared with a critical velocity value derived with the limiting assumption of constant discharge per unit width.

4.4 Suggested Revisions to Ancillary Calculations

To reconcile the inconsistencies between independently calculated velocities derived from Manning's Equation and the accepted method of derivation of critical depths and critical velocities based on the assumption of constant discharge per unit width, discharge at each panel was calculated as

$$q_n = v_m y$$

where q_n = discharge at panel n

v_m = Manning's velocity at panel n

y = measured water depth at panel n.

Revised discharge per panel, q_n, was then substituted into the equation for critical depth at each panel

$$y_c = (q_n\text{^}2/g)\text{^}0.33$$

The revised values of critical depths were then substituted into the equation for critical velocity at each panel

$$v_c = (gy_c)\text{^}0.5$$

The ratios Depth / Critical Depth y/y_c and Velocity / Critical Velocity v/v_c at each panel were recalculated (Digital Appendix III) and plotted against the previously calculated Froude Number Fr_m. The results are shown in the bottom graphs in Figures 16 through 19.

4.4.1 Revised Froude Number Fr_m v. Depth / Critical Depth y/y_c

While exhibiting some data scatter, both the full depth and adjusted depth calculations show an inverse linear relationship between the Froude Number Fr_m and the ratio of Depth / Critical Depth y/y_c, similar to the relationship found in Section 4.3.2 above with calculations based on assumptions of constant discharge per unit width (Figures 16 and 17). Even though critical depth, y_c, does not remain constant across the section, the ratio y/y_c still varies directly with depth, y, in each panel. The value of the calculated Froude Number,

$$Fr_m = v_m/(gy/1.30)\text{^}0.5$$

varies inversely with depth y. Therefore, an inverse linear relationship exists between Froude Number Fr_m and the ratio Depth / Critical Depth y/y_c, regardless of the use of the full or adjusted depth. The data scatter could be attributed to imprecise survey of the bedrock in the upper several cross sections.

4.4.2 Revised Froude Number Fr_m v. Velocity / Critical Velocity v/v_c

Both the full depth and adjusted depth calculations show a linear relationship between the

Froude Number Fr_m and the ratio of Velocity / Critical Velocity v/v_c, very similar to the relationship found in Section 4.3.3 above (Figures 18 and 19). Velocity, v, varies directly with depth,

$$v_m = 1.49(y\text{^}0.67)(S\text{^}0.5)/n$$

Critical depth, y_c, also varies directly with depth,

$$y_c = (q_n\text{^}2/g)\text{^}0.33 = ((v_m y)\ \text{^}2/g)\text{^}0.33$$

Critical velocity, v_c, varies directly with critical depth, y_c,

$$v_c = (gy_c)\text{^}0.5$$

and thus with depth, y. Even though critical depth, y_c, and therefore critical velocity, v_c, do not remain constant across the section, the ratio v/v_c still varies directly with velocity, v, in each panel because both velocity, v, and critical velocity, v_c, vary directly with depth, y. The value of the calculated Froude Number,

$$Fr_m = v_m/(gy/1.30)\text{^}0.5$$

also varies directly with velocity v_m. Therefore, a linear relationship exists between Froude Number Fr_m and the ratio Velocity / Critical Velocity v/v_c, regardless of the use of the full or adjusted depth.

4.4.3 Summation of Panel Discharge Calculations

To check the validity of the calculation of individual panel discharge values, the discharge values of each panel within a cross section were summed, multiplied by the panel width (10 feet) to obtain a calculated total discharge value for each cross section

and compared with the measured discharge value recorded by USGS Stream Gage 04213500 for water levels 4.70 and 6.34 (Figure 20).

$$Q_{cal}=(\sum q_n)b_i$$

where Q_{cal} = calculated discharge

$\sum q_n$ = summation of discharge values of each panel

b_i = panel width

Cross Sections 0+00 and 8+00 were excluded from each water level because slope, hence Manning's velocity, was not determined beyond the upper and lower limits of the study reach. Cross Section 4+00 at water level 4.70 was excluded because no photo was recorded at the time of measurement.

The stream maintained a steady discharge value of 3470 cfs through the data collection period for the 4.70 event. However, the stream rose significantly during data collection for the 6.34 event. Discharge at the stream gage was recorded at the beginning and end of data collection. For the 6.34 event, the initial discharge value of 6780 cfs was assigned to Cross Sections 0+00 through 2+00. The final discharge value of 7520 cfs was assigned to Cross Sections 6+00 through 8+00. An intermediate discharge value of 7070 cfs was assigned to Cross Sections 3+00 through 5+00. The tabulated results, in cfs, are shown below.

Water level	Measured Discharge Gage (cfs)	Calculated Discharge 1+00 (cfs)	Calculated Discharge 2+00 (cfs)	Calculated Discharge 3+00 (cfs)	Calculated Discharge 4+00 (cfs)	Calculated Discharge 5+00 (cfs)	Calculated Discharge 6+00 (cfs)	Calculated Discharge 7+00 (cfs)
4.7	3470	18755	8669	5115		2423	3326	4056
6.34	6780	15800	12138					
6.34	7070			21771	11484	7028		
6.34	7520						7517	8122

Table 2. Measured v. Calculated Discharge at Water Levels 4.70 and 6.34

Results at both water levels indicate poor correlation between calculated and measured discharge values at Cross Sections 1+00 through 4+00 and good to excellent correlation at Cross Sections 5+00 through 7+00 (Figure 20).

The calculated discharge values for the upstream cross sections all significantly exceed the measured discharge values. Conversely, the calculated discharge values for the downstream cross sections reasonably match the measured discharge values. Similar results between the two water levels suggest that changing discharge values during the 6.34 event did not seriously impact data collection and the subsequent calculations. Instead, it is suggested that the lack of inter-channel high area details during initial streambed surveys of the upstream cross sections result in overly high water depth values for many panels. Since individual panel discharge values, q, vary directly with depth, y,

$$q_n = v_m y$$

panel discharge values across the upper cross sections are erroneously high, resulting in erroneously high total calculated discharge values. Conversely, good streambed details for the downstream cross sections yield more accurate water depths, and subsequently more accurate total calculated discharge values.

Further investigation, under controlled conditions, is warranted to verify the validity of panel discharge values. Acceptable correlation between measured discharge values and calculated total discharge values, based on panel discharge values derived from Manning's velocity and measured depths, would suggest that Froude Numbers similarly derived from Manning's velocity and measured depths would be valid.

Comparison of Measured v. Calculated Discharge Values at Two Water Levels

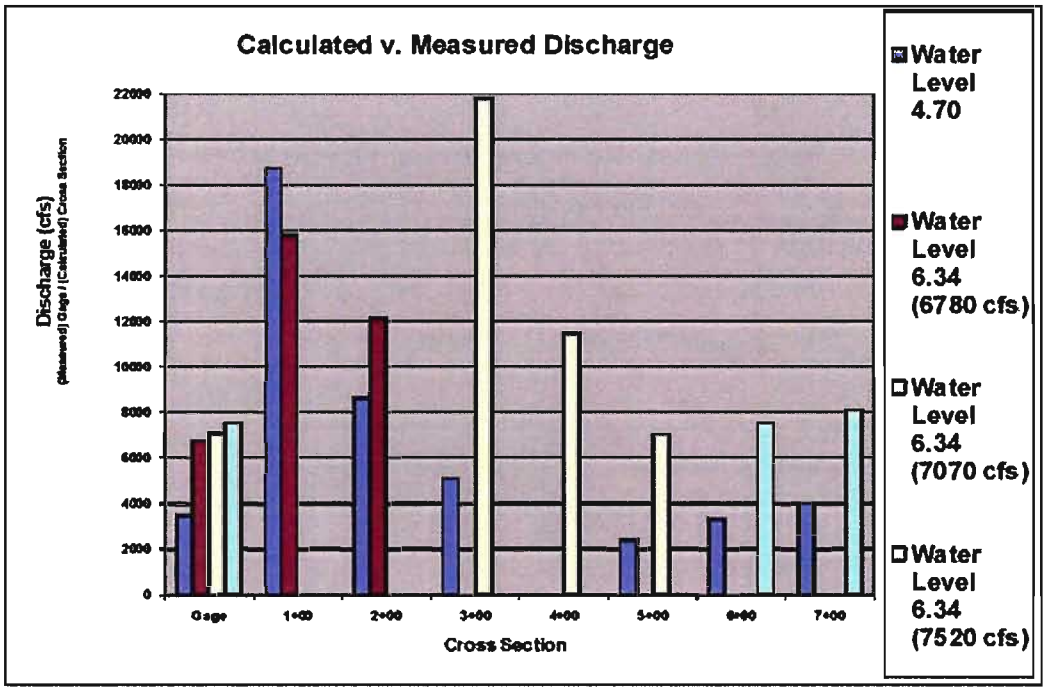

Water level	Measured Discharge Gage (cfs)	Calculated Discharge 1+00 (cfs)	Calculated Discharge 2+00 (cfs)	Calculated Discharge 3+00 (cfs)	Calculated Discharge 4+00 (cfs)	Calculated Discharge 5+00 (cfs)	Calculated Discharge 6+00 (cfs)	Calculated Discharge 7+00 (cfs)
4.7	3470	16755	8669	5115		2423	3326	4056
6.34	6780	15800	12136					
6.34	7070			21771	11484	7028		
6.34	7520						7517	8122

Discharge Measured at USGS Gage No. 04213500

Discharge Calculated as sum of (discharge in each panel X width of panel)

Figure. 20. Calculated v. Measured Discharge

4.5 Comparison of Accuracies Among Results

The following general observations come from comparison of overall accuracies among the various methods of Froude Number calculation when critical flow is reclassified as $F=0.84$ and supercritical flow is defined as $Fr>0.84$ (Figure 10).

1. Velocities derived from Manning's Equation produced more accurate Froude Numbers than velocities derived from discharge data.
2. Accuracy increased with increasing velocity coefficient.
3. Depth adjustment for possible vertical shearing within the panels significantly increased the accuracy of Froude Numbers derived from discharge data.
4. Depth adjustment for possible vertical shearing within the panels slightly decreased the accuracy of Froude Numbers derived from Manning's Equation.

4.5.1 Comparison of Results by Water Level

The following observations come from comparison of accuracies among the various methods of Froude Number calculation by water level (Figure 11).

1) Water level 2.76 yielded the least accurate results for Froude Numbers derived from Manning's Equation at both full and adjusted water depths, possibly due to a greater influence of streambed roughness, n, than assumed in the calculations.
2) Water level 6.99 yields the least accurate results for Froude Numbers derived from discharge data at full depth, Fr_h, possibly due to the suppressed velocities and

subsequent Froude Numbers that vary inversely with water depth (see Section 4.3.2 above). Accuracy increases significantly at water level 6.99 for Froude Numbers derived from discharge data at adjusted depth, Fr_{ha} in comparison with Froude Numbers derived from discharge data at full depth, Fr_h.

3) Similarly, accuracy increases significantly at all water levels higher than 2.76 for Froude Numbers derived from discharge data at adjusted depth, Fr_{ha}, suggesting that the inverse relationship between velocity and depth, required to maintain the assumption of constant discharge per unit width, produces erroneously low velocities, in agreement with the results of Richardson and Carling (2006). The adjusted depths allow for increased velocities and subsequently increased Froude Numbers that more accurately predict observed supercritical flow. The adjusted depths could also more accurately account for possible vertical shearing in the panels.
4) Accuracy decreases slightly at water level 2.76 for Froude Numbers derived from discharge data at adjusted depth, Fr_{ha}, possibly due to the lack of vertical shearing in the water column at shallow depth.
5) Accuracy decreases slightly at all water levels for most Froude Numbers derived from Manning's Equation at adjusted depth, Fr_{ma}, possibly due to the ubiquitous application of adjusted depth values. Since velocity derived from Manning's Equation varies directly with depth,

$$v_m = 1.49(y\text{^}0.67)(S\text{^}0.5)/n$$

the subsequent Froude Number also varies directly with depth. Full depth Froude Number values near the subcritical/supercritical interface at $Fr = 0.84$ may become erroneously suppressed at adjusted depths. Blanket application of depth adjustments

could assume vertical shearing in non-shearing panels. Further investigation, under controlled conditions, of minimum depth for shearing and likely shearing panel locations, such as the thalweg, may shed light on this matter. The significant decrease in accuracy at water level 5.18 and recovery of accuracy at water level 6.99 for both full and adjusted depths might indicate the shearing/non-shearing interface water depth range for the study area. Alternatively, ubiquitous supercritical flow throughout the reach might suppress velocity differences between central and flanking flow (minimal eddies) and inhibit creation of vertically separated flow.

4.5.2 Comparison of Results by Cross Section

The following observations come from comparison of accuracies among the various methods of Froude Number calculation by cross section (Figure 12).

1) Accuracy increases significantly for Froude Numbers derived from discharge data when depth is adjusted, Fr_{ha}, in comparison with full depth calculations, at Cross Sections 0+00 through 3+00, possibly due to erroneously low Froude Numbers calculated at full depth that result from the lack of inter-channel high area details during initial streambed surveys of the upper cross sections. Water depth adjustment at Cross Section 1+00 may not raise the resultant Froude Numbers enough to compensate for the survey inaccuracies as efficiently as at the other cross sections.

2) Accuracy increases significantly for Froude Numbers derived from discharge data when depth is adjusted, Fr_{ha}, at Cross Section 6+00, possibly due to vertical shearing in the panels.

3) Accuracy decreases significantly for Froude Numbers derived from discharge data with both full and adjusted depths at Cross Section 7+00 at water levels 2.76 through 6.34, possibly due to the presence of a hydraulic jump over a pool immediately downstream of a shelf very near the cross section. Since hydraulic jumps can oscillate upstream and downstream through time (Tinkler, 1997b), water depth, and thus Froude Number, can also oscillate, rendering accurate prediction of flow condition very difficult. At water level 6.99, the hydraulic jump has washed out. However, lack of accurate right bank water edge location data prohibits subsequent Froude Number calculations.

4) Accuracy continues to decrease significantly for Froude Numbers derived from discharge data with both full and adjusted depths at Cross Section 8+00 at water levels 2.76 through 5.18, possibly due to the presence of a widening thalweg and adjacent shallow water eddies. Deeper water in the thalweg would result in suppressed Froude Numbers derived from discharge data. The eddies cannot be predicted by simple cross sections without upstream and downstream data. Therefore, based simply on water depth and the assumption of constant discharge per stream width, erroneously high Froude Numbers are predicted for the eddies. At water levels 6.34 and 6.99, lack of accurate right bank water edge location data prohibits subsequent Froude Number calculations.

5) Accuracy decreases for Froude Numbers derived from Manning's Equation with both full and adjusted depths at Cross Section 2+00, possibly due to the presence of transitional waves here classified as supercritical flow, based on the appearance of

diagonal waves and downstream hydraulic jumps. Froude Number values hover near the subcritical/supercritical interface at $Fr = 0.84$ at water levels 2.76, 3.26, 6.34 and 6.99. More accurate streambed details and refinement of flow condition classifications may increase accuracy.

6) Accuracy decreases for Froude Numbers derived from Manning's Equation with both full and adjusted depths at Cross Section 6+00, possibly due to the presence of a hydraulic jump and very shallow water along the sloping stream banks. Since hydraulic jumps can oscillate upstream and downstream through time, water depth, and thus Froude Number, can also oscillate, rendering accurate prediction of flow condition very difficult. Very shallow water along the sloping stream banks results in low Froude Numbers derived from Manning's Equation, in contradiction to observed diagonal waves that suggest supercritical flow conditions.

7) Accuracy remains depressed for Froude Numbers derived from Manning's Equation with both full and adjusted depths at Cross Section 7+00, possibly due to the presence of a hydraulic jump over a pool immediately downstream of a shelf very near the cross section. Since hydraulic jumps can oscillate upstream and downstream through time, water depth, and thus Froude Number, can also oscillate, rendering accurate prediction of flow condition very difficult.

4.6 Presentation of Preferred Calculations as Froude Maps

Based on the above accuracy analysis, Froude Numbers that result from the calculations that utilized full depth measurements, velocities derived from Manning's Equation and a

velocity coefficient set at $\alpha = 1.30$ are plotted on plan view maps of the study reach at each water level (Appendix IV). Subcritical Froude Numbers are plotted in blue. Critical Froude Numbers are plotted in green. Supercritical Froude Numbers are plotted in red.

In general, the maps show that supercritical flow occurs throughout the study reach at all measured water levels with isolated pockets of subcritical or critical flow. Variations in calculated Froude Number values with changing water levels at each cross section mimic observed water surface variations recorded via photographs during data collection. Although not common (Trieste, 1992; Grant, 1997), sustained supercritical flow throughout the 800 foot long study reach over two orders of magnitude of discharge levels is similar to conditions observed upstream, in the left channel of naturally occurring Refrigerator Island rapids in Zoar Valley Gorge (Appendix I).

4.6.1 Froude Number Contour Maps

Appendix V contains a series of Froude Number Contour Maps for each water level. In general, the maps show relatively constant Froude Numbers across most of each section, but a sinusoidal pattern of rising and falling Froude Numbers in the downstream direction. Photos of each entire water level event also appear in Appendix V for correlation with the graphs. Figure 21 shows the progressive changes in Froude Number values in the thalweg at each cross section at each water level. Further investigation is warranted to explore the causes of the sinusoidal pattern.

4.6.2 Changes in Froude Numbers with Increasing Water Levels

Froude Numbers at each panel were plotted against water level for each cross section (Appendix VI). Photos of each cross section at each water level also appear in Appendix 6 for correlation with the graphs. The following general observations were noted.

1) Calculated Froude Number values between 0.8 and 1.1 correlate well with observed transitional flow, defined as the first appearance of small diagonal waves.
2) Calculated Froude Numbers tend to group near transitional flow values or well into the range of supercritical flow.
3) Calculated Froude Numbers tend to move from transitional to supercritical flow as water level increases, then back to transitional flow at the highest water levels. The corresponding photographs accurately record flow state changes from transitional flow to supercritical flow, then back toward transitional flow. The tendency of flow to become supercritical with increasing discharge agrees with observations by Tinkler (1997a) of a rockbed stream in Ontario, Canada. The tendency of Froude Numbers in supercritical flow to decrease with increasing discharge agrees with mathematical models of sloping bedrock reaches in California, USA, as reported by Valle and Pasternack (2006).
4) Minor streambed irregularities tend to toward insignificance as water levels increase.

5) At all water levels, calculated Froude Number values near the edges of the stream drop off dramatically, probably due to the decrease in water depth and subsequent mathematical influence on calculation of velocities and Froude Numbers for those panels.
6) Observed hydraulic jumps correlate with transitional to supercritical Froude Number values. The migratory nature of hydraulic jumps upstream or downstream of the sections may result in fluctuating Froude Number values as water levels change.

Individual cross section results are discussed in the following sections.

4.6.2.1 Cross Section 0+00

Since the study reach starts at Cross Section 0+00, no upgradient slope data is available for derivation of velocity from Manning's Equation. Therefore, no Froude Numbers are calculated for analysis.

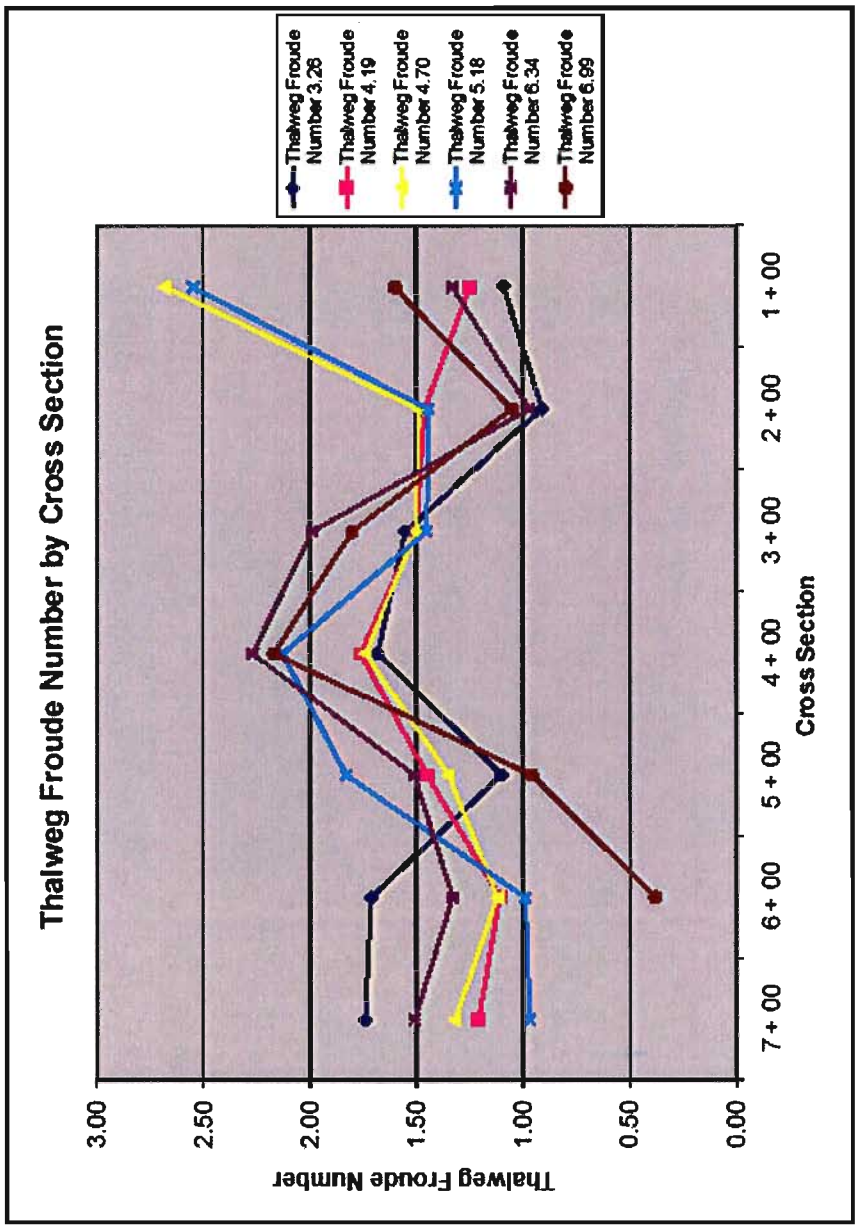

Figure 21. Thalweg Froude Number by Cross Section

4.6.2.2 Cross Section 1+00

At lower water levels 2.76 to 3.26, Froude Numbers across the section progressively increase, but remain at or below 1.1, indicative of transitional flow. At intermediate water level 4.19, Froude Numbers across the section increase in value to hover above 1.2, indicative of supercritical flow that approaches transitional flow. At intermediate water levels 4.70 to 5.18, Froude Numbers across the section jump in value to hover near 2.5, well within the range of supercritical flow. At higher water levels 6.34 to 6.99, Froude Numbers across the section return to lower values, generally less than 1.6, indicative of supercritical flow that approaches transitional flow. Examination of the corresponding photos (Appendix VI) reveals incipient and growing diagonal waves with increasing water levels, culminating in strong diagonal waves at 5.18, then progressively less obvious diagonal waves as water levels increase through 6.99.

4.6.2.3 Cross Section 2+00

At lower water levels 2.76 to 3.26, Froude Numbers across the section progressively increase, but remain below 1.0, indicative of transitional flow. At intermediate water levels 4.19 to 5.18, Froude Numbers across the section jump in value to hover near 1.4, indicative of supercritical flow that approaches transitional flow. At higher water levels 6.34 to 6.99, Froude Numbers across the section return to lower values, generally less than 1.1, indicative of transitional flow. Examination of the corresponding photos (Appendix VI) reveals incipient and growing diagonal waves with increasing water

levels, culminating in development of a hydraulic jump immediately downstream of the section at 4.19 to 5.18, then progressively less obvious diagonal waves as water levels increase through 6.99.

4.6.2.4 Cross Section 3+00

Values at water level 2.76 were not used due to the failure of the author to photograph the cross section at the time of data collection. At lower to intermediate water levels 3.26 to 5.18, Froude Numbers across the section progressively slightly decrease, but remain between 1.4 and 1.6, indicative of supercritical flow that approaches transitional flow. At higher water level 6.34, Froude Numbers across the section jump in value to hover near 2.1, well within the range of supercritical flow. At highest water level 6.99, Froude Numbers across the section decrease slightly in value to hover near 1.7, indicative of supercritical flow that approaches transitional flow. Examination of the corresponding photos (Appendix VI) reveals developed and growing diagonal waves with increasing water levels through 6.34. At 6.99, the diagonal waves appear to lose some definition, perhaps indicating a return toward transitional flow.

4.6.2.5 Cross Section 4+00

Values at water level 2.76 were not used due to the failure of the author to photograph the cross section at the time of data collection. At lower to intermediate water levels, from 3.26 to 4.70, Froude Numbers across the section progressively increase, but remain

between 1.4 and 1.8, indicative of supercritical flow that approaches transitional flow. At intermediate to higher water levels, from 5.18 to 6.99, Froude Numbers across the section jump in value to hover between 2.0 and 2.3, well within the range of supercritical flow. The Froude Number values decrease slightly from water levels 6.34 to 6.99. Examination of the corresponding photos (Appendix VI) reveals developed and growing diagonal waves with increasing water levels through water level 6.34. At 6.99, the diagonal waves appear to lose some definition, perhaps indicating a return toward transitional flow.

4.6.2.6 Cross Section 5+00

Values at water level 2.76 were not used due to the unreliability of the slope values at low water along an irregular streambed. Values at water level 5.18 were not used due to the failure of the author to photograph the cross section at the time of data collection. At low water level 3.26, Froude Numbers across the section hover near 1.1, indicative of transitional flow. At intermediate to higher water levels, from 4.19 to 6.34, Froude Numbers across the section increase in value to hover between 1.2 and 1.6, indicative of supercritical flow that approaches transitional flow. At the highest water level 6.99, Froude Numbers across the section decrease to hover below 1.0, indicative of transitional flow. Examination of the corresponding photos (Appendix VI) reveals developed and growing diagonal waves with increasing water levels through water level 6.34. At 6.99, the diagonal waves lose considerable definition, indicating a return to transitional flow.

4.6.2.7 Cross Section 6+00

Values at water level 2.76 were not used due to the unreliability of the slope values at low water along an irregular streambed. At low water level 3.26, Froude Numbers across the section fluctuate between 1.4 and 1.7, indicative of supercritical flow that approaches transitional flow. A dip in the Froude Numbers at panels between 80 to 120 feet from baseline partly correlates with a dip in the streambed geometry at a distance of 101 feet from the baseline. At higher water levels, the dip lessens to insignificance. At intermediate water levels from 4.19 to 5.18, Froude Numbers across the section decrease in value to hover between 0.8 and 1.1, indicative of transitional flow. At the higher water level 6.34, Froude Numbers across the section increase to hover between 1.2 and 1.4, indicative of supercritical flow that approaches transitional flow. At the highest water level 6.99, Froude Numbers across the section decrease dramatically to hover below 0.4, indicative of subcritical flow. Examination of the corresponding photos (Appendix VI) reveals developed diagonal waves at water level 3.26, with a developing and growing stream wide hydraulic jump with increasing water levels through water level 5.18. At 6.34, the hydraulic jump has migrated downstream, with diagonal waves across the section. At the highest water level 6.99, the diagonal waves lose considerable definition, with an exploding central standing wave, indicating a return to transitional flow. Alternatively, inaccurate data could have produced erroneous calculated Froude Numbers. At the higher water level, projection of a flat water surface elevation across the entire section is problematic in such a dynamic system. Lateral pressure from

flanking water panels that show supercritical flow at the surface but subcritical flow at depth could lift the standing wave (Tinkler, unpublished communication).

4.6.2.8 Cross Section 7+00

Values at water level 2.76 were not used due to the unreliability of the slope values at low water along an irregular streambed. At low water level 3.26, Froude Numbers across the section fluctuate between 1.5 and 1.8, indicative of supercritical flow that approaches transitional flow. At intermediate water levels 4.19 to 5.18, Froude Numbers across the section fluctuate in value between 0.9 and 1.3, indicative of transitional to supercritical flow. At the higher water level 6.34, Froude Numbers across the section increase to hover above 1.4, indicative of supercritical flow that approaches transitional flow. At the highest water level 6.99, Froude Numbers across the section increase to hover above 1.9, indicative of supercritical flow. Examination of the corresponding photos (Appendix VI) reveals developed diagonal waves at water level 3.26, with a developing and growing stream wide hydraulic jump with increasing water levels through water level 5.18. The transitory location of the hydraulic jump relative to the section may result in the fluctuating Froude Numbers with changing water levels. At the higher water level 6.34, the stream wide hydraulic jump begins to lose definition, replaced along the near bank by diagonal waves. At the highest water level 6.99, diagonal waves flank a central standing wave train that overlies the thalweg. The standing wave train is not predicted by the calculations, possibly due to inaccurate data collection. At the highest water level, projection of a flat water surface elevation across the entire section is problematic in such

a dynamic system. Lateral pressure from flanking water panels that show supercritical flow at the surface but subcritical flow at depth could lift the central panels, increasing the water depth to critical depth and producing standing waves, in support of Tinkler's unpublished communication.

4.6.2.9 Cross Section 8+00

Since the study reach ends at Cross Section 8+00, no downgradient slope data is available for derivation of velocity from Manning's Equation. Therefore, no Froude Numbers were calculated for analysis.

5. Summary and Conclusions

5.1 General Summary

Water flows through open channels in one of three regimes, known as subcritical, critical or supercritical flow. The traditional method of calculation of the Froude Number, a mathematical definition of each flow state, assumes constant discharge across the entire width of the channel, a condition rarely found in nature. This study explores variations in determination of the key variables, water velocity, water depth and velocity coefficient, that are used in the calculations that define the state of flow. Results are compared with photographs of the study reach at several levels of discharge across two orders of magnitude to determine accuracies of the calculation variations.

5.2 Summary of Froude Equation Variations

The following variations of the Froude Equation were examined in this study.

Name	Equation	Origin of Velocity Value	Velocity Coefficient	Depth
Simplified Froude Number	$F_{hs}= v_h/ (gy)^{0.5}$	discharge data	1	full
Manning's *v* Simplified Froude Number	$F_{ms}= v_m/(gy)^{0.5}$	Manning's Equation	1	full
Original Froude Number	$F_h=v_h/ (gy/1.15)^{0.5}$	discharge data	1.15	full
Manning's *v* Original Froude Number	$F_m=v_m/ (gy/1.15)^{0.5}$	Manning's Equation	1.15	full
Original Froude Number	$F_h=v_h/ (gy/1.30)^{0.5}$	discharge data	1.3	full
Manning's *v* Original Froude Number	$F_m=v_m/ (gy/1.30)^{0.5}$	Manning's Equation	1.3	full
Panel Froude Number	$F_{pan}= v/(gy)^{0.5}$	discharge data/panel	1	full
Depth Adjusted Simplified Froude Number	$F_{hsa}= v_h/ (gy_a)^{0.5}$	discharge data	1	0.66*y*
Depth Adjusted Manning's *v* Simplified Froude Number	$F_{msa}= v_m/(gy_a)0.5$	Manning's Equation	1	0.66*y*
Depth Adjusted Original Froude Number	$F_{ha}=v_h/ (gy_a/1.15)^{0.5}$	discharge data	1.15	0.66*y*
Depth Adjusted Manning's *v* Original Froude Number	$F_{ma}=v_m/ (gy_a/1.15)^{0.5}$	Manning's Equation	1.15	0.66*y*
Depth Adjusted Original Froude Number	$F_{ha}=v_h/ (gy_a/1.30)^{0.5}$	discharge data	1.3	0.66*y*
Depth Adjusted Manning's *v* Original Froude Number	$F_{ma}=v_m/ (gy_a/1.30)^{0.5}$	Manning's Equation	1.3	0.66*y*

Table 1 (again). Summary of Froude Equation Variations

5.3 Summary of Results

1) When critical flow is defined by Froude Number as $0.84 <= Fr <= 1.00$, accuracies of the various calculation methods range from poor to fair (Figures 7 through 9). However, when the flow states are re-classified as critical flow when $Fr = 0.84$ and supercritical flow when $Fr > 0.84$, the accuracy of the revised results increases dramatically. Comparison of the results of the various calculation methods with the photos reveals excellent to poor accuracy (Figures 10 through 12).
2) At 94%, the most accurate method is the Original Froude Equation, with a velocity coefficient of $\alpha = 1.30$ and velocity derived from Manning's Equation,

$$Fr_m = v_m/(gy/1.30)^{0.5}.$$

3) At 43%, the least accurate method is the Panel Froude Equation, with velocity as a function of the percentage of discharge passing through each panel,

$$Fr_{pan} = v_{pan}/(gy)^{0.5}.$$

4) Velocities derived from Manning's Equation produce more accurate Froude Numbers than velocities derived from discharge data.
5) Accuracy increases with increasing velocity coefficient.
6) In general, depth adjustment for possible vertical shearing within the panels significantly increases the accuracy of Froude Numbers derived from discharge data, Fr_{ha}, when compared with Froude Numbers derived from discharge data at full depth, Fr_h, suggesting that the inverse relationship between velocity and depth, required to maintain the assumption of constant discharge per unit width,

produces erroneously low velocities. The adjusted depths could also more accurately account for possible vertical shearing in the panels.

7) Depth adjustment for possible vertical shearing within the panels slightly decreases the accuracy of Froude Numbers derived from Manning's Equation, Fr_{ma}, in comparison with Froude Numbers derived from Manning's Equation at full depth, Fr_m, possibly due to the ubiquitous application of adjusted depth values, supercritical flow throughout the reach at all water levels, or both.
8) The lowest water level 2.76 yields the least accurate results for Froude Numbers derived from Manning's Equation at both full and adjusted water depths, possibly due to a greater influence of streambed roughness, n, than assumed in the calculations.
9) Accuracy decreases for all analyzed Froude Number derivation methods, regardless of depth considerations, in the presence of a hydraulic jump.
10) Very shallow water along the sloping stream banks results in low Froude Numbers derived from Manning's Equation, in contradiction to observed diagonal waves that suggest supercritical flow conditions.
11) Accuracy decreases significantly for Froude Numbers derived from discharge data with both full and adjusted depths in the presence of a widening thalweg and adjacent shallow eddies.

5.4 Summary of Ancillary Calculations

To check the results of this study with theoretical results under ideal conditions, three additional sets of calculations were performed. Critical depth y_c and critical velocity v_c were calculated as per Section 1.3.3.2 above and divided by the actual water depth and calculated velocity, respectively. Based on overall accuracy of the varying calculation methods, calculations with data from water levels 4.70 and 6.34, with velocity determined from discharge data and from Manning's Equation, respectively, the velocity coefficient set at α=1.30, and at full and adjusted depths, were plotted in a series of graphs of Froude Number Fr v. Specific Energy E, Depth / Critical Depth y/y_c and Velocity / Critical Velocity v/v_c (Figures 14 through 19) and compared with ideal results as illustrated in Henderson (1966) (Figure 13).

Subsequent analysis revealed the following observations.

1) Regardless of depth, calculations with velocity derived from discharge, v_h, produce graphs (Figures 14 through 19) that closely mirror the ideal graphs found in Henderson (1966) and in http://nptel.iitm.ac.in/courses/IIT-MADRAS/Hydraulics/pdfs/Unit8/8_1.pdf, reproduced in Figure 13. Although apparently mathematically consistent, the initial unrealistic assumption of constant discharge per unit width yields inaccurate velocities and invalid predictions of flow conditions.

2) Conversely, regardless of depth, calculations with velocity derived from Manning's Equation, v_m, produce graphs that are meaningless. A Froude Number Fr_m calculated from the independently derived velocity cannot be logically compared with a specific energy, critical depth or critical velocity value derived with the limiting assumption of constant discharge per unit width.

3) Recalculation of discharge at each panel, from velocity derived from Manning's Equation and measured depth, $q_n = v_m y$, substitution into the equation for critical depth, $y_c = (q_n\text{^}2/g)\text{^}0.33$, and subsequent substitution into the equation for critical velocity, $v_c = (gy_c)\text{^}0.5$, yields recalculated ratios Depth / Critical Depth, y/y_c, and Velocity / Critical Velocity, v/v_c, that were plotted against the previously calculated Froude Number Fr_m. The results are shown in the bottom graphs in Figures 16 through 19. While exhibiting some data scatter, both the full depth and adjusted depth calculations produce graphs similar to the ideal graphs produced by calculations based on assumptions of constant discharge per unit width.

4) Similarities between results based on the ideal assumed constant discharge and observed variable discharge suggest that variable discharge per unit width may allow valid application of velocities derived from Manning's Equation to the Froude Equation in analysis of flow state in individual panels across a section.

5) Calculated discharge values were compared with the measured discharge values recorded by USGS Stream Gage 04213500 for water levels 4.70 and 6.34 (Figure 20 and Table 1). Results at both water levels indicate poor correlation between calculated and measured discharge values at Cross Sections 1+00 through 4+00

and good to excellent correlation at Cross Sections 5+00 through 7+00 (Figure 17). The lack of inter-channel high area details during initial streambed surveys of the upper cross sections may result in overly high water depth values for many panels, and subsequently erroneously high panel discharge and total discharge values. Conversely, good streambed details for the lower cross sections yield more accurate water depths, and subsequently more accurate total calculated discharge values.

6) Further investigation, under controlled conditions, is warranted to verify the validity of panel discharge values.

5.5 Summary of Presentation of Preferred Calculations as Froude Maps

5.5.1 Froude Number Maps

Based on the accuracy analysis, Froude Numbers that resulted from the calculations that utilized full depth measurements, velocities derived from Manning's Equation and a velocity coefficient set at $\alpha = 1.30$ were plotted on plan view maps of the study reach at each water level (Appendix IV). In general, the maps show that supercritical flow occurs throughout the study reach at all measured water levels with isolated pockets of subcritical or critical flow. The results support previous assertions by Trieste (1992) and Grant (1997) that supercritical flow may be maintained for more than short distances, provided that flow occurs in steep gradient bedrock channels.

5.5.2 Froude Number Contour Maps

Appendix V contains a series of Froude Number Contour Maps for each water level. Photos of each entire water level event also appear in Appendix 5 for correlation with the graphs. In general, the maps show relatively constant Froude Numbers across most of each section, but a sinusoidal pattern of rising and falling Froude Numbers in the downstream direction. Figure 21 shows the progressive changes in Froude Number values in the thalweg at each cross section at each water level. Further investigation is warranted to explore the causes of the sinusoidal pattern.

5.5.3 Changes in Froude Numbers with Increasing Water Levels

Froude Numbers at each panel were plotted against water level for each cross section (Appendix VI). Photos of each cross section at each water level also appear in Appendix VI for correlation with the graphs. Variations in calculated Froude Number values with changing water levels at each cross section mimic observed water surface variations recorded via photographs during data collection. The following general observations were noted.

1) Calculated Froude Number values between 0.8 and 1.1 correlate well with observed transitional flow, defined as the first appearance of small diagonal waves.
2) Calculated Froude Numbers tend to group near transitional flow values or well into the range of supercritical flow.

3) Calculated Froude Numbers tend to move from transitional to supercritical flow as water level increases, then back to transitional flow at the highest water levels. The corresponding photographs accurately record flow state changes from transitional flow to supercritical flow, then back toward transitional flow.
4) Minor streambed irregularities tend to toward insignificance as water levels increase.
5) At all water levels, calculated Froude Number values near the edges of the stream drop off dramatically, probably due to the decrease in water depth and subsequent mathematical influence on calculation of velocities and Froude Numbers for those panels.
6) Observed hydraulic jumps correlate with transitional to supercritical Froude Number values. The migratory nature of hydraulic jumps upstream or downstream of the sections may result in fluctuating Froude Number values as water levels change.

5.6 Conclusions

Previous workers have relied on the assumption of constant discharge across most or all of a stream cross section to model or analyze individual features or cross sections mathematically, in the lab or in the field. Determination of velocity from measured discharge data introduces the assumption of decreasing velocity with increasing depth

across the entire section and produces mathematically consistent but potentially invalid and unrealistic Froude Number and other calculation results.

The present field study analyzes flow conditions through two orders of magnitude of discharge across and along a very dynamic system in the field that is 800 feet long and up to 200 or more feet wide. The results suggest that calculation of Froude Number, critical velocity and critical depth for individual panels across an entire section of a steep gradient rockbed stream do not need to be constrained by the unrealistic assumption of constant discharge across the section, provided that:

1) the streambed geometry is accurately surveyed;
2) water surface elevation and location is accurately measured;
3) velocity in determined from Manning's Equation;
4) the appropriate velocity coefficient is chosen.

6.0 Recommendations for Further Study

Replication of the field study, with a new streambed survey to account for erosional changes, combined with controlled experiments in a flume, could investigate the relative accuracies of the various methods of calculation of Froude Number and the ancillary calculations with much greater precision.

1) With more precise values of streambed geometry, water depth at each panel, water surface widths, water surface slopes and discharge rates, calculated velocities determined from discharge data and from Manning's Equation,

respectively, could be checked against measured velocities for relative accuracies of the two methods.

2) Subsequent calculation of Froude Numbers, using the variations examined in the present study, could be compared with photos of the water surface in the flume to determine relative accuracies of the variations of the Froude Equation.
3) Manipulation of the variables to produce subcritical, critical and supercritical flow could more accurately define the Froude Numbers at the transition points among the states of flow.
4) Manipulation of the streambed geometry to produce subcritical, critical and supercritical flow across individual sections and subsequent velocity measurements throughout the water columns at individual panels could more accurately examine the occurrence of lateral and vertical flow separation in a rough dynamic environment.
5) Investigation of the apparent sinusoidal fluctuations in Froude Numbers in the downstream direction under controlled conditions could shed further light on energy distribution throughout open channel flow. Does the sinusoidal pattern observed in supercritical flow in a rock bedded stream mimic pool-riffle-pool geomorphology found in alluvial streams?
6) The ancillary calculations could be performed with more precise data to assess the validity of the calculated discharge per panel derived from velocity determined from Manning's Equation. If proven valid, such a calculated discharge method might prove useful along streams without gages, but with known streambed geometry and water surface slope.

Literature Cited

1. Bakhmeteff, B.A., 1932, Hydraulics of Open Channels, New York: McGraw-Hill Book Company, Inc., Chapter 8.

2. Beffa, C., 1996, Backwater computation for transcritical flows, J. Hydraulic Engineering, 122, 12: 745-748.

3. Beinkafner, K.J., 1983, Terminal expression of decollement in Chautauqua County, New York, Northeastern Geology, 5, 3/4: 160-171.

4. Benton, G.S., 1954, The occurrence of critical flow and hydraulic jumps in a multi-layered fluid system, J. Meteorology, 11:139-150.

5. Blank, H.R., 1958, Pothole grooves in the bed of the James River, Mason County, Texas, Texas Journal of Science, p.293-301.

6. Blank, H.R., 1970, Incised Meanders in Mason County, Texas, Geol. Soc. Amer. Bull., 81: 3135-3140.

7. Carll, J.F., 1880, The geology of the oil regions of Warren, Venango, Clarion and Butler Counties, 2nd Pa. Geol. Surv. Rpt. 13: 1-10, 77-79, 330-397.

8. Carollo, F.G., Ferro, V. and Pampalone, V., 2007, Hydraulic jumps on rough beds, J. Hydraulic Engineering, 133, 9: 989-999.

9. Catella, M., Paris, E. and Solan, L., 2008, Conservative scheme for numerical modeling of flow in natural geometry, J. Hydraulic Engineering, 134, 6: 736-748.

10. Causon, D.M., Mingham, C.G. and Ingram, D.M., 1999, Advances in calculation methods for supercritical flow in spillway channels, J. Hydraulic Engineering, 125, 10: 1039-1050.

11. Chanson, H., 2006, Minimum specific energy and critical flow conditions in open channels, J. Irrigation and Drainage Engineering, 132, 5: 498-502.

12. Cheel, R.J., 1990, Horizontal lamination and the sequence of bed phases and stratification under upper-flow-regime conditions, Sedimentology, 37: 517-529.

13. Chow, V.T., 1959, Open-Channel Hydraulics, New York: McGraw-Hill Book Company, Inc., Chapter 5.

14. Eyles, N., Arnaud, E., Scheidegger, A.E. and Eyles, C.H., 1997, Bedrock jointing and geomorphology in southwestern Ontario, Canada: an example of tectonic pre-design, Geomorphology, 19: 17-34.

15. Eyles, N. and Scheidegger, A.E., 1995, Environmental significance of bedrock jointing in southern Ontario, Canada, Environmental Geology, 26: 269-277.

16. Grant, G.E., 1997, Critical flow constrains flow hydraulics in mobile-bed streams: A new hypothesis, Water Resources Research, 33, 2: 349-358.

17. Guo, J.C.Y., 1999, Critical flow section in collector channel, J. Hydraulic Engineering, 125, 4: 422-425.

18. HEC-2 Water Surface Profiles User's Manual September 1990: Revised September, 1991.

19. HEC-RAS River Analysis System Hydraulic Reference Manual Version 4.0 March 2008.

20. Henderson, F.M., 1966, Open Channel Flow, New York: MacMillan Publishing Co., Inc., Chapters 1-4.

21. Jacobi, R.D., Baudo, A., Lowenstein, S., and Fountain, J., 1999, Faults exposed in Zoar Valley, western New York, and their possible relation to geophysical anomalies, Landsat lineaments and seismicity, Geol. Soc. Amer. Northeastern Section Meeting, Abstract with Programs, 2, no.2.

22. Jimenez, O.F. and Chaudhry, M.H., 1988, Computation of supercritical free-surface flows, J. Hydraulic Engineering, 114, 4: 377-395.

23. Kennedy, J.F., 1963, The mechanics of dunes and antidunes in erodible-bed channels, J. Fluid Mechanics, 16: 521-544.

24. King, H.W. and Brater, E.F., 1963, Handbook of Hydraulics, New York: McGraw-Hill, Inc., Fifth Edition.

25. Meselhe, E.A., Sotiropoulos, F. and Holly Jr., F.M., 1997, Numerical simulation of transcritical flow in open channels, J. Hydraulic Engineering, 123, 9: 774-783.

26. Meyers, M.J., 1999, Geology of Zoar Valley gorge of Cattaraugus Creek, Cattaraugus and Erie counties, New York, in Guidebook for NY State Geol. Assn. Field Trip Guidebook, Lash, G.G., editor: F1-F15.

27. Ohtsu, I. and Yasuda, Y., 1991, Hydraulic jump in sloping channels, J. Hydraulic Engineering, 117, 7: 905-921.

28. Richardson, K. and Carling, P.A., 2006, The hydraulics of a straight bedrock channel: Insights from solute dispersion studies, Geomorphology, 82: 98-125.

29. Sarma, K.V.N. and Syamula, P., 1991, Supercritical flow in smooth open channels, J. Hydraulic Engineering, 117, 1: 54-63.

30. Schoellhamer, D.H., 1983, Calculation of critical depth and subdivision froude number in HEC2, thesis presented to the University of Calfornia, at Davis, Calif., in partial fulfillment of the requirements for the degree of Master of Science.

31. Schoellhamer, D.H., Peters, J.C. and Larock, B.E., 1985, Subdivision froude number, J. Hydraulic Engineering, 111, 7: 1099-1104.

32. Shepherd, R.G. and Schumm, S.A., 1974, Experimental study of river incision, Geol. Soc. Amer. Bull., 85: 1783-1800.

33. Tesmer, I.H., 1975, Geology of Cattaraugus County, New York: Buffalo Society of Natural Sciences Bulletin, no. 27, 105p.

34. Tinkler, K.J., 1982, Avoiding error with the Manning equation, J. Geology, 90: 326-328.

35. Tinkler, K.J., 1997a, Critical flow in rockbed streams with estimated values for Manning's *n*, Geomorphology, 20: 147-164.

36. Tinkler, K.J., 1997b, Indirect velocity measurement from standing waves in rockbed rivers, J. Hydraulic Engineering, 123, 10: 918-921.

37. Trieste, D.J., 1992, Evaluation of supercritical/subcritical flows in high-gradient channel, J. Hydraulic Engineering, 118, 8: 1107-1118.

38. Turowski, J.M., Hovius, Meng-Long, H., Lague, D. and Men-Chiang, C., 2008, Distribution of erosion across bedrock channels, Earth Surface Processes and Landforms, 33: 353-363.

39. Turowski, J.M., Hovius, N, Wilson, A. and Horng, M.J., 2008, Hydraulic geometry, river sediment and the definition of bedrock channels, Geomorphology, 99: 26-38.

40. Valle, B.L. and Pasternack, G.B., 2006, Submerged and unsubmerged natural hydraulic jumps in a bedrock step-pool mountain channel, Geomorphology, 82: 146-159.

41. Van Tyne, A.M., Kamakaris, D.G., and Corbo, S., 1980, Structure Contours on Base of the Dunkirk, Morgantown Energy Technology Center, Eastern Gas Shales Project Series III.

42. Ven Te Chow, 1959, Open-Channel Hydraulics, New York: McGraw-Hill Book Company, Inc., Chapter 5.

Appendix I
Streambed Contour Map
Stream Bed Cross Sections
Refrigerator Island Rapid Photos

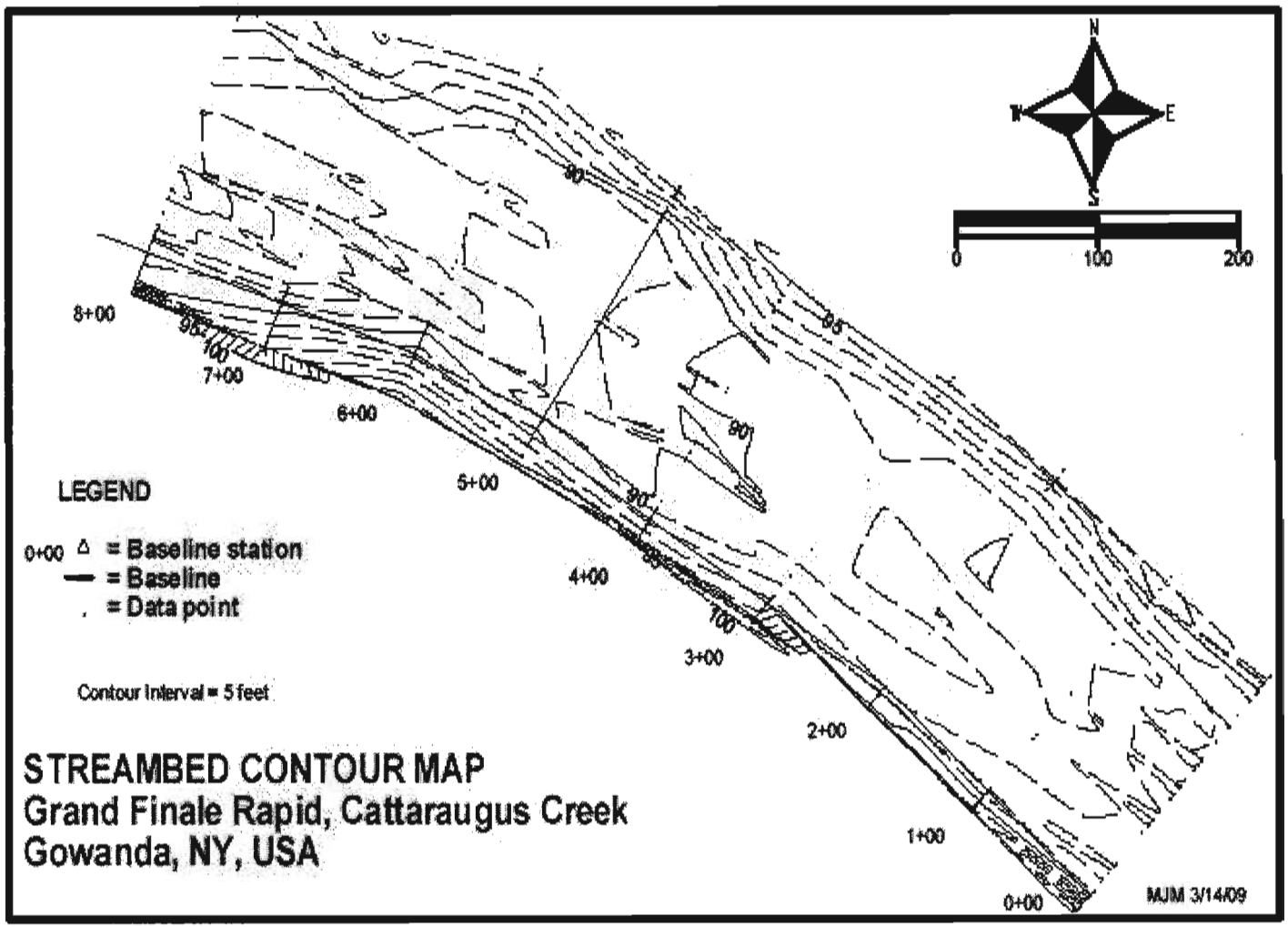
N
W
E
S
0
100
200
8+00
7+00
6+00
5+00
4+00
3+00
2+00
1+00
0+00
90
95
100
LEGEND
0+00 Δ = Baseline station
— = Baseline
. = Data point
Contour Interval = 5 feet
STREAMBED CONTOUR MAP
Grand Finale Rapid, Cattaraugus Creek
Gowanda, NY, USA
MJM 3/14/09

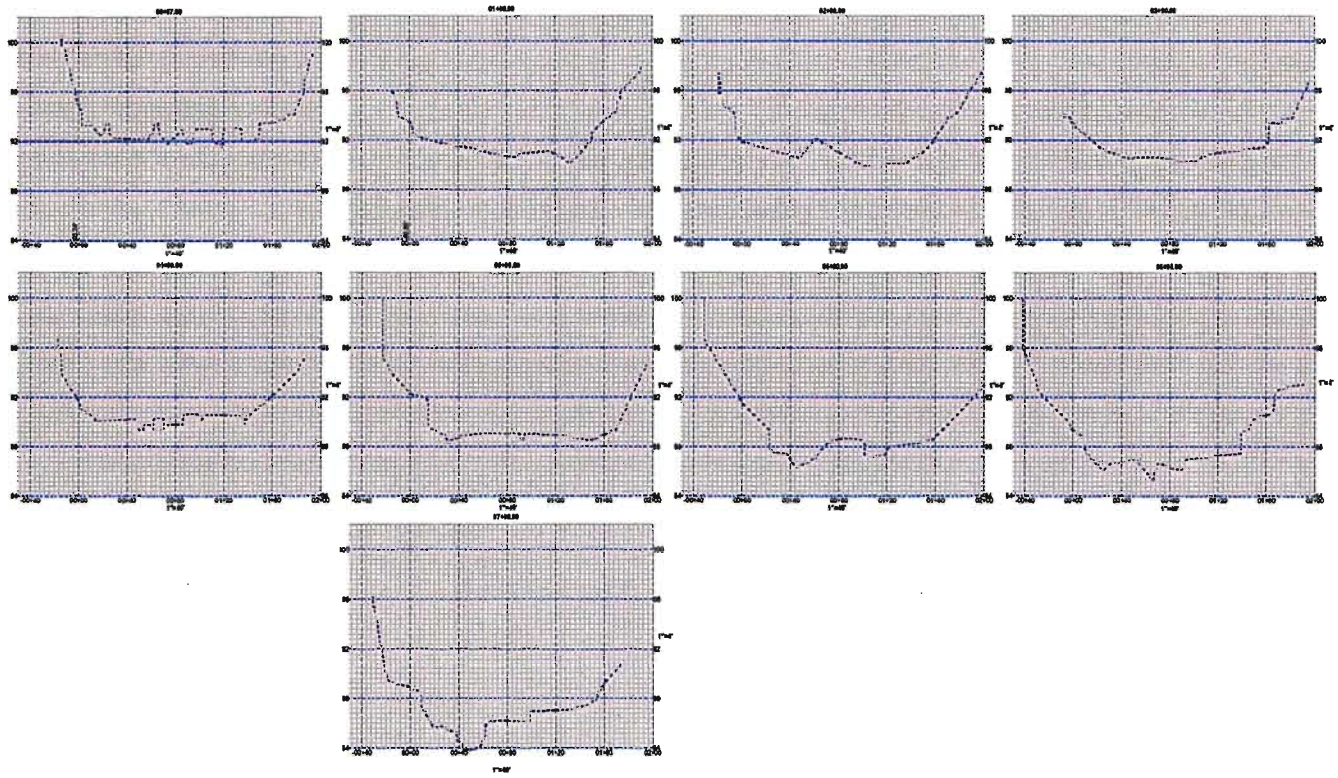

Horizontal Scale one inch = 40 feet

Vertical Scale one inch = 4 feet

STREAM BED CROSS SECTIONS
Grand Finale Rapid
Cattaraugus Creek
Gowanda, New York, USA

Refrigerator Island Rapid at Water Level 2.7

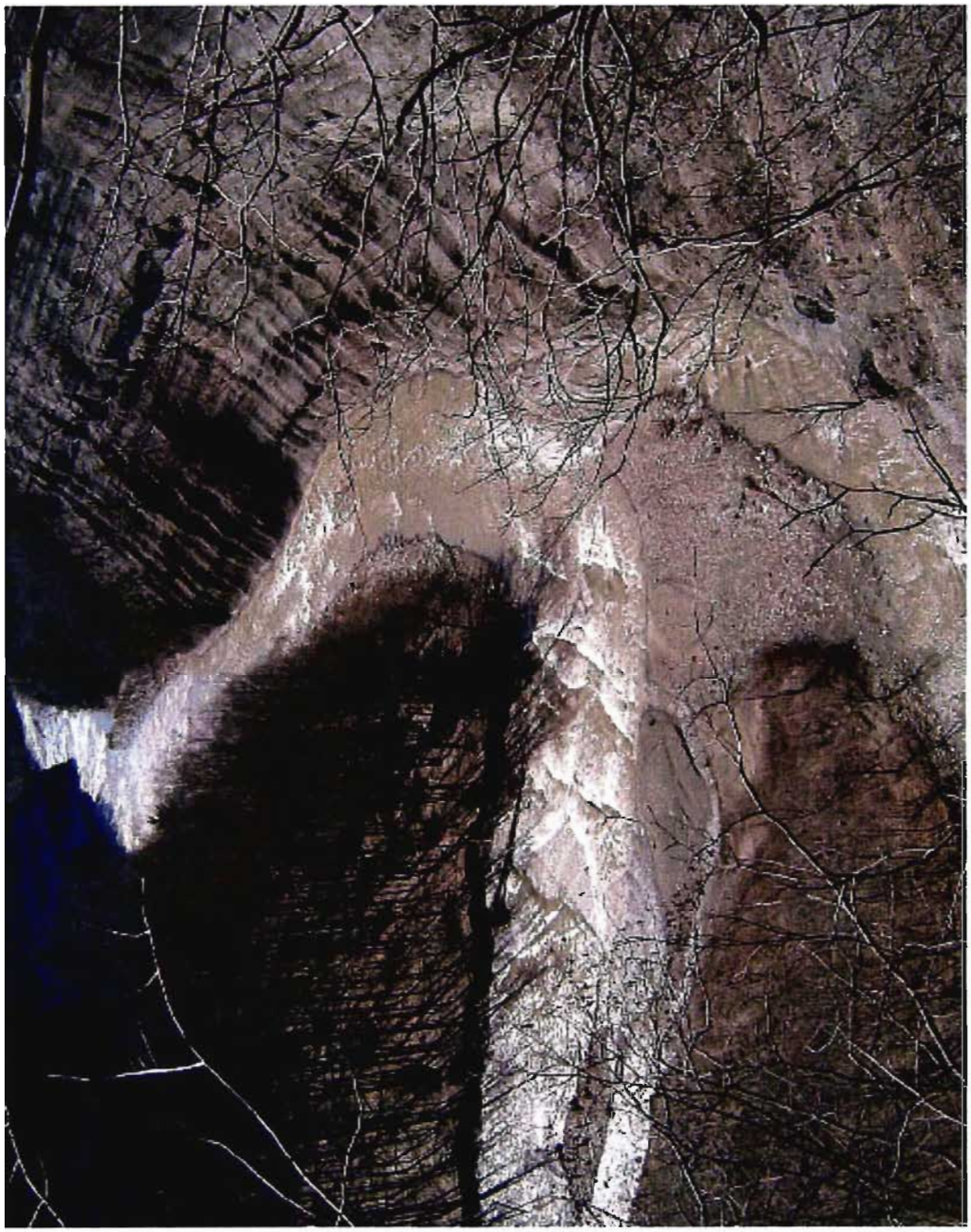

Refrigerator Island Rapid at Water Level 3.4

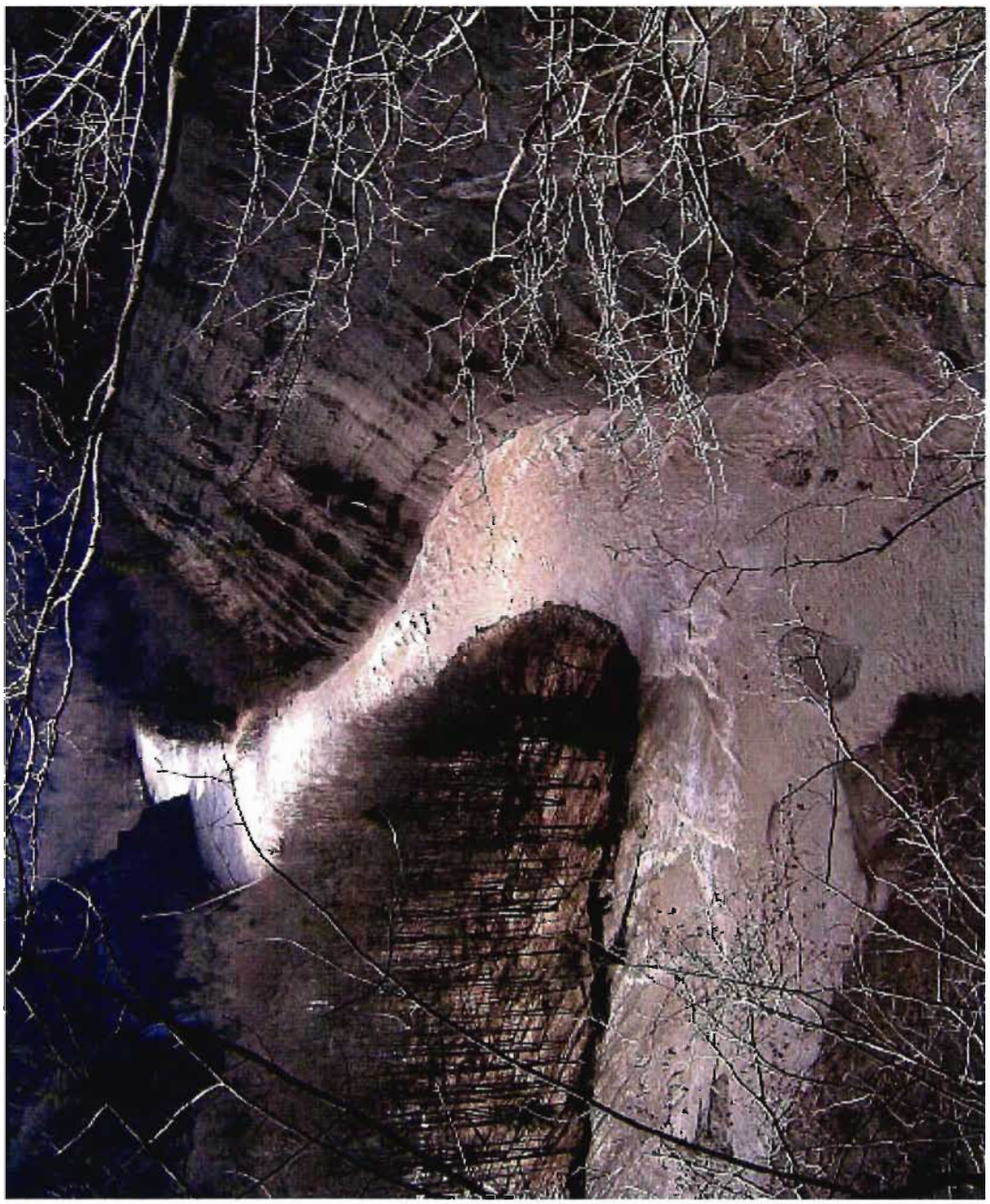

Refrigerator Island Rapid at Water Level 5.7

Appendix II

Cross Section Areas

Areas by AVERAGE END AREA
Fri Nov 14 15:28:59 2008
Project: Cattaraugus Creek Study.PCS
Water Level 2.76

Station	Area
0.000000	0.000000
100.000000	389.608595
200.000000	418.967807
290.000000	326.781947
300.000000	310.367092
400.000000	97.456466
500.000000	82.213703
600.000000	83.359973
695.000000	158.715033
7.000000	273.436967
700.000000	151.888730
790.000000	46.265235
800.000000	0.000000

Areas by AVERAGE END AREA
Tue Nov 11 17:15:42 2008
Project: Cattaraugus Creek Study.PCS
Water level 3.26

Station	Area
0.000000	0.000000
100.000000	424.575722
200.000000	418.780885
290.000000	334.422633
300.000000	317.423647
400.000000	140.261861
500.000000	162.806539
600.000000	261.684648
695.000000	231.600486
7.000000	326.230550
700.000000	224.607201
790.000000	122.070494
800.000000	0.000000

Areas by AVERAGE END AREA
Tue Nov 11 17:19:08 2008
Project: Cattaraugus Creek Study.PCS
Water Level 4.19

Station	Area
0.000000	0.000000
100.000000	708.523986
200.000000	584.320885
290.000000	392.460892
300.000000	383.154299
400.000000	299.748624
500.000000	255.923789
600.000000	265.720876
695.000000	326.372444
7.000000	510.483123
700.000000	329.875121
790.000000	338.572901
800.000000	0.000000

Areas by AVERAGE END AREA
Tue Nov 11 17:22:37 2008
Project: Cattaraugus Creek Study.PCS
Water Level 4.70

Station	Area
0.000000	0.000000
100.000000	20.229046
200.000000	622.162066
290.000000	418.227985
300.000000	409.249688
400.000000	339.809519
500.000000	303.938100
600.000000	400.393040
695.000000	378.201194
7.000000	0.000000
700.000000	381.148510
790.000000	400.964533
800.000000	0.582344

Areas by AVERAGE END AREA
Tue Nov 18 15:24:53 2008
Project: Cattaraugus Creek Study.PCS
Water Level 5.18

Station	Area
0.000000	0.000000
100.000000	31.833142
200.000000	775.584999
290.000000	617.750724
300.000000	611.740014
400.000000	513.506109
500.000000	322.136255
600.000000	322.476534
695.000000	421.341308
7.000000	0.000000
700.000000	425.973953
790.000000	435.028273
800.000000	2.391983

Areas by AVERAGE END AREA
Tue Nov 18 15:37:14 2008
Project: Cattaraugus Creek Study.PCS
Water Level 6.34

Station	Area
0.000000	1.941470
100.000000	1037.760384
200.000000	1023.650750
290.000000	968.225167
300.000000	951.048962
400.000000	592.804847
500.000000	552.350617
600.000000	634.015044
695.000000	567.767354
7.000000	979.613079
700.000000	566.823695
790.000000	12.961387
800.000000	1.982608

Areas by AVERAGE END AREA
Tue Nov 11 17:27:31 2008
Project: Cattaraugus Creek Study.PCS
Water Level 6.99

Station	Area
0.000000	17.006083
100.000000	1183.662633
200.000000	1211.385840
290.000000	1094.259468
300.000000	1083.605015
400.000000	826.166935
500.000000	802.129835
600.000000	1146.213488
695.000000	615.867074
7.000000	1202.695037
700.000000	584.272508
790.000000	25.181533
800.000000	0.053888

Appendix III

Example of Calculation Spreadsheet

Example of Cross Section Photo with Froude Numbers

Calculation Spreadsheet
Velocity from Discharge
Full Depth

Interval (n)	Discharge (Q) cfs.	Water Elevation (WE)	Interval Elevation (En)	Water Depth (y) ft.	Channel width (b_n) ft.	Acceleration due to gravity (g) ft/sec/sec	$q=Q/b_n$	Henderson's Velocity $v_h=q/y$	Critical Depth $y_c=(q^2/g)^{0.33}$	Critical Velocity $v_c=(g(yc))^{0.5}$
6+00										
-40 to -30										
-30 to -20	4210	90	95.7	-5.7	156.4	32	26.92	-4.72	2.80	9.47
-20 to -10	4210	90	94	-4	156.4	32	26.92	-6.73	2.80	9.47
-10 to 0	4210	90	92.4	-2.4	156.4	32	26.92	-11.22	2.80	9.47
0 to 10	4210	90	91.1	-1.1	156.4	32	26.92	-24.47	2.80	9.47
10 to 20	4210	90	90.1	-0.1	156.4	32	26.92	-269.18	2.80	9.47
20 to 30	4210	90	88.2	1.8	156.4	32	26.92	14.95	2.80	9.47
30 to 40	4210	90	87.4	2.6	156.4	32	26.92	10.35	2.80	9.47
40 to 50	4210	90	86.6	3.4	156.4	32	26.92	7.92	2.80	9.47
50 to 60	4210	90	86.8	3.2	156.4	32	26.92	8.41	2.80	9.47
60 to 70	4210	90	87.6	2.4	156.4	32	26.92	11.22	2.80	9.47
70 to 80	4210	90	88.5	1.5	156.4	32	26.92	17.95	2.80	9.47
80 to 90	4210	90	88.7	1.3	156.4	32	26.92	20.71	2.80	9.47
90 to 100	4210	90	88.6	1.4	156.4	32	26.92	19.23	2.80	9.47
100 to 110	4210	90	87.5	2.5	156.4	32	26.92	10.77	2.80	9.47
110 to 120	4210	90	87.3	2.7	156.4	32	26.92	9.97	2.80	9.47
120 to 130	4210	90	87.9	2.1	156.4	32	26.92	12.82	2.80	9.47
130 to 140	4210	90	88.1	1.9	156.4	32	26.92	14.17	2.80	9.47
140 to 150	4210	90	88.2	1.8	156.4	32	26.92	14.95	2.80	9.47
150 to 160	4210	90	88.5	1.5	156.4	32	26.92	17.95	2.80	9.47
160 to 170	4210	90	89.3	0.7	156.4	32	26.92	38.45	2.80	9.47
170 to 180	4210	90	90.3	-0.3	156.4	32	26.92	-89.73	2.80	9.47
180 to 190	4210	90	91.3	-1.3	156.4	32	26.92	-20.71	2.80	9.47
190 to 200	4210	90	92.3	-2.3	156.4	32	26.92	-11.70	2.80	9.47

Cross Section 6+00
Water Level 5.18

Calculation Spreadsheet
Velocity from Discharge
Full Depth

Interval (ft)	Simplified Froude Number F_{hs}= $v_h/(gy)^{0.5}$	Simplified Specific Energy $E=y+v_h^2/2g$	Original Froude Number $F_h=v_h/(gy/1.15)^{0.5}$	Original Specific Energy $E=y+1.15v_h^2/2g$	Original Froude Number $F_h=v_h/(gy/1.30)^{0.5}$	Original Specific Energy $E=y+1.30v_h^2/2g$	Depth/ Critical Depth y/y_c	Velocity/ Critical Velocity v_h/v_c
6+00								
-40 to -30								
-30 to -20	#NUM!	-5.35	#NUM!	-5.30	#NUM!	-5.25	-2.04	-0.50
-20 to -10	#NUM!	-3.29	#NUM!	-3.19	#NUM!	-3.08	-1.43	-0.71
-10 to 0	#NUM!	-0.43	#NUM!	-0.14	#NUM!	0.16	-0.86	-1.18
0 to 10	#NUM!	8.26	#NUM!	9.66	#NUM!	11.06	-0.39	-2.59
10 to 20	#NUM!	1132.07	#NUM!	1301.89	#NUM!	1471.72	-0.04	-28.44
20 to 30	1.97	5.29	2.11	5.82	2.25	6.34	0.64	1.58
30 to 40	1.14	4.27	1.22	4.53	1.29	4.78	0.93	1.09
40 to 50	0.76	4.38	0.81	4.53	0.87	4.67	1.21	0.84
50 to 60	0.83	4.31	0.89	4.47	0.95	4.64	1.14	0.89
60 to 70	1.28	4.37	1.37	4.66	1.46	4.96	0.86	1.18
70 to 80	2.59	6.53	2.78	7.29	2.95	8.04	0.54	1.90
80 to 90	3.21	8.00	3.44	9.00	3.66	10.01	0.46	2.19
90 to 100	2.87	7.18	3.08	8.04	3.28	8.91	0.50	2.03
100 to 110	1.20	4.31	1.29	4.58	1.37	4.85	0.89	1.14
110 to 120	1.07	4.25	1.15	4.49	1.22	4.72	0.96	1.05
120 to 130	1.56	4.67	1.68	5.05	1.78	5.44	0.75	1.35
130 to 140	1.82	5.04	1.95	5.51	2.07	5.98	0.68	1.50
140 to 150	1.97	5.29	2.11	5.82	2.25	6.34	0.64	1.58
150 to 160	2.59	6.53	2.78	7.29	2.95	8.04	0.54	1.90
160 to 170	8.12	23.81	8.71	27.27	9.26	30.74	0.25	4.06
170 to 180	#NUM!	125.50	#NUM!	144.37	#NUM!	163.24	-0.11	-9.48
180 to 190	#NUM!	5.40	#NUM!	6.40	#NUM!	7.41	-0.46	-2.19
190 to 200	#NUM!	-0.16	#NUM!	0.16	#NUM!	0.48	-0.82	-1.24

Cross Section 6+00
Water Level 5.18

Calculation Spreadsheet
Velocity from Manning's Equation
Full Depth

Interval (n)	Slope S	Manning's Velocity v_m= $(1.49)(y^{0.67})s^{0.5}/n$ where n=0.025	Manning's v Simplified Froude Number $F_{ms}=v_m/(gy)^{0.5}$	Manning's v Simplified Specific Energy $E=y+v_m^2/2g$	Manning's v Simplified Velocity/ Critical Velocity v_m/v_c	Manning's v Original Froude Number $F_m=v_m/(gy/1.15)^{0.5}$	Manning's v Original Specific Energy $E=y+1.15v_m^2/2g$	Manning's v Original Froude Number $F_m=v_m/(gy/1.30)^{0.5}$	Manning's v Original Specific Energy $E=y+1.30v_m^2/2g$
6+00									
-40 to -30									
-30 to -20	0.0045	#NUM!	#NUM!	#NUM!	#NUM!	#NUM!	#NUM!	#NUM!	#NUM!
-20 to -10	0.0045	#NUM!	#NUM!	#NUM!	#NUM!	#NUM!	#NUM!	#NUM!	#NUM!
-10 to 0	0.0045	#NUM!	#NUM!	#NUM!	#NUM!	#NUM!	#NUM!	#NUM!	#NUM!
0 to 10	0.0045	#NUM!	#NUM!	#NUM!	#NUM!	#NUM!	#NUM!	#NUM!	#NUM!
10 to 20	0.0045	#NUM!	#NUM!	#NUM!	#NUM!	#NUM!	#NUM!	#NUM!	#NUM!
20 to 30	0.0045	5.93	0.78	2.35	0.63	0.84	2.43	0.89	2.51
30 to 40	0.0045	7.58	0.83	3.50	0.80	0.89	3.63	0.95	3.77
40 to 50	0.0045	9.08	0.87	4.69	0.96	0.93	4.88	0.99	5.07
50 to 60	0.0045	8.72	0.86	4.39	0.92	0.92	4.56	0.98	4.74
60 to 70	0.0045	7.19	0.82	3.21	0.76	0.88	3.33	0.94	3.45
70 to 80	0.0045	5.25	0.76	1.93	0.55	0.81	1.99	0.86	2.06
80 to 90	0.0045	4.77	0.74	1.65	0.50	0.79	1.71	0.84	1.76
90 to 100	0.0045	5.01	0.75	1.79	0.53	0.80	1.85	0.85	1.91
100 to 110	0.0045	7.39	0.83	3.35	0.78	0.89	3.48	0.94	3.61
110 to 120	0.0045	7.78	0.84	3.65	0.82	0.90	3.79	0.95	3.93
120 to 130	0.0045	6.57	0.80	2.77	0.69	0.86	2.88	0.91	2.98
130 to 140	0.0045	6.15	0.79	2.49	0.65	0.85	2.58	0.90	2.67
140 to 150	0.0045	5.93	0.78	2.35	0.63	0.84	2.43	0.89	2.51
150 to 160	0.0045	5.25	0.76	1.93	0.55	0.81	1.99	0.86	2.06
160 to 170	0.0045	3.15	0.67	0.85	0.33	0.71	0.88	0.76	0.90
170 to 180	0.0045	#NUM!	#NUM!	#NUM!	#NUM!	#NUM!	#NUM!	#NUM!	#NUM!
180 to 190	0.0045	#NUM!	#NUM!	#NUM!	#NUM!	#NUM!	#NUM!	#NUM!	#NUM!
190 to 200	0.0045	#NUM!	#NUM!	#NUM!	#NUM!	#NUM!	#NUM!	#NUM!	#NUM!

Cross Section 6+00
Water Level 5.18

Calculation Spreadsheet
Velocity from Discharge
Adjusted Depth

Interval (n)	Discharge (Q) cfs.	Water Elevation (WE)	Interval Elevation (E_n)	Adjusted Water Depth (y_a) ft.	Channel width (b_n) ft.	Acceleration due to gravity (g) ft/sec/sec	$q=Q/b_n$	Henderson's Velocity $v_n=q/y_a$	Critical Depth $y_c=$ $(q^2/g)^{0.33}$	Critical Velocity $v_c=$ $(g(y_c))^{0.5}$
6+00										
-40 to -30										
-30 to -20	4210	90	95.7	-3.76	156.4	32	26.92	-7.16	2.80	9.47
-20 to -10	4210	90	94	-2.64	156.4	32	26.92	-10.20	2.80	9.47
-10 to 0	4210	90	92.4	-1.58	156.4	32	26.92	-16.99	2.80	9.47
0 to 10	4210	90	91.1	-0.73	156.4	32	26.92	-37.08	2.80	9.47
10 to 20	4210	90	90.1	-0.07	156.4	32	26.92	-407.85	2.80	9.47
20 to 30	4210	90	88.2	1.19	156.4	32	26.92	22.66	2.80	9.47
30 to 40	4210	90	87.4	1.72	156.4	32	26.92	15.69	2.80	9.47
40 to 50	4210	90	86.6	2.24	156.4	32	26.92	12.00	2.80	9.47
50 to 60	4210	90	86.8	2.11	156.4	32	26.92	12.75	2.80	9.47
60 to 70	4210	90	87.6	1.58	156.4	32	26.92	16.99	2.80	9.47
70 to 80	4210	90	88.5	0.99	156.4	32	26.92	27.19	2.80	9.47
80 to 90	4210	90	88.7	0.86	156.4	32	26.92	31.37	2.80	9.47
90 to 100	4210	90	88.6	0.92	156.4	32	26.92	29.13	2.80	9.47
100 to 110	4210	90	87.5	1.65	156.4	32	26.92	16.31	2.80	9.47
110 to 120	4210	90	87.3	1.78	156.4	32	26.92	15.11	2.80	9.47
120 to 130	4210	90	87.9	1.39	156.4	32	26.92	19.42	2.80	9.47
130 to 140	4210	90	88.1	1.25	156.4	32	26.92	21.47	2.80	9.47
140 to 150	4210	90	88.2	1.19	156.4	32	26.92	22.66	2.80	9.47
150 to 160	4210	90	88.5	0.99	156.4	32	26.92	27.19	2.80	9.47
160 to 170	4210	90	89.3	0.46	156.4	32	26.92	58.26	2.80	9.47
170 to 180	4210	90	90.3	-0.20	156.4	32	26.92	-135.95	2.80	9.47
180 to 190	4210	90	91.3	-0.86	156.4	32	26.92	-31.37	2.80	9.47
190 to 200	4210	90	92.3	-1.52	156.4	32	26.92	-17.73	2.80	9.47

Cross Section 6+00
Water Level 5.18

Calculation Spreadsheet
Velocity from Discharge
Adjusted Depth

Interval (n)	Depth Adjusted Simplified Froude Number F_{hsa}= $v_h/(gy_a)^{0.5}$	Depth Adjusted Simplified Specific Energy $E = y_a + v_h^2/2g$	Depth Adjusted Original Froude Number F_{ha}= $v_h/(gy_a/1.15)^{0.5}$	Depth Adjusted Original Specific Energy $E=y+1.15v_h^2/2g$	Depth Adjusted Original Froude Number F_{ha}= $v_h/(gy_a/1.30)^{0.5}$	Depth Adjusted Original Specific Energy $E=y_a+1.30v_h^2/2g$	Depth Adjusted Depth/ Critical Depth y_a/y_c	Depth Adjusted Velocity/ Critical Velocity v_h/v_c
6+00								
-40 to -30								
-30 to -20	#NUM!	-2.96	#NUM!	-2.84	#NUM!	-2.72	-1.34	-0.76
-20 to -10	#NUM!	-1.02	#NUM!	-0.77	#NUM!	-0.53	-0.94	-1.08
-10 to 0	#NUM!	2.93	#NUM!	3.61	#NUM!	4.28	-0.57	-1.80
0 to 10	#NUM!	20.75	#NUM!	23.98	#NUM!	27.20	-0.26	-3.92
10 to 20	#NUM!	2599.03	#NUM!	2988.90	#NUM!	3378.76	-0.02	-43.09
20 to 30	3.67	9.21	3.94	10.41	4.19	11.62	0.42	2.39
30 to 40	2.12	5.56	2.27	6.14	2.41	6.71	0.61	1.66
40 to 50	1.42	4.49	1.52	4.83	1.61	5.17	0.80	1.27
50 to 60	1.55	4.65	1.66	5.03	1.77	5.41	0.75	1.35
60 to 70	2.39	6.10	2.56	6.77	2.72	7.45	0.57	1.80
70 to 80	4.83	12.54	5.18	14.27	5.51	16.01	0.35	2.87
80 to 90	5.99	16.24	6.42	18.54	6.83	20.85	0.31	3.31
90 to 100	5.36	14.18	5.75	16.17	6.11	18.16	0.33	3.08
100 to 110	2.25	5.81	2.41	6.43	2.56	7.06	0.59	1.72
110 to 120	2.00	5.35	2.15	5.88	2.28	6.42	0.64	1.60
120 to 130	2.92	7.28	3.13	8.16	3.33	9.05	0.50	2.05
130 to 140	3.39	8.45	3.63	9.53	3.86	10.61	0.45	2.27
140 to 150	3.67	9.21	3.94	10.41	4.19	11.62	0.42	2.39
150 to 160	4.83	12.54	5.18	14.27	5.51	16.01	0.35	2.87
160 to 170	15.15	53.50	16.25	61.46	17.28	69.42	0.17	6.16
170 to 180	#NUM!	288.59	#NUM!	331.91	#NUM!	375.23	-0.07	-14.36
180 to 190	#NUM!	14.52	#NUM!	16.83	#NUM!	19.14	-0.31	-3.31
190 to 200	#NUM!	3.40	#NUM!	4.13	#NUM!	4.87	-0.54	-1.87

Cross Secion 6+00
Water Level 5.18

Calculation Spreadsheet
Velocity from Manning's Equation
Adjusted Depth

Interval (n)	Slope S	Depth Adjusted Manning's Velocity v_m= (1.49)(y_a^0.67)s^0.5/ n where n=0.025	Depth Adjusted Manning's v Simplified Froude Number F_{msa}= v_m/(gy_a)^0.5	Depth Adjusted Manning's v Simplified Specific Energy E=y_a+ v_m^2/2g	Depth Adjusted Manning's v Simplified Velocity/ Critical Velocity v_m/v_c	Depth Adjusted Manning's v Original Froude Number F_{ma}= v_m/ (gy_a/1.15)^0.5	Depth Adjusted Manning's v Original Specific Energy E=y_a+ 1.15v_m^2/2g	Depth Adjusted Manning's v Original Froude Number F_{ma}=v_m/ (gy_a/1.30)^0.5	Depth Adjusted Manning's v Original Specific Energy E=y_a+ 1.30v_m^2/2g
6+00									
-40 to '-30									
-30 to '-20	0.0045	#NUM!	#NUM!	#NUM!	#NUM!	#NUM!	#NUM!	#NUM!	#NUM!
-20 to '-10	0.0045	#NUM!	#NUM!	#NUM!	#NUM!	#NUM!	#NUM!	#NUM!	#NUM!
-10 to 0	0.0045	#NUM!	#NUM!	#NUM!	#NUM!	#NUM!	#NUM!	#NUM!	#NUM!
0 to 10	0.0045	#NUM!	#NUM!	#NUM!	#NUM!	#NUM!	#NUM!	#NUM!	#NUM!
10 to 20	0.0045	#NUM!	#NUM!	#NUM!	#NUM!	#NUM!	#NUM!	#NUM!	#NUM!
20 to 30	0.0045	4.49	0.73	1.50	0.47	0.78	1.55	0.83	1.60
30 to 40	0.0045	5.74	0.77	2.23	0.61	0.83	2.31	0.88	2.39
40 to 50	0.0045	6.87	0.81	2.98	0.73	0.87	3.09	0.92	3.20
50 to 60	0.0045	6.60	0.80	2.79	0.70	0.86	2.89	0.92	3.00
60 to 70	0.0045	5.44	0.76	2.05	0.57	0.82	2.12	0.87	2.19
70 to 80	0.0045	3.97	0.71	1.24	0.42	0.76	1.27	0.80	1.31
80 to 90	0.0045	3.61	0.69	1.06	0.38	0.74	1.09	0.79	1.12
90 to 100	0.0045	3.79	0.70	1.15	0.40	0.75	1.18	0.80	1.22
100 to 110	0.0045	5.59	0.77	2.14	0.59	0.83	2.21	0.88	2.29
110 to 120	0.0045	5.89	0.78	2.32	0.62	0.84	2.40	0.89	2.49
120 to 130	0.0045	4.98	0.75	1.77	0.53	0.80	1.83	0.85	1.89
130 to 140	0.0045	4.65	0.73	1.59	0.49	0.79	1.64	0.84	1.69
140 to 150	0.0045	4.49	0.73	1.50	0.47	0.78	1.55	0.83	1.60
150 to 160	0.0045	3.97	0.71	1.24	0.42	0.76	1.27	0.80	1.31
160 to 170	0.0045	2.38	0.62	0.55	0.25	0.66	0.56	0.71	0.58
170 to 180	0.0045	#NUM!	#NUM!	#NUM!	#NUM!	#NUM!	#NUM!	#NUM!	#NUM!
180 to 190	0.0045	#NUM!	#NUM!	#NUM!	#NUM!	#NUM!	#NUM!	#NUM!	#NUM!
190 to 200	0.0045	#NUM!	#NUM!	#NUM!	#NUM!	#NUM!	#NUM!	#NUM!	#NUM!

Cross Section 6+00
Water Level 5.18

Calculation Spreadsheet
Panel Froude Equation

Interval (n)	Discharge (Q) cfs.	Channel Area (A_c)	Water Elevation (WE)	Interval Elevation (E_n)	Water Depth (y) ft.	Interval width (b_i) ft.	Interval Area (A_I)	Area Ratio (A_r)=Area Interval (A_T)/Area Channel (A_c)	Acceleration due to gravity (g) ft/sec/sec	Discharge in Interval $Q_n=Q(A_r)$	$q_{pan}=Q_n/b_i$
6+00											
-40 to '-30											
-30 to '-20	4210	312.35	90	95.7	-5.7	10	-57	-0.18	32	-768.3	-76.83
-20 to '-10	4210	312.35	90	94	-4	10	-40	-0.13	32	-539.1	-53.91
-10 to 0	4210	312.35	90	92.4	-2.4	10	-24	-0.08	32	-323.5	-32.35
0 to 10	4210	312.35	90	91.1	-1.1	10	-11	-0.04	32	-148.3	-14.83
10 to 20	4210	312.35	90	90.1	-0.1	10	-1	0.00	32	-13.5	-1.35
20 to 30	4210	312.35	90	88.2	1.8	10	18	0.06	32	242.6	24.26
30 to 40	4210	312.35	90	87.4	2.6	10	26	0.08	32	350.4	35.04
40 to 50	4210	312.35	90	86.6	3.4	10	34	0.11	32	458.3	45.83
50 to 60	4210	312.35	90	86.8	3.2	10	32	0.10	32	431.3	43.13
60 to 70	4210	312.35	90	87.6	2.4	10	24	0.08	32	323.5	32.35
70 to 80	4210	312.35	90	88.5	1.5	10	15	0.05	32	202.2	20.22
80 to 90	4210	312.35	90	88.7	1.3	10	13	0.04	32	175.2	17.52
90 to 100	4210	312.35	90	88.6	1.4	10	14	0.04	32	188.7	18.87
100 to 110	4210	312.35	90	87.5	2.5	10	25	0.08	32	337.0	33.70
110 to 120	4210	312.35	90	87.3	2.7	10	27	0.09	32	363.9	36.39
120 to 130	4210	312.35	90	87.9	2.1	10	21	0.07	32	283.1	28.31
130 to 140	4210	312.35	90	88.1	1.9	10	19	0.06	32	256.1	25.61
140 to 150	4210	312.35	90	88.2	1.8	10	18	0.06	32	242.6	24.26
150 to 160	4210	312.35	90	88.5	1.5	10	15	0.05	32	202.2	20.22
160 to 170	4210	312.35	90	89.3	0.7	10	7	0.02	32	94.4	9.44
170 to 180	4210	312.35	90	90.3	-0.3	10	-3	-0.01	32	-40.4	-4.04
180 to 190	4210	312.35	90	91.3	-1.3	10	-13	-0.04	32	-175.2	-17.52
190 to 200	4210	312.35	90	92.3	-2.3	10	-23	-0.07	32	-310.0	-31.00

Cross Section 6+00
Water Level 5.18

Calculation Spreadsheet
Panel Froude Equation

Interval (n)	Velocity $v=q_{pan}/y$	Critical Depth (y_c) = $(q_{pan}\text{^}2/g)\text{^}0.33$	Critical Velocity $v_c=(g(y_c))\text{^}0.5$	Froude Number F_{pan} = $v/(gy)\text{^}0.5$	Specific Energy $E = y+ v\text{^}2/2g$	Depth/ Critical Depth y/y_c	Velocity/ Critical Velocity v/v_c
6+00							
-40 to -30							
-30 to -20	13.48	5.68	13.48	#NUM!	-2.86	-1.00	1.00
-20 to -10	13.48	4.49	11.98	#NUM!	-1.16	-0.89	1.12
-10 to 0	13.48	3.19	10.11	#NUM!	0.44	-0.75	1.33
0 to 10	13.48	1.90	7.80	#NUM!	1.74	-0.58	1.73
10 to 20	13.48	0.38	3.51	#NUM!	2.74	-0.26	3.84
20 to 30	13.48	2.64	9.19	1.78	4.64	0.68	1.47
30 to 40	13.48	3.37	10.38	1.48	5.44	0.77	1.30
40 to 50	13.48	4.03	11.35	1.29	6.24	0.84	1.19
50 to 60	13.48	3.87	11.13	1.33	6.04	0.83	1.21
60 to 70	13.48	3.19	10.11	1.54	5.24	0.75	1.33
70 to 80	13.48	2.34	8.65	1.95	4.34	0.64	1.56
80 to 90	13.48	2.12	8.24	2.09	4.14	0.61	1.64
90 to 100	13.48	2.23	8.45	2.01	4.24	0.63	1.60
100 to 110	13.48	3.28	10.25	1.51	5.34	0.76	1.32
110 to 120	13.48	3.45	10.51	1.45	5.54	0.78	1.28
120 to 130	13.48	2.92	9.67	1.64	4.94	0.72	1.39
130 to 140	13.48	2.73	9.35	1.73	4.74	0.69	1.44
140 to 150	13.48	2.64	9.19	1.78	4.64	0.68	1.47
150 to 160	13.48	2.34	8.65	1.95	4.34	0.64	1.56
160 to 170	13.48	1.41	6.71	2.85	3.54	0.50	2.01
170 to 180	13.48	0.80	5.06	#NUM!	2.54	-0.38	2.66
180 to 190	13.48	2.12	8.24	#NUM!	1.54	-0.61	1.64
190 to 200	13.48	3.10	9.97	#NUM!	0.54	-0.74	1.35

Cross Section 6+00
Water Level 5.18

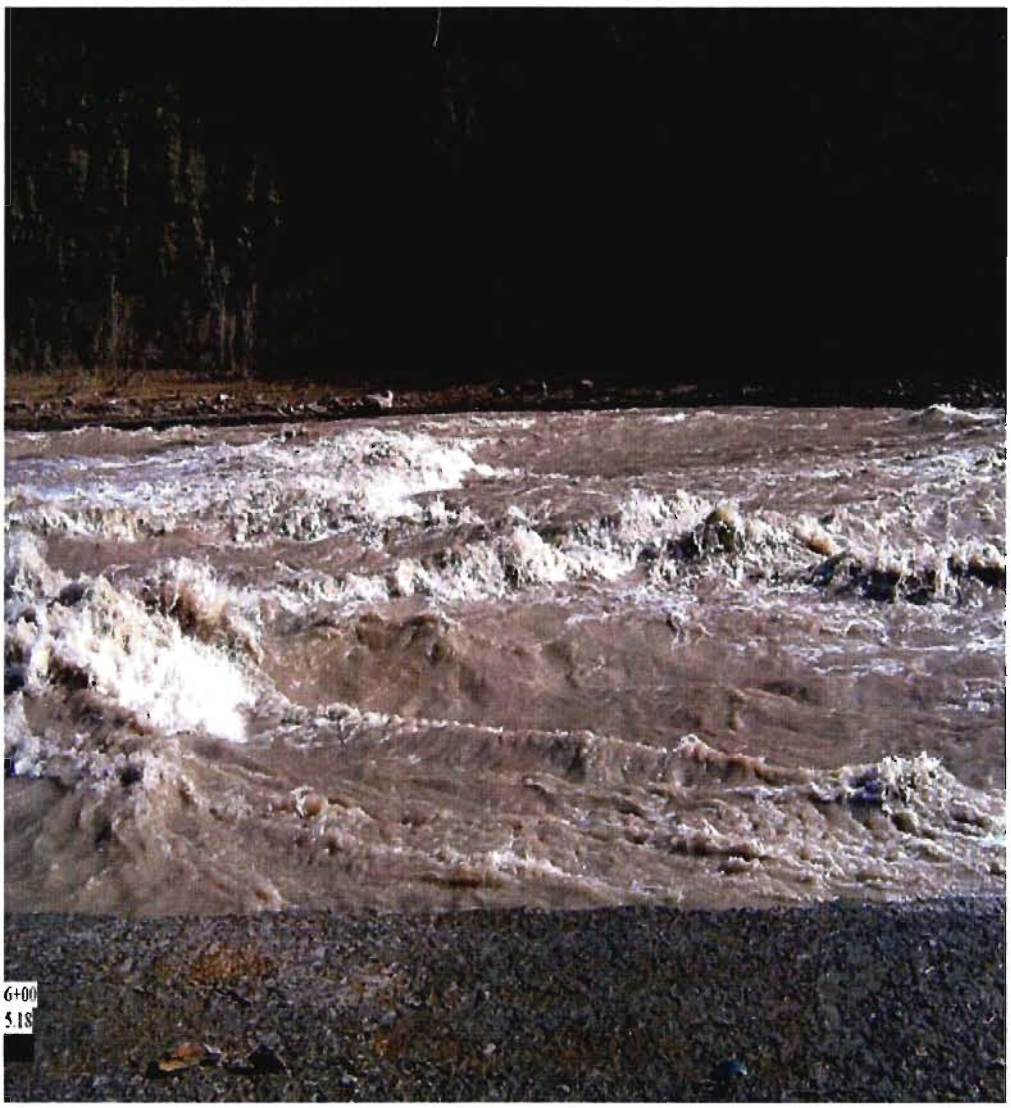

Cross Section 6+00
Water Level 5.18

Interval (n)	Flow Condition	Comments	Simplified Froude Number $F_{fs}=v_f/(gy)^{0.5}$	Manning's v Simplified Froude Number $F_{ms}=v_m/(gy)^{0.5}$	Original Froude Number $F_f=v_f/(gy/1.15)^{0.5}$	Manning's v Original Froude Number $F_m=v_m/(gy/1.15)^{0.5}$	Original Froude Number $F_f=v_f/(gy/1.30)^{0.5}$	Manning's v Original Froude Number $F_m=v_m/(gy/1.30)^{0.5}$
6+00								
-40 to -30								
-30 to -20								
-20 to -10								
-10 to 0								
0 to 10								
10 to 20								
20 to 30	super	diagonal waves	1.97	0.78	2.11	0.84	2.25	0.89
30 to 40	super	smooth	1.14	0.83	1.22	0.89	1.29	0.95
40 to 50	super	smooth	0.76	0.87	0.81	0.93	0.87	0.99
50 to 60	super	diagonal waves	0.83	0.86	0.89	0.92	0.95	0.98
60 to 70	super	smooth	1.28	0.82	1.37	0.88	1.46	0.94
70 to 80	super	smooth	2.59	0.76	2.78	0.81	2.95	0.86
80 to 90	super	smooth	3.21	0.74	3.44	0.79	3.66	0.84
90 to 100	super	smooth	2.87	0.75	3.08	0.80	3.28	0.85
100 to 110	super	smooth	1.20	0.83	1.29	0.89	1.37	0.94
110 to 120	super	smooth	1.07	0.84	1.15	0.90	1.22	0.95
120 to 130	super	smooth	1.56	0.80	1.68	0.86	1.78	0.91
130 to 140	super	smooth	1.82	0.79	1.95	0.85	2.07	0.90
140 to 150	super	smooth	1.97	0.78	2.11	0.84	2.25	0.89
150 to 160	super	smooth	2.59	0.76	2.78	0.81	2.95	0.86
160 to 170	super	smooth	8.12	0.67	8.71	0.71	9.26	0.76
170 to 180								
180 to 190								
190 to 200								

Cross Section 6+00
Water Level 5.18

Interval (n)	Flow Condition	Comments	Simplified Froude Number $F_{hs}=v_h/(gy)^{0.5}$	Manning's v Simplified Froude Number $F_{ms}=v_m/(gy)^{0.5}$	Original Froude Number $F_h=v_h/(gy/1.15)^{0.5}$	Manning's v Original Froude Number $F_m=v_m/(gy/1.15)^{0.5}$	Original Froude Number $F_h=v_h/(gy/1.30)^{0.5}$	Manning's v Original Froude Number $F_m=v_m/(gy/1.30)^{0.5}$
6+00								
-40 to -30								
-30 to -20								
-20 to -10								
-10 to 0								
0 to 10								
10 to 20								
20 to 30	super	diagonal waves	1.97	0.78	2.11	0.84	2.25	0.89
30 to 40	super	smooth	1.14	0.83	1.22	0.89	1.29	0.95
40 to 50	super	smooth	0.76	0.87	0.81	0.93	0.87	0.99
50 to 60	super	diagonal waves	0.83	0.86	0.89	0.92	0.95	0.98
60 to 70	super	smooth	1.28	0.82	1.37	0.88	1.46	0.94
70 to 80	super	smooth	2.59	0.76	2.78	0.81	2.95	0.86
80 to 90	super	smooth	3.21	0.74	3.44	0.79	3.66	0.84
90 to 100	super	smooth	2.87	0.75	3.08	0.80	3.28	0.85
100 to 110	super	smooth	1.20	0.83	1.29	0.89	1.37	0.94
110 to 120	super	smooth	1.07	0.84	1.15	0.90	1.22	0.95
120 to 130	super	smooth	1.56	0.80	1.68	0.86	1.78	0.91
130 to 140	super	smooth	1.82	0.79	1.95	0.85	2.07	0.90
140 to 150	super	smooth	1.97	0.78	2.11	0.84	2.25	0.89
150 to 160	super	smooth	2.59	0.76	2.78	0.81	2.95	0.86
160 to 170	super	smooth	8.12	0.67	8.71	0.71	9.26	0.76
170 to 180								
180 to 190								
190 to 200								

Cross Section 6+00
Water Level 5.18

Appendix IV

Froude Number Maps

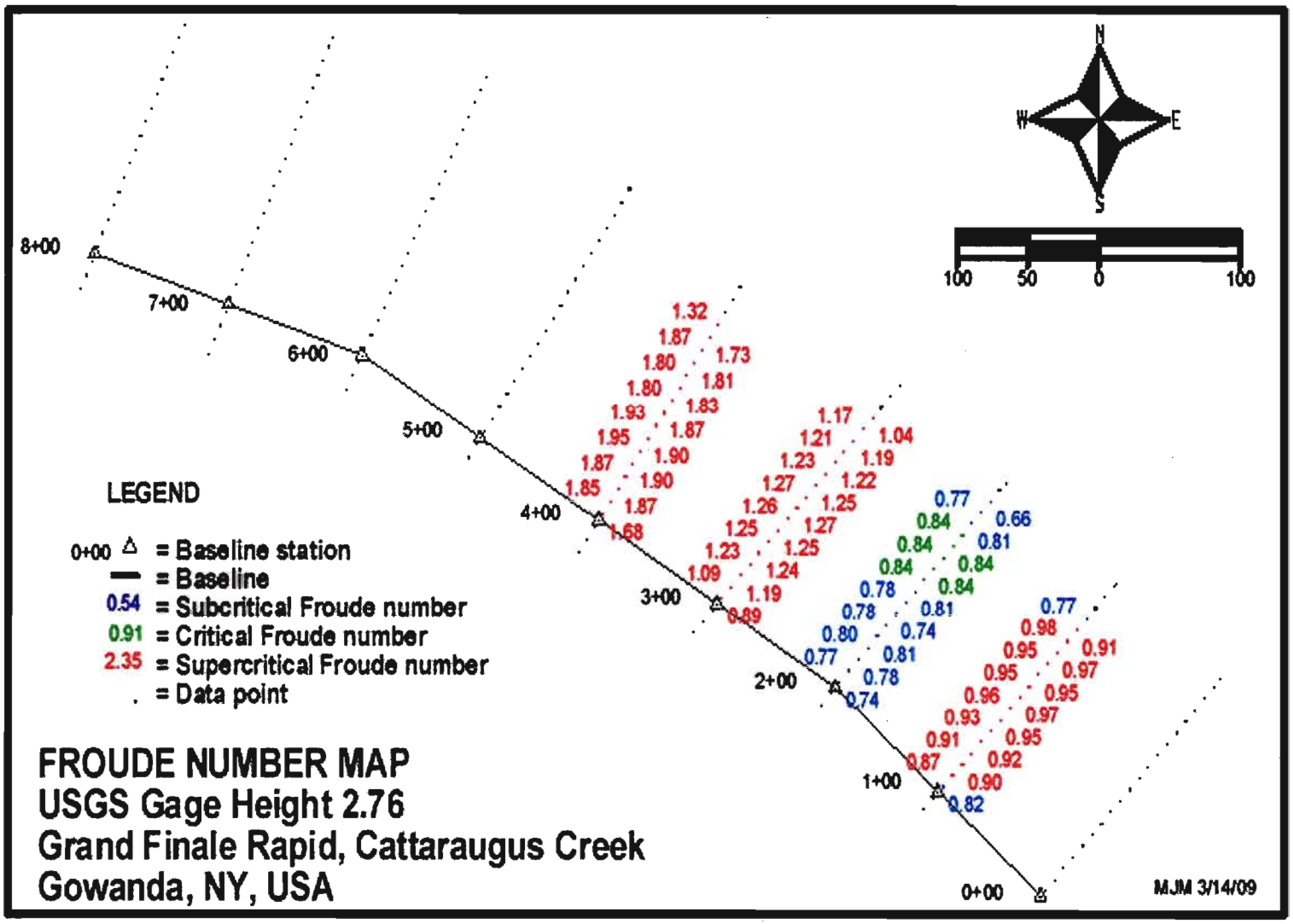
N
W
E
S
100
50
0
100
8+00
7+00
6+00
5+00
4+00
3+00
2+00
1+00
0+00
1.32
1.87
1.80
1.73
1.80
1.81
1.93
1.83
1.95
1.87
1.87
1.90
1.85
1.90
1.87
1.68
1.17
1.21
1.04
1.23
1.19
1.27
1.22
1.26
1.25
1.25
1.27
1.23
1.25
1.09
1.24
1.19
0.89
0.77
0.84
0.66
0.84
0.81
0.84
0.84
0.78
0.84
0.78
0.81
0.80
0.74
0.77
0.81
0.78
0.74
0.77
0.98
0.95
0.91
0.95
0.97
0.96
0.95
0.93
0.97
0.91
0.95
0.87
0.92
0.90
0.82
LEGEND
0+00 = Baseline station
= Baseline
0.54 = Subcritical Froude number
0.91 = Critical Froude number
2.35 = Supercritical Froude number
. = Data point
FROUDE NUMBER MAP
USGS Gage Height 2.76
Grand Finale Rapid, Cattaraugus Creek
Gowanda, NY, USA
MJM 3/14/09

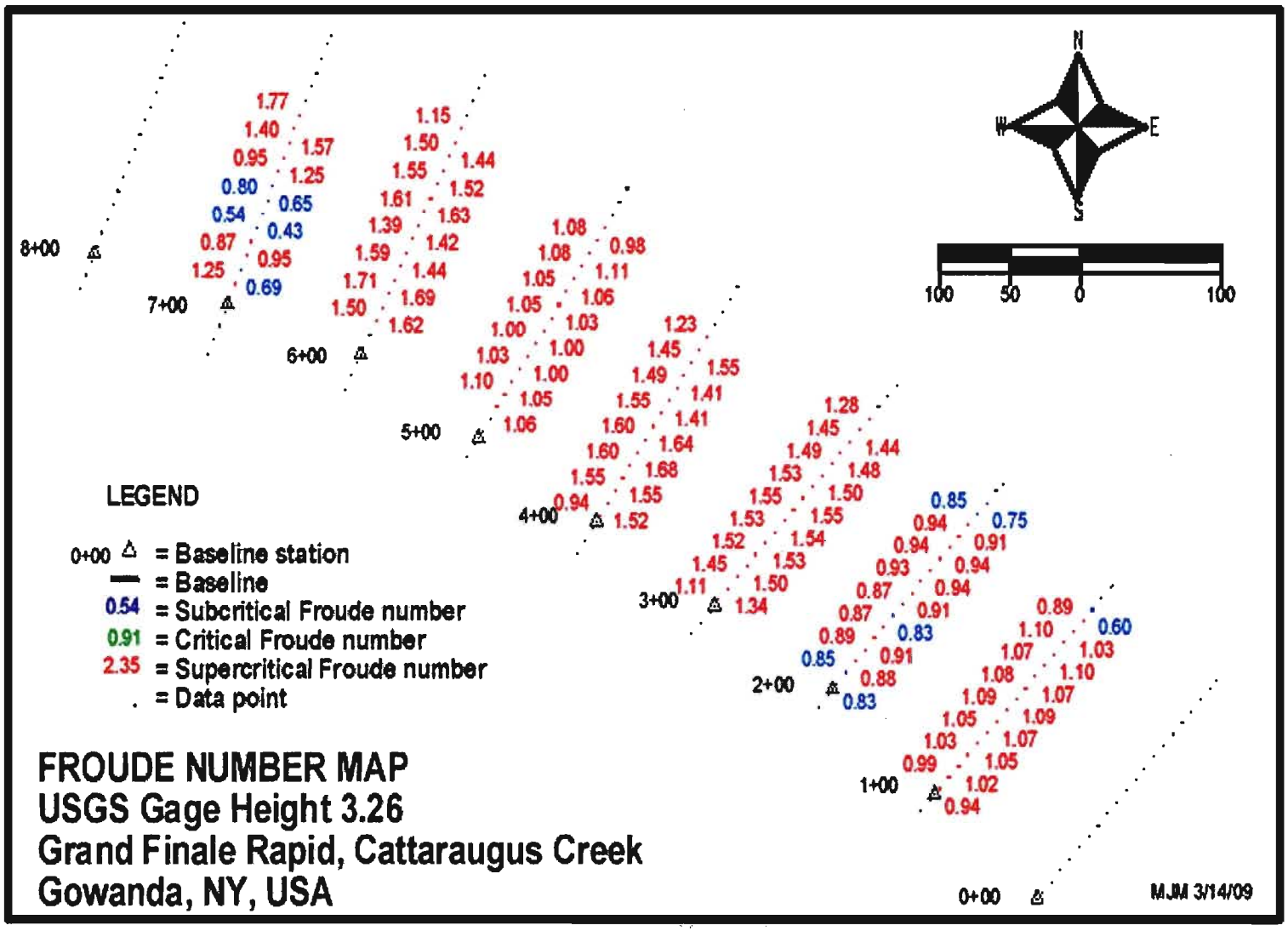
8+00
7+00
6+00
5+00
4+00
3+00
2+00
1+00
0+00
1.77
1.40
0.95
0.80
0.54
0.87
1.25
1.57
1.25
0.65
0.43
0.95
0.69
1.15
1.50
1.55
1.61
1.39
1.59
1.71
1.50
1.44
1.52
1.63
1.42
1.44
1.69
1.62
1.08
1.08
1.05
1.05
1.00
1.03
1.10
0.98
1.11
1.06
1.03
1.00
1.00
1.05
1.06
1.23
1.45
1.49
1.55
1.55
1.60
1.60
1.55
0.94
1.41
1.41
1.64
1.68
1.55
1.52
1.28
1.45
1.49
1.53
1.55
1.53
1.52
1.45
1.11
1.44
1.48
1.50
1.55
1.54
1.53
1.50
1.34
0.85
0.94
0.94
0.93
0.87
0.87
0.89
0.85
0.75
0.91
0.94
0.94
0.91
0.83
0.91
0.88
0.83
0.89
1.10
1.07
1.08
1.09
1.05
1.03
0.99
0.94
0.60
1.03
1.10
1.07
1.09
1.07
1.05
1.02
N
W
E
S
100
50
0
100
LEGEND
0+00 = Baseline station
= Baseline
0.54 = Subcritical Froude number
0.91 = Critical Froude number
2.35 = Supercritical Froude number
. = Data point
FROUDE NUMBER MAP
USGS Gage Height 3.26
Grand Finale Rapid, Cattaraugus Creek
Gowanda, NY, USA
MJM 3/14/09

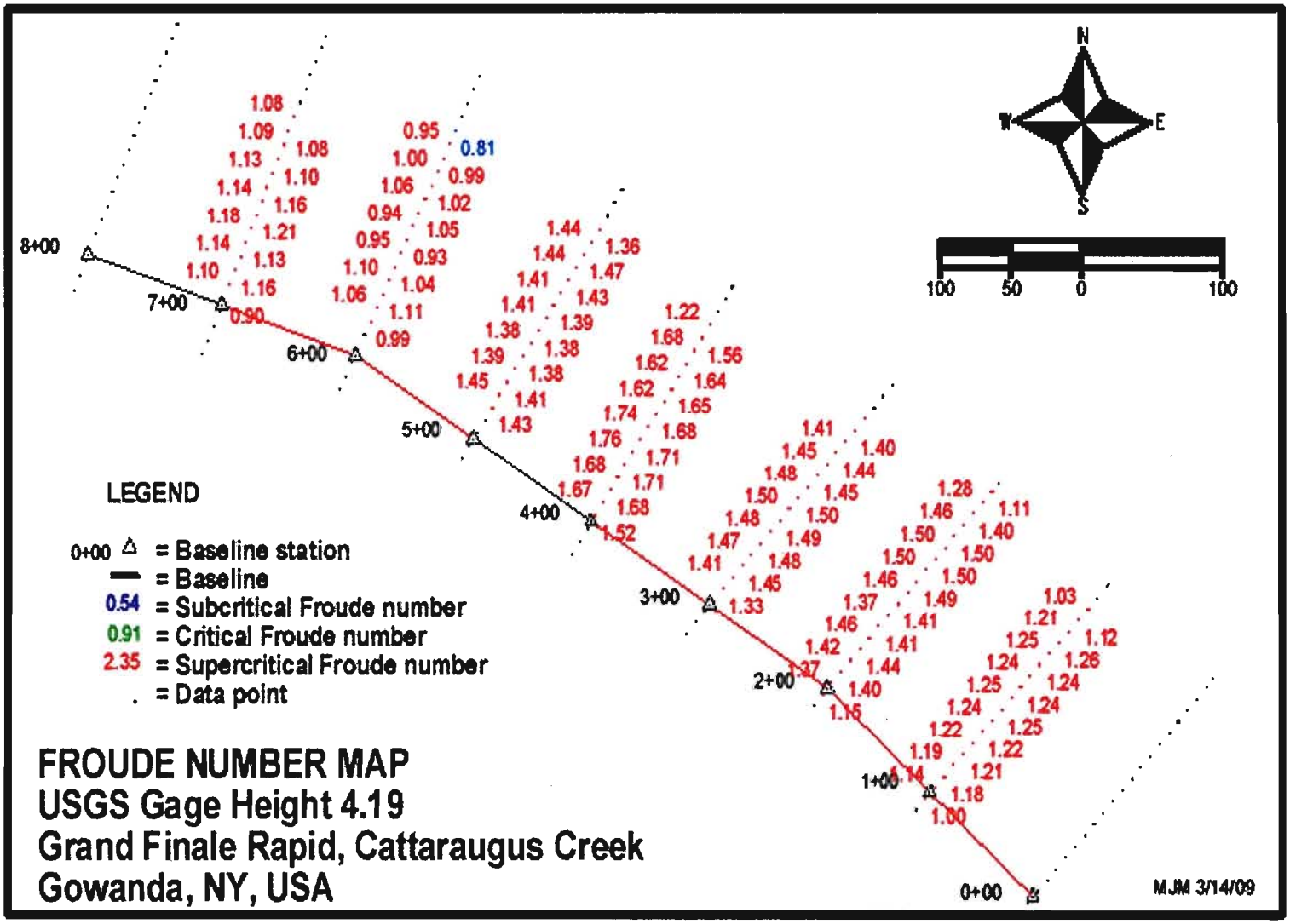
N
W
E
S
100 50 0 100
8+00
7+00
6+00
5+00
4+00
3+00
2+00
1+00
0+00
LEGEND
0+00 = Baseline station
= Baseline
0.54 = Subcritical Froude number
0.91 = Critical Froude number
2.35 = Supercritical Froude number
. = Data point
FROUDE NUMBER MAP
USGS Gage Height 4.19
Grand Finale Rapid, Cattaraugus Creek
Gowanda, NY, USA
MJM 3/14/09

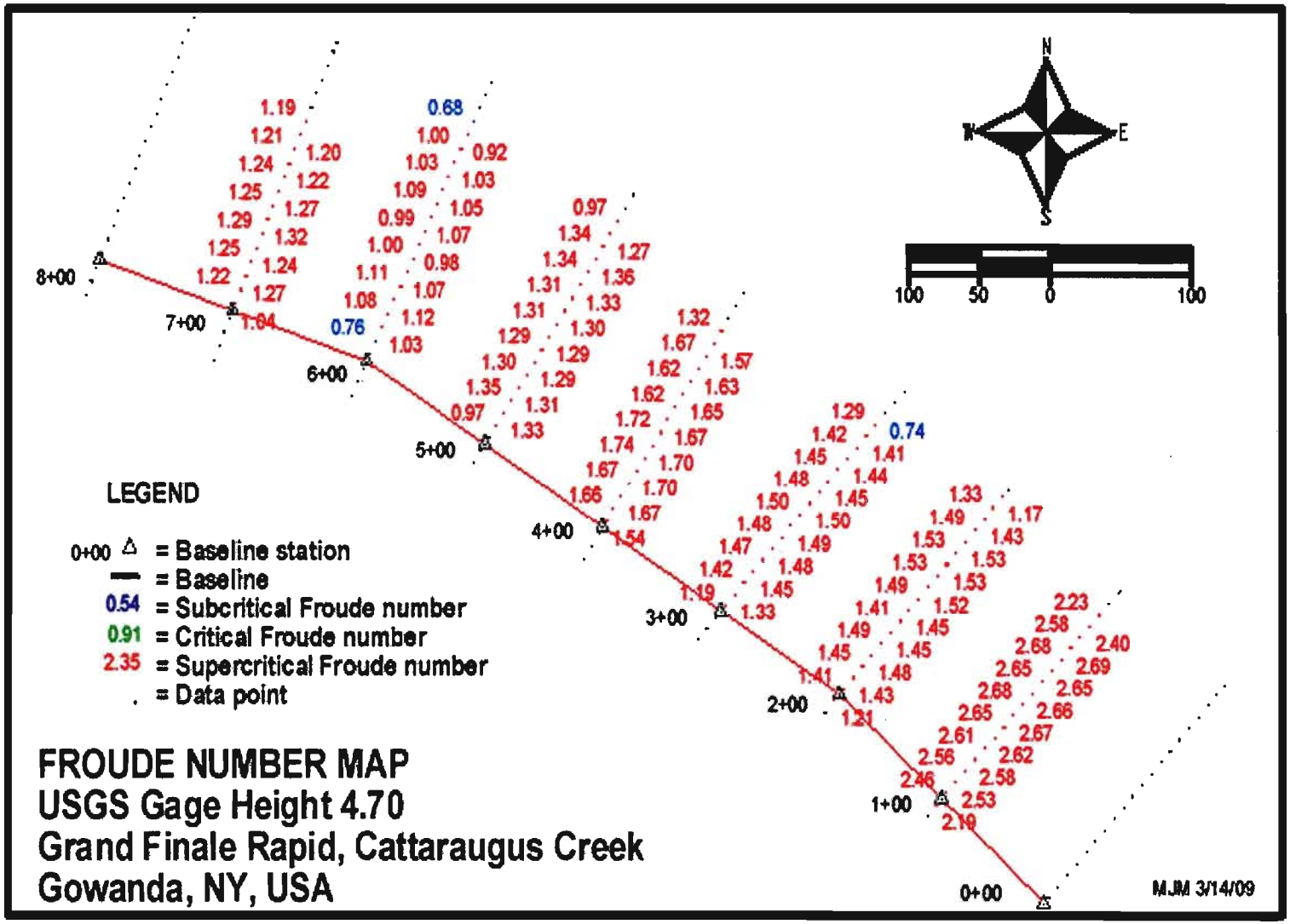
N
W
E
S
100 50 0 100
8+00
7+00
6+00
5+00
4+00
3+00
2+00
1+00
0+00
LEGEND
0+00 = Baseline station
= Baseline
0.54 = Subcritical Froude number
0.91 = Critical Froude number
2.35 = Supercritical Froude number
. = Data point
FROUDE NUMBER MAP
USGS Gage Height 4.70
Grand Finale Rapid, Cattaraugus Creek
Gowanda, NY, USA
MJM 3/14/09

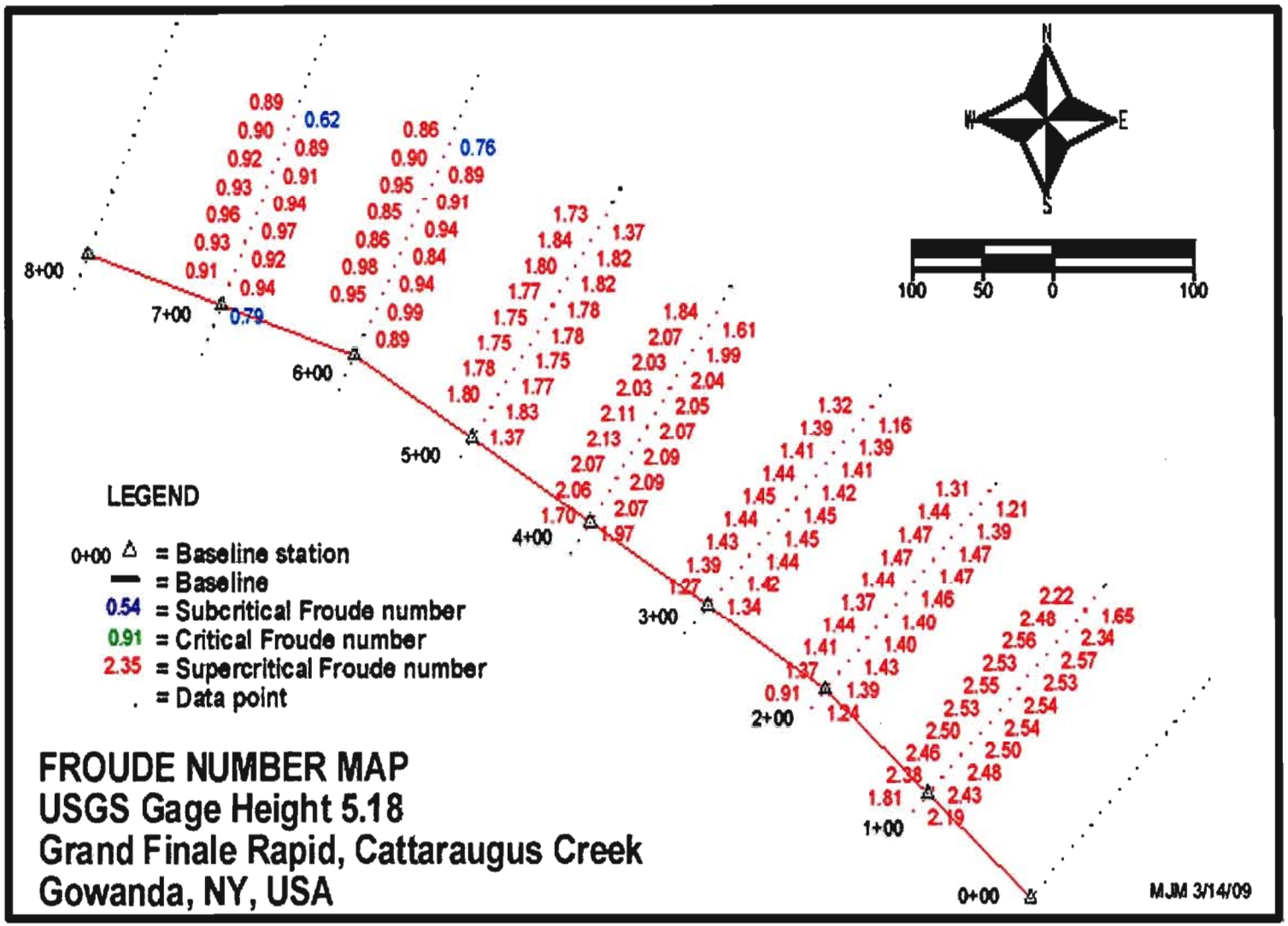
N
W
E
S
100
50
0
100
8+00
7+00
6+00
5+00
4+00
3+00
2+00
1+00
0+00
LEGEND
0+00 = Baseline station
= Baseline
0.54 = Subcritical Froude number
0.91 = Critical Froude number
2.35 = Supercritical Froude number
. = Data point
FROUDE NUMBER MAP
USGS Gage Height 5.18
Grand Finale Rapid, Cattaraugus Creek
Gowanda, NY, USA
MJM 3/14/09

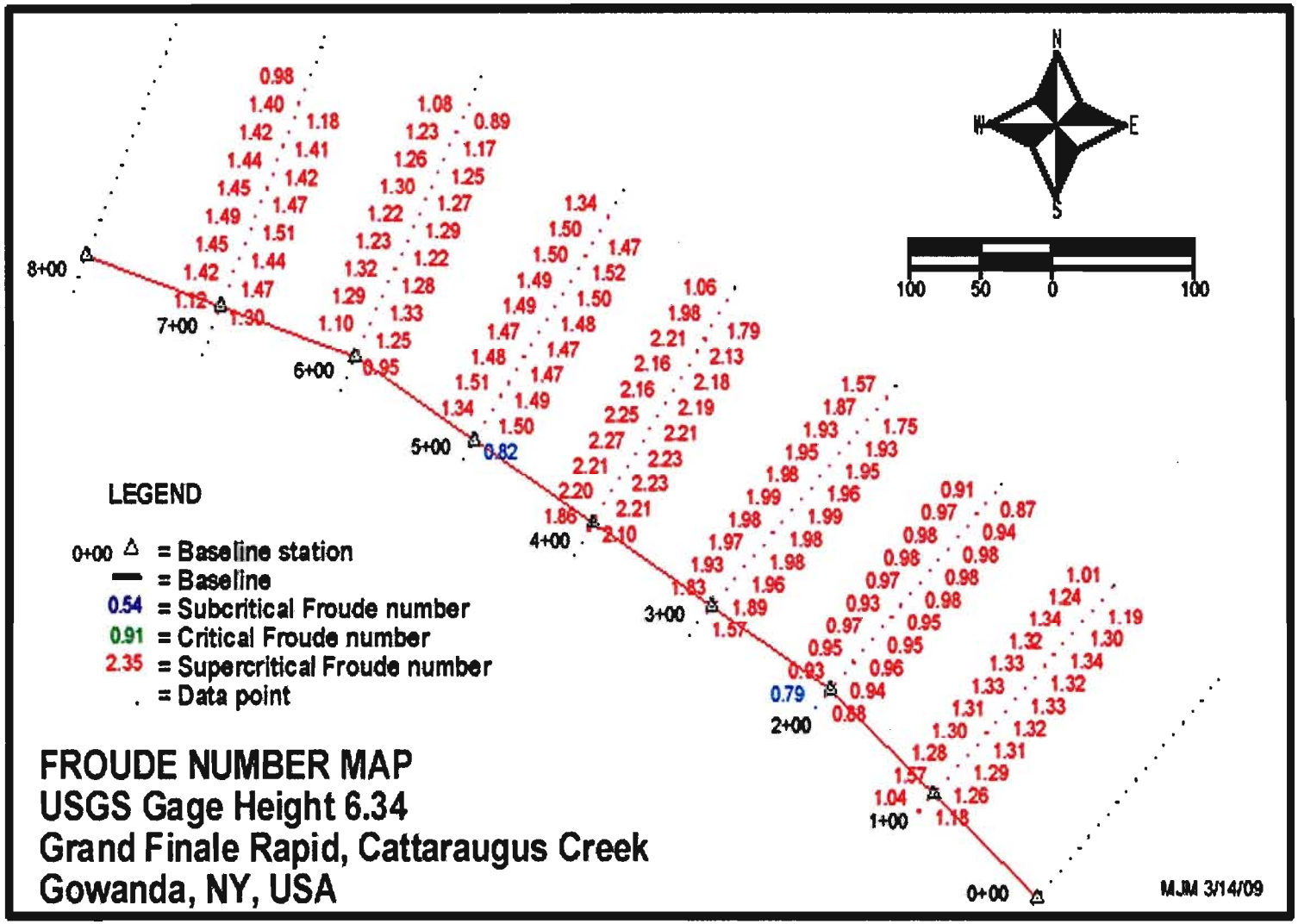
N
W
E
S
100
50
0
100
8+00
7+00
6+00
5+00
4+00
3+00
2+00
1+00
0+00
LEGEND
0+00 = Baseline station
= Baseline
0.54 = Subcritical Froude number
0.91 = Critical Froude number
2.35 = Supercritical Froude number
. = Data point
FROUDE NUMBER MAP
USGS Gage Height 6.34
Grand Finale Rapid, Cattaraugus Creek
Gowanda, NY, USA
MJM 3/14/09

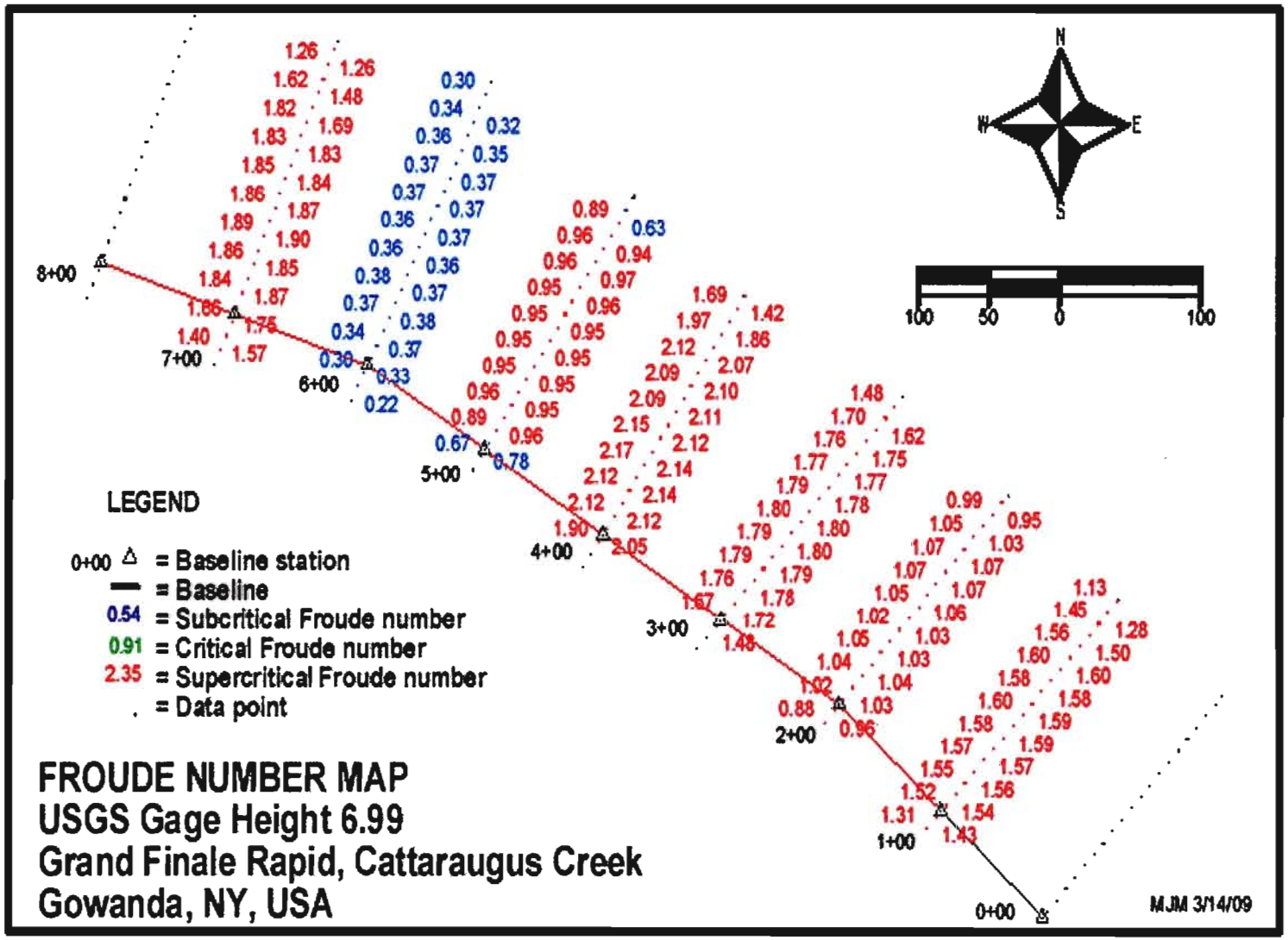
N
W
E
S
100 50 0 100
8+00
7+00
6+00
5+00
4+00
3+00
2+00
1+00
0+00
LEGEND
0+00 = Baseline station
= Baseline
0.54 = Subcritical Froude number
0.91 = Critical Froude number
2.35 = Supercritical Froude number
. = Data point
FROUDE NUMBER MAP
USGS Gage Height 6.99
Grand Finale Rapid, Cattaraugus Creek
Gowanda, NY, USA
MJM 3/14/09

Appendix V

Froude Number Contour Maps

Water Level by Cross Section Photos

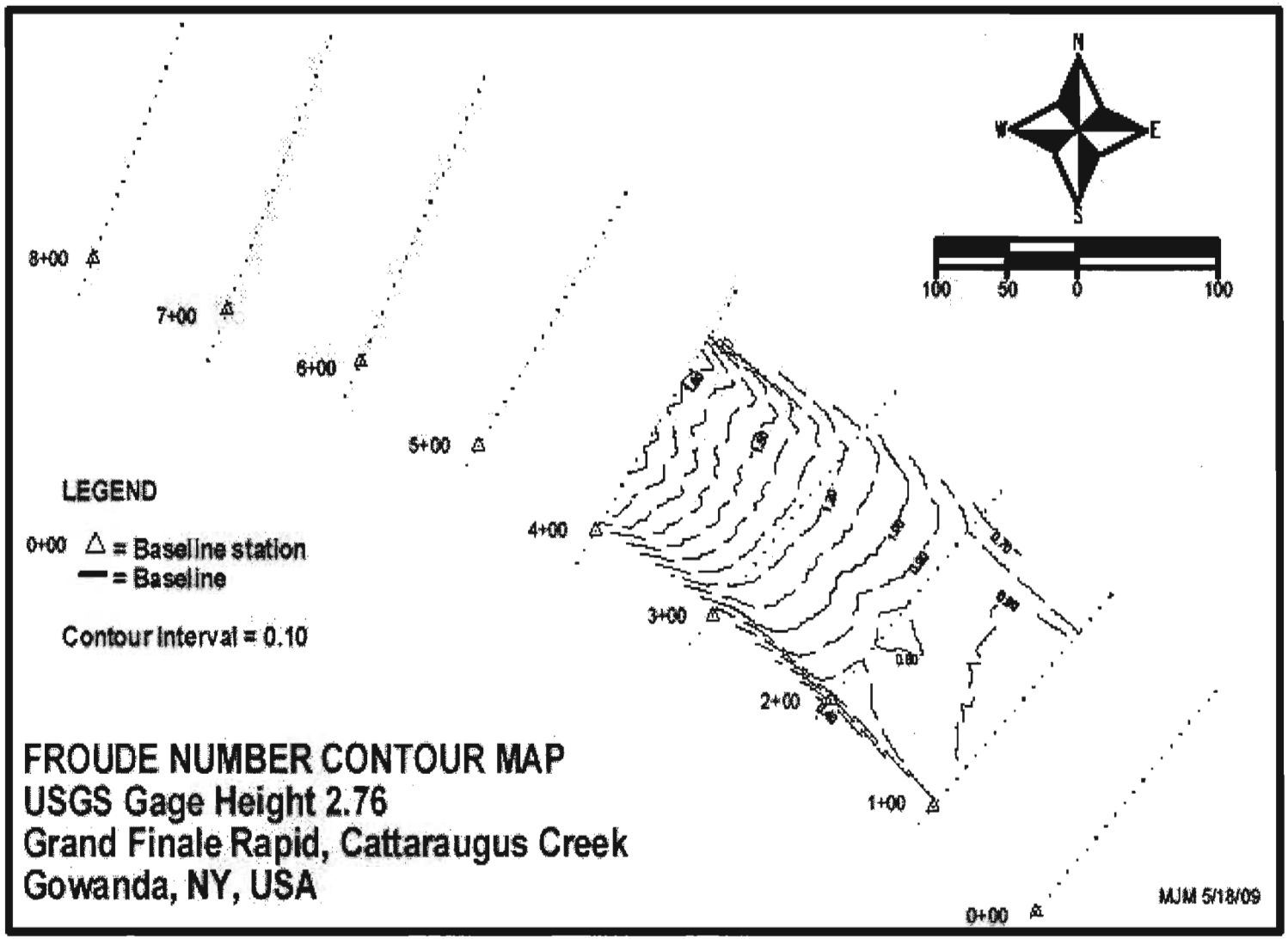
N
W
E
S
100
50
0
100
8+00
7+00
6+00
5+00
4+00
3+00
2+00
1+00
0+00
LEGEND
0+00 △ = Baseline station
— = Baseline
Contour Interval = 0.10
FROUDE NUMBER CONTOUR MAP
USGS Gage Height 2.76
Grand Finale Rapid, Cattaraugus Creek
Gowanda, NY, USA
MJM 5/18/09

1+00

2+00

3+00

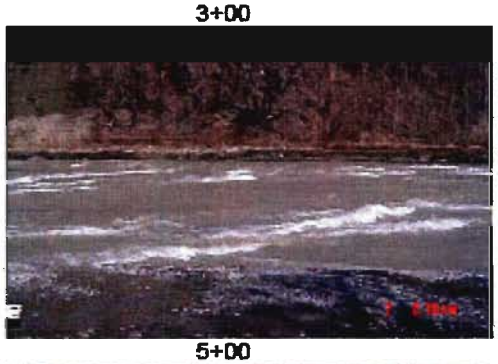

4+00

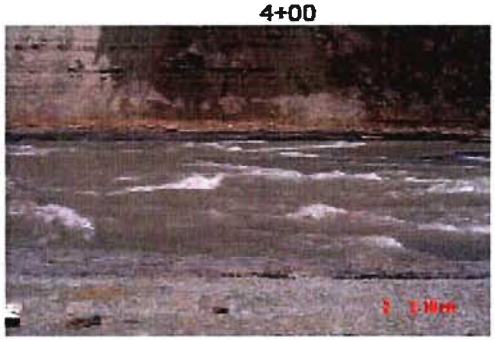

5+00

6+00

7+00

Water Level 2.76
by Cross Section

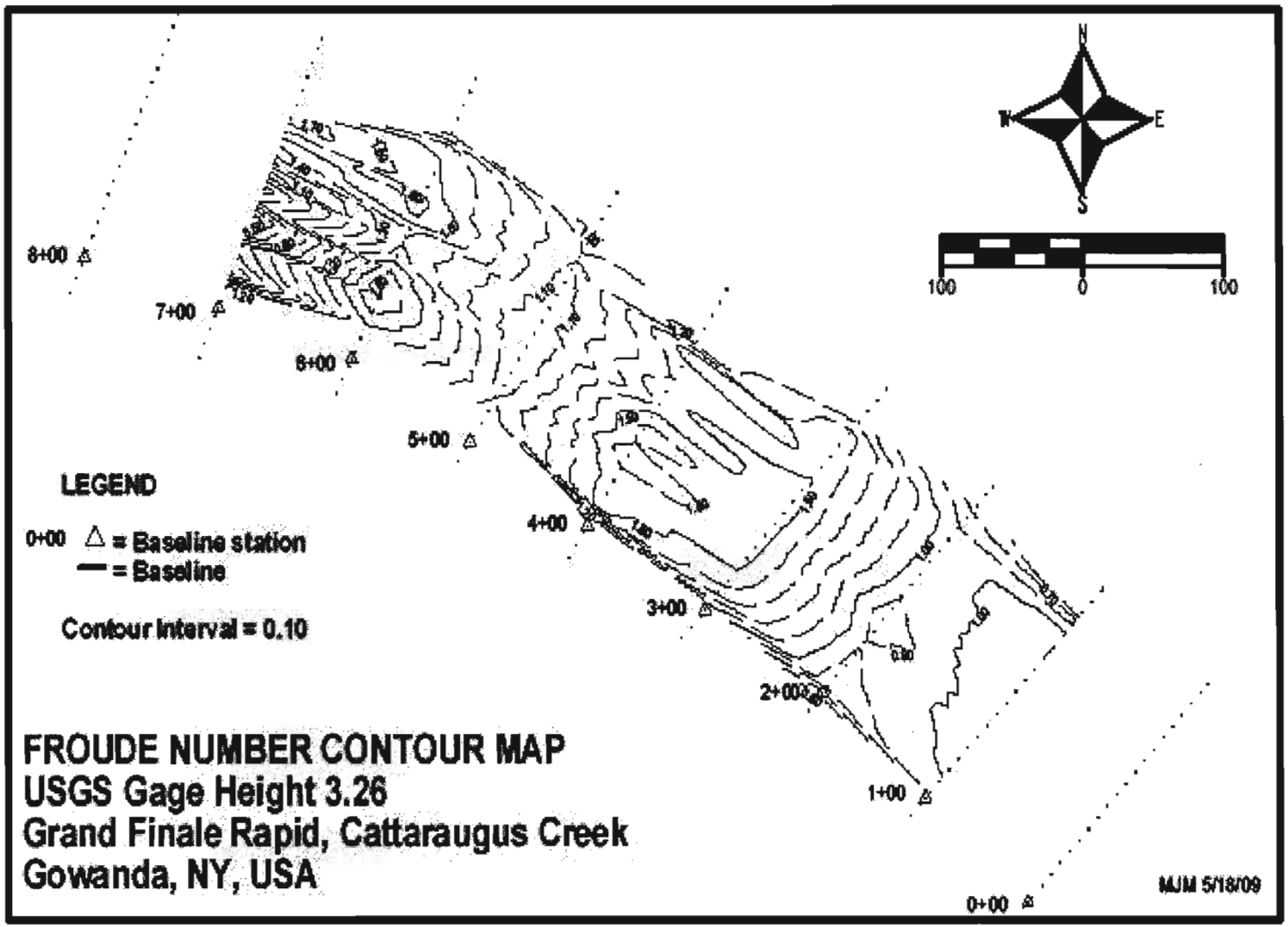
N
W
E
S
100
0
100
8+00
7+00
6+00
5+00
4+00
3+00
2+00
1+00
0+00
LEGEND
0+00 △ = Baseline station
— = Baseline
Contour Interval = 0.10
FROUDE NUMBER CONTOUR MAP
USGS Gage Height 3.26
Grand Finale Rapid, Cattaraugus Creek
Gowanda, NY, USA
MJM 5/18/09

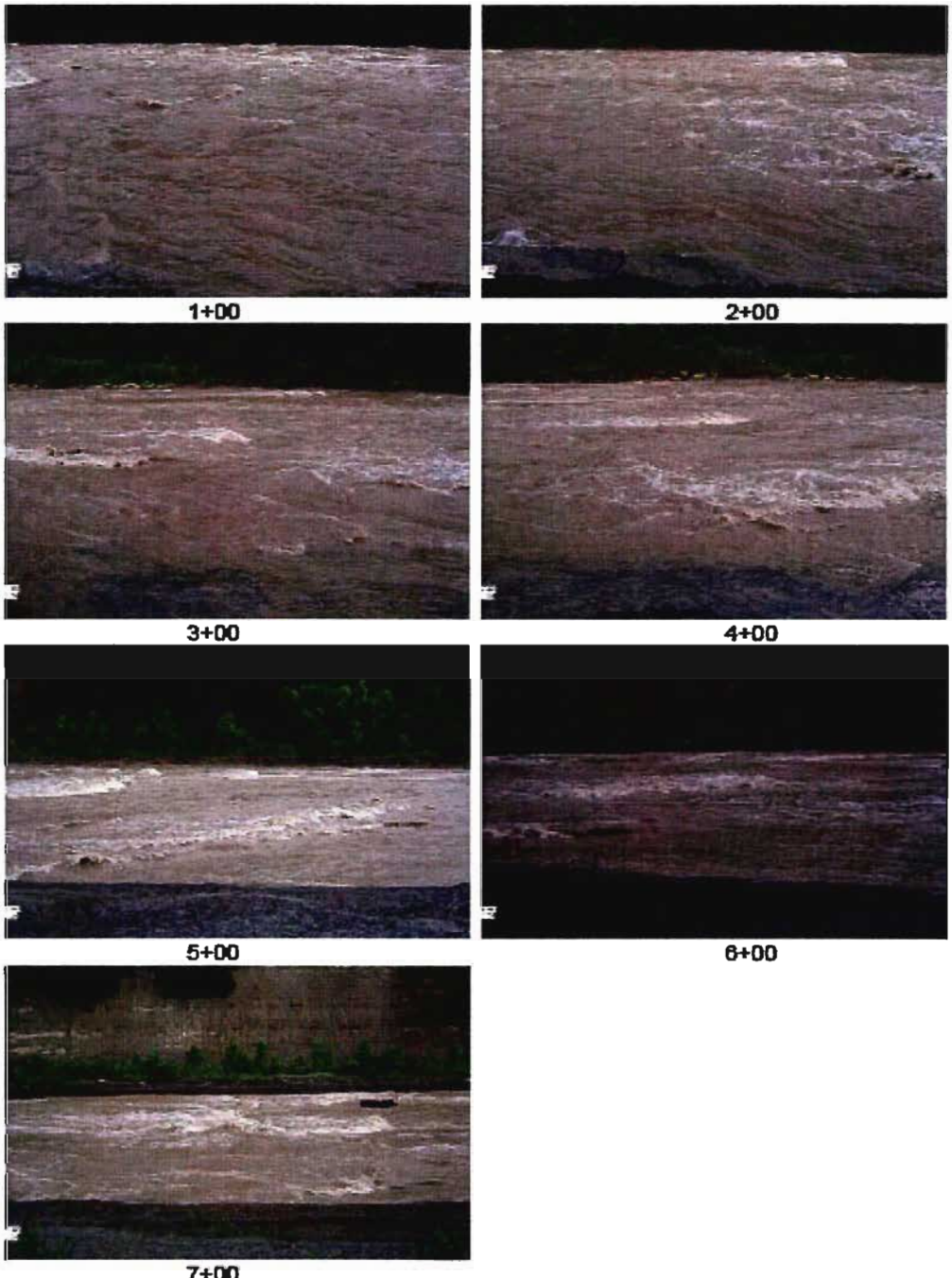

Water Level 3.26
by Cross Section

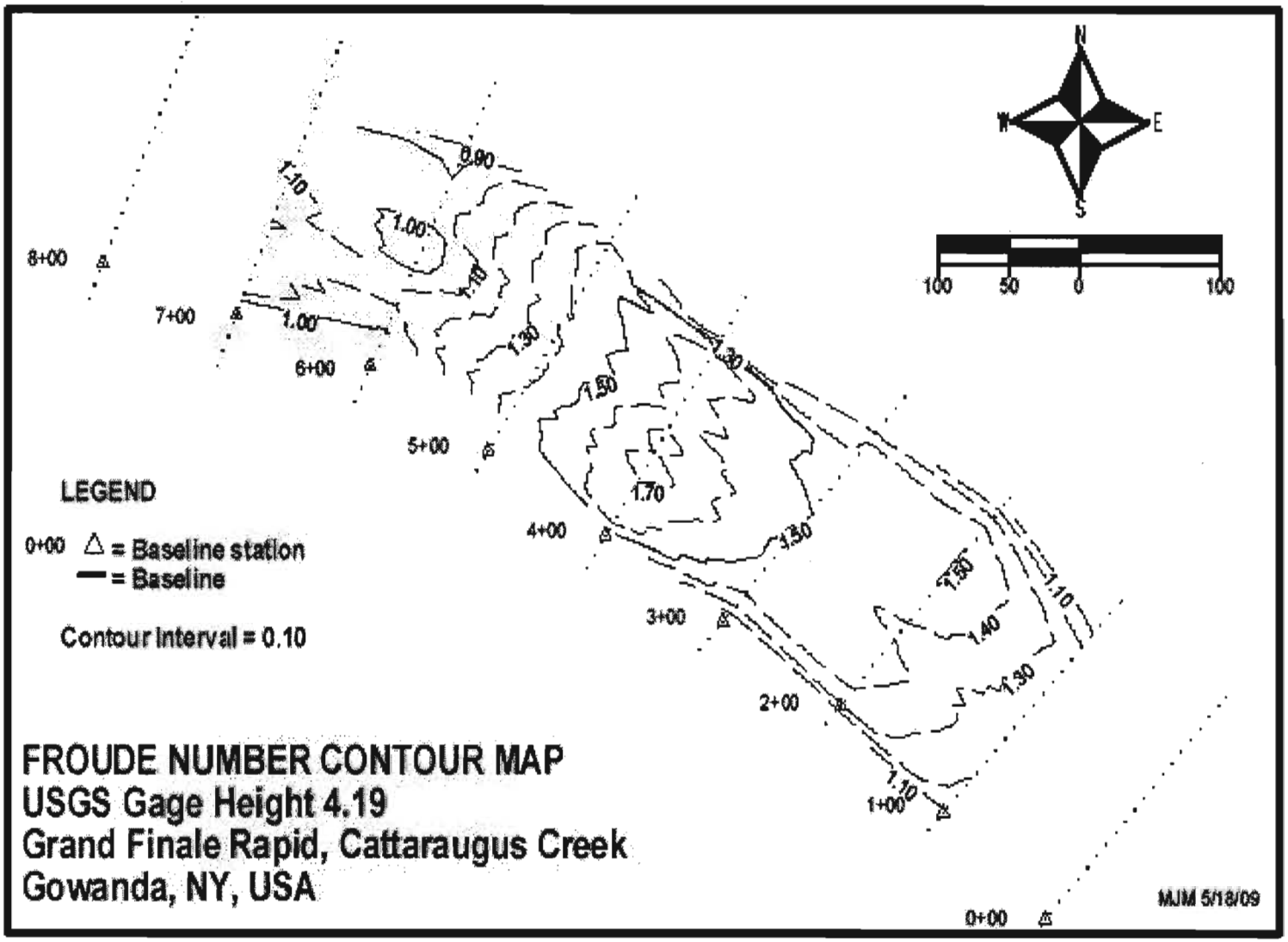
N
W
E
S
100
50
0
100
8+00
7+00
6+00
5+00
4+00
3+00
2+00
1+00
0+00
0.90
1.00
1.10
1.30
1.50
1.70
1.40
LEGEND
= Baseline station
= Baseline
Contour Interval = 0.10
FROUDE NUMBER CONTOUR MAP
USGS Gage Height 4.19
Grand Finale Rapid, Cattaraugus Creek
Gowanda, NY, USA
MJM 5/18/09

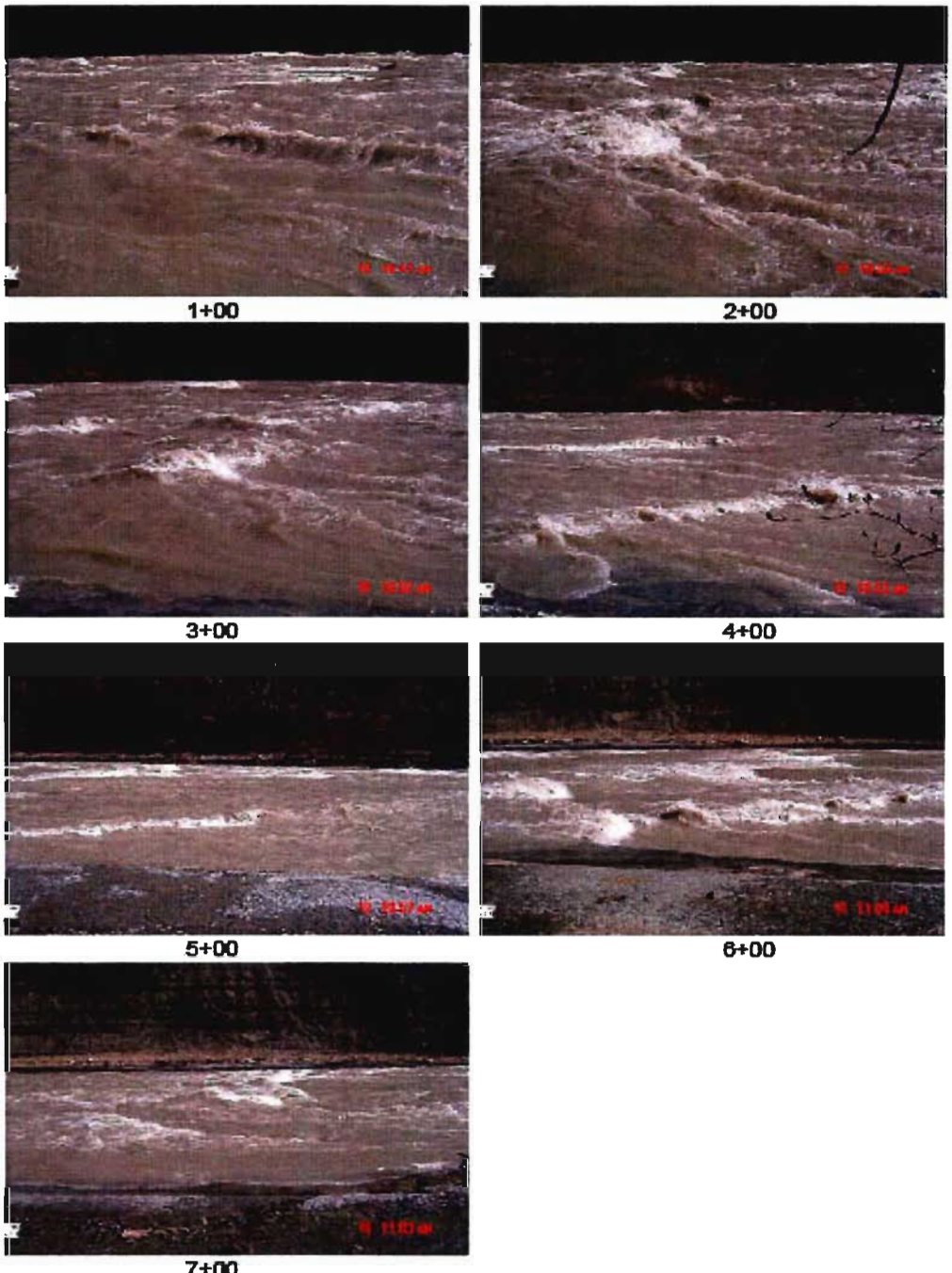

Water Level 4.19
by Cross Section

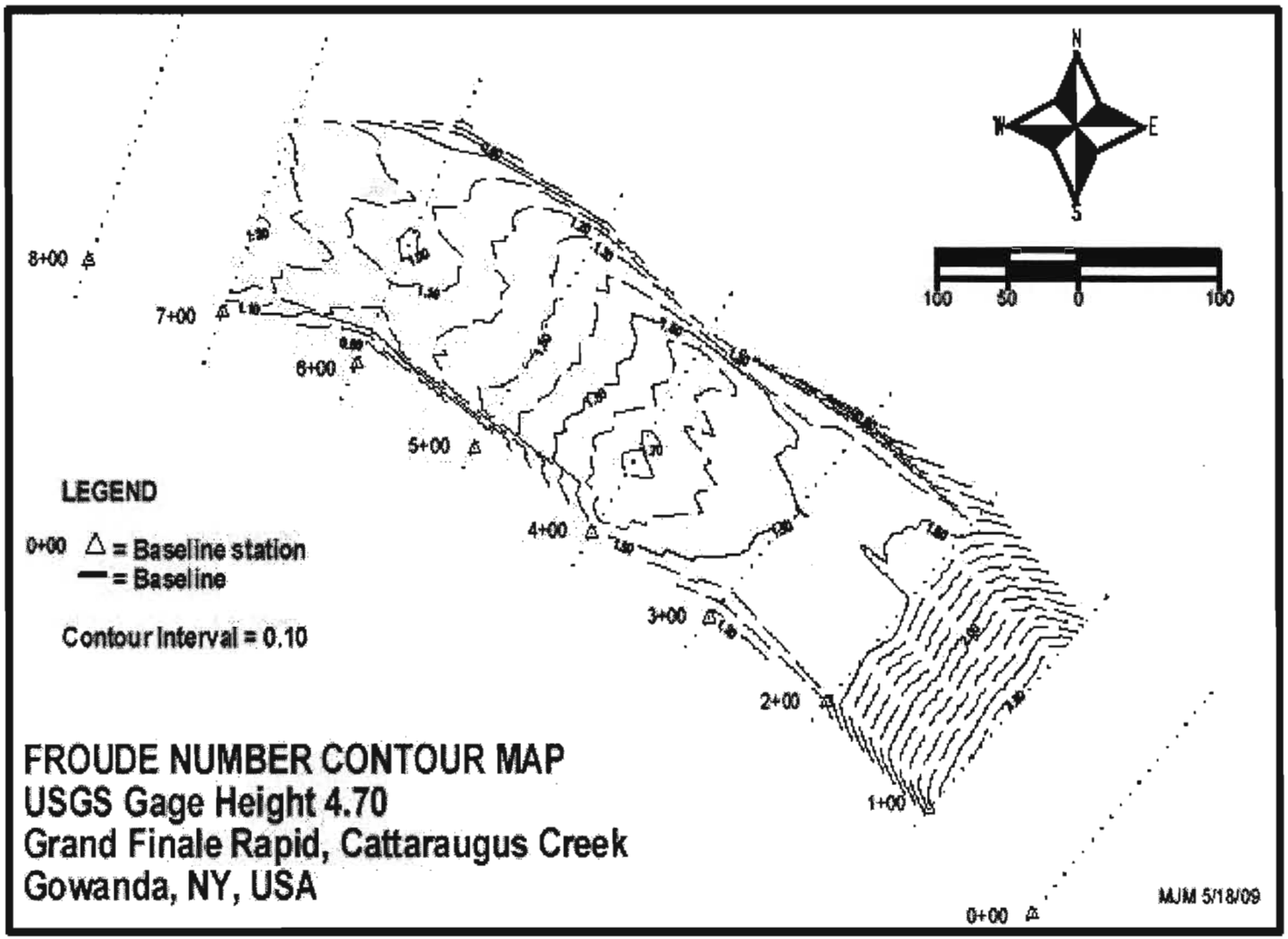
N
W
E
S
100
50
0
100
8+00
7+00
6+00
5+00
4+00
3+00
2+00
1+00
0+00
LEGEND
0+00 △ = Baseline station
— = Baseline
Contour Interval = 0.10
FROUDE NUMBER CONTOUR MAP
USGS Gage Height 4.70
Grand Finale Rapid, Cattaraugus Creek
Gowanda, NY, USA
MJM 5/18/09

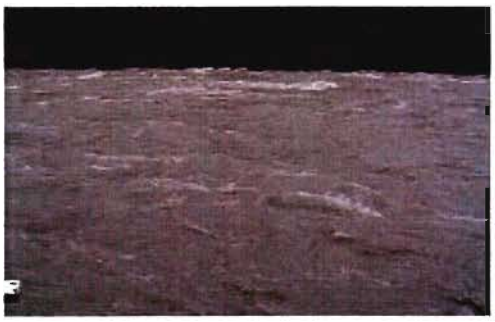

1+00

2+00

3+00

4+00

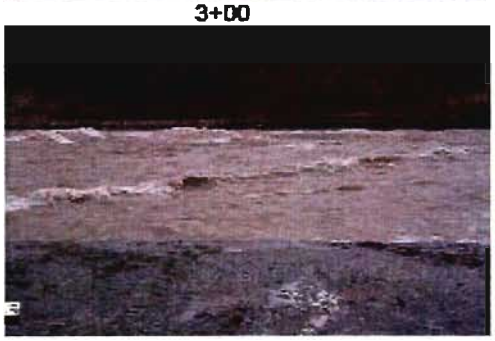

5+00

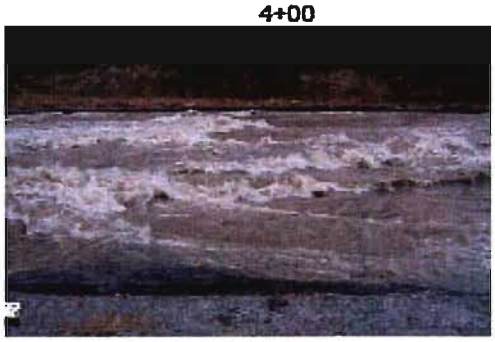

6+00

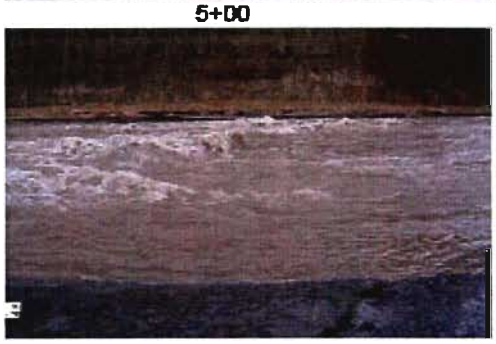

7+00

Water Level 4.70
by Cross Section

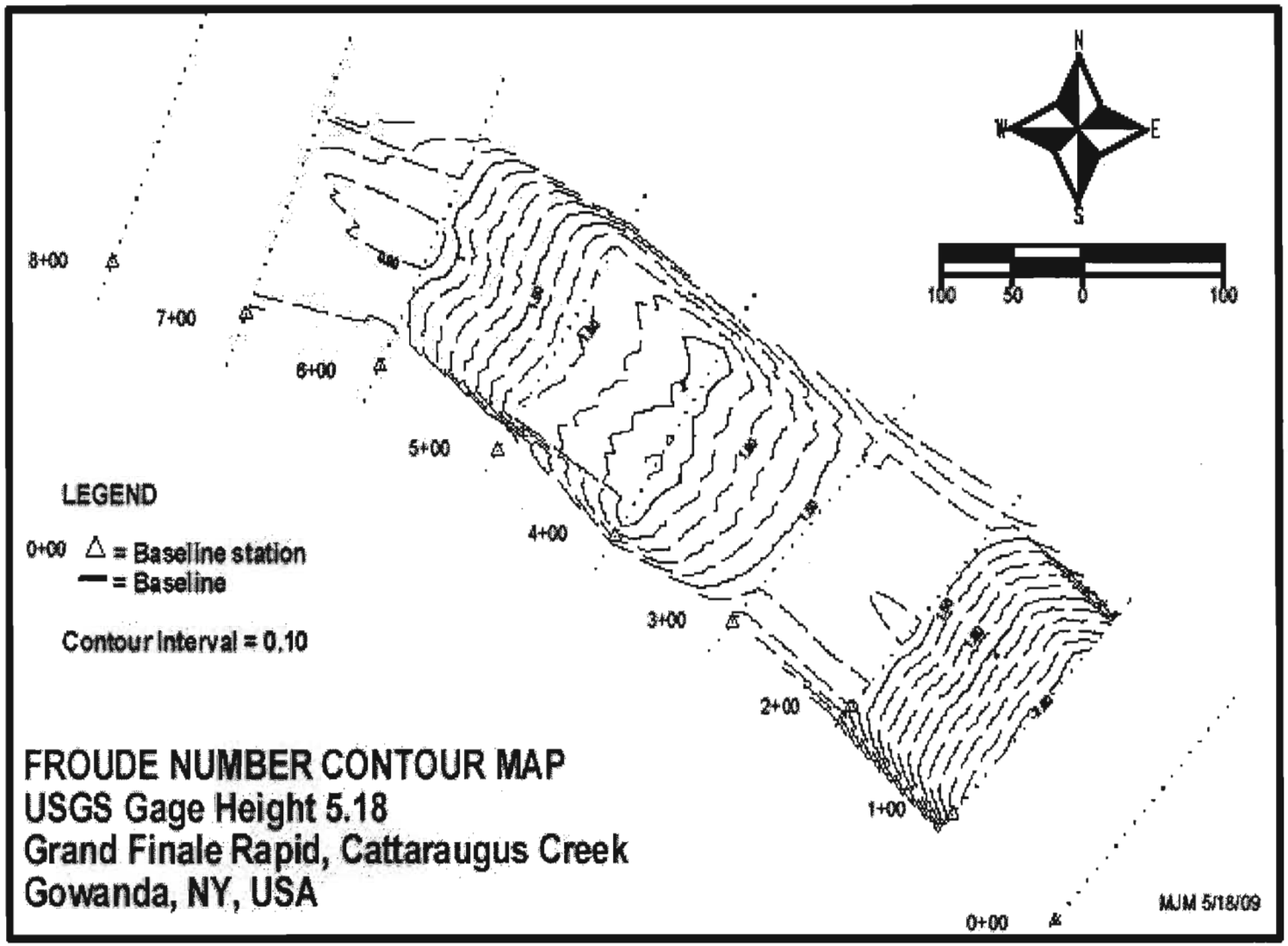
N
W
E
S
100
50
0
100
8+00
7+00
6+00
5+00
4+00
3+00
2+00
1+00
0+00
LEGEND
△ = Baseline station
= Baseline
Contour Interval = 0.10
FROUDE NUMBER CONTOUR MAP
USGS Gage Height 5.18
Grand Finale Rapid, Cattaraugus Creek
Gowanda, NY, USA
MJM 5/18/09

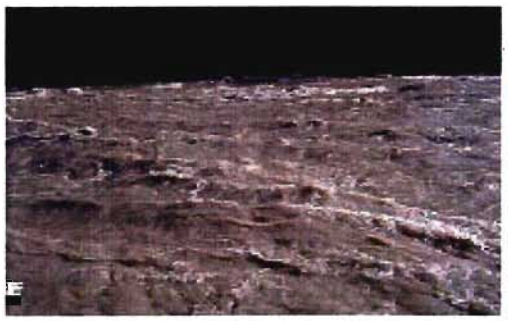

1+00

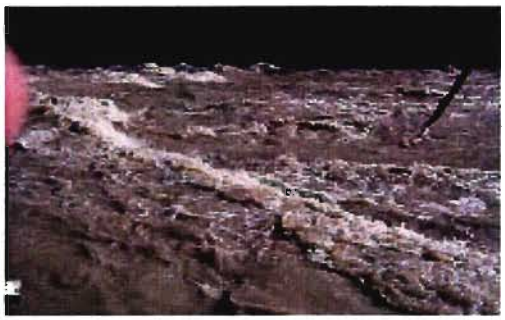

2+00

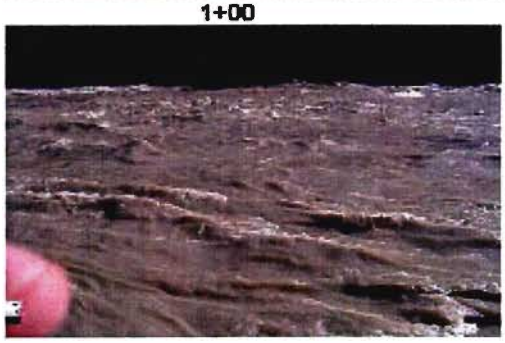

3+00

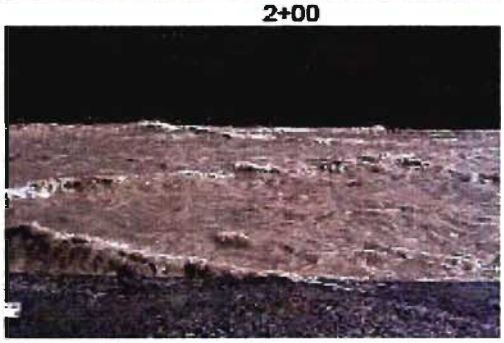

4+00

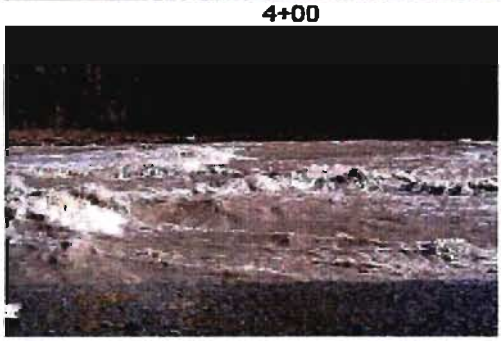

6+00

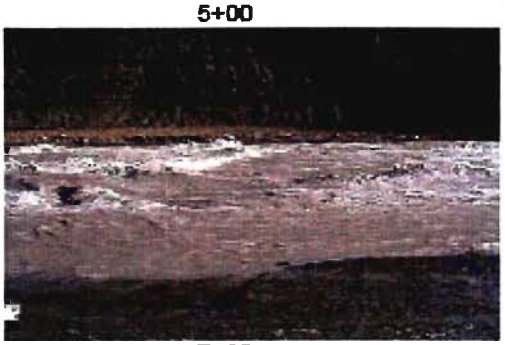

5+00

7+00

Water Level 5.18
by Cross Section

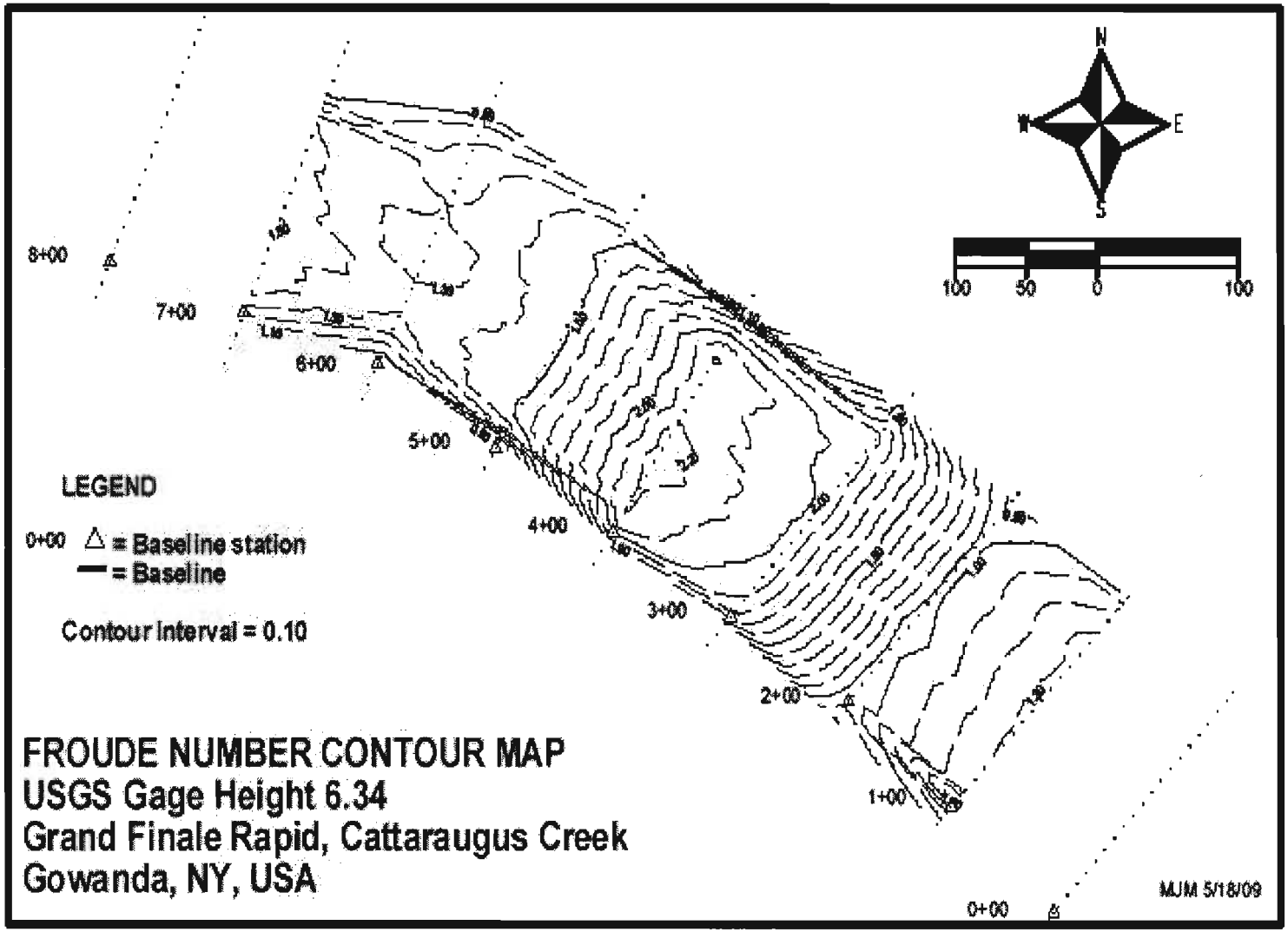
N
W
E
S
100
50
0
100
8+00
7+00
6+00
5+00
4+00
3+00
2+00
1+00
0+00
LEGEND
△ = Baseline station
= Baseline
Contour Interval = 0.10
FROUDE NUMBER CONTOUR MAP
USGS Gage Height 6.34
Grand Finale Rapid, Cattaraugus Creek
Gowanda, NY, USA
MJM 5/18/09

1+00

2+00

3+00

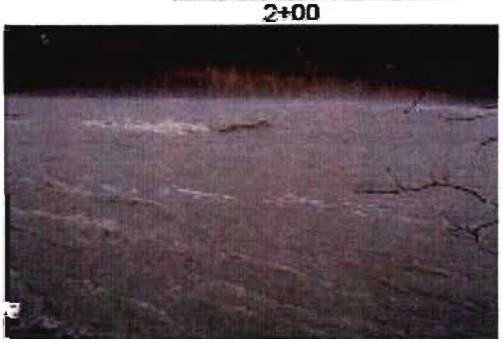

4+00

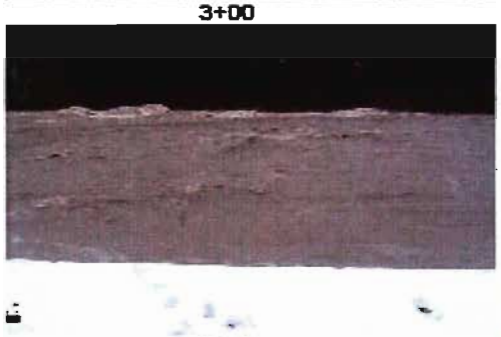

5+00

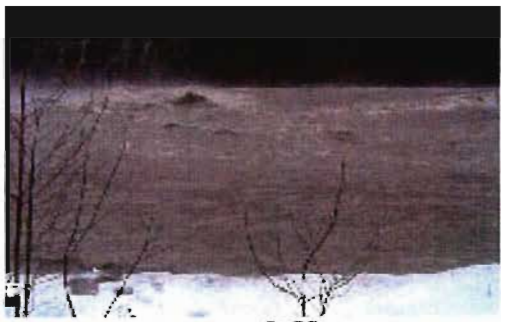

6+00

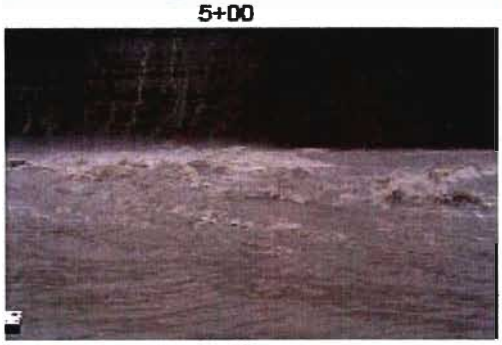

7+00

Water Level 6.34
by Cross Section

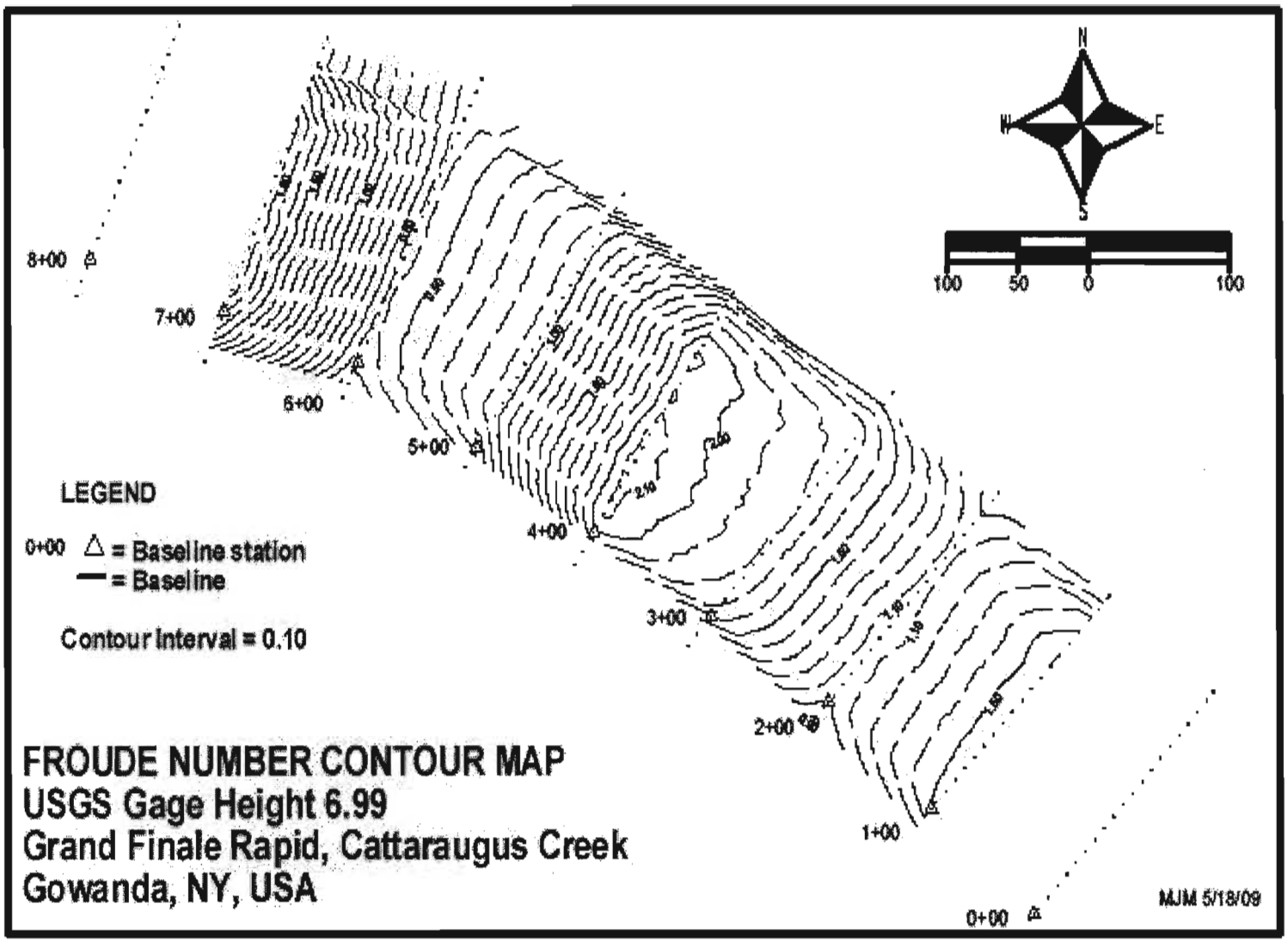
N
W
E
S
100
50
0
100
8+00
7+00
6+00
5+00
4+00
3+00
2+00
1+00
0+00
LEGEND
0+00 △ = Baseline station
— = Baseline
Contour Interval = 0.10
FROUDE NUMBER CONTOUR MAP
USGS Gage Height 6.99
Grand Finale Rapid, Cattaraugus Creek
Gowanda, NY, USA
MJM 5/18/09

1+00

2+00

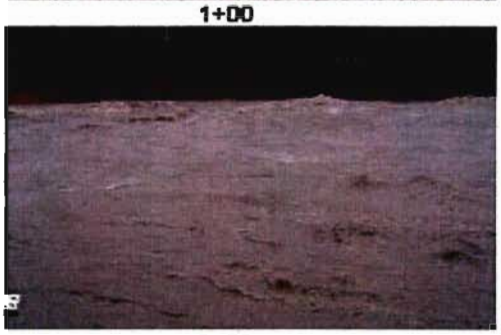

3+00

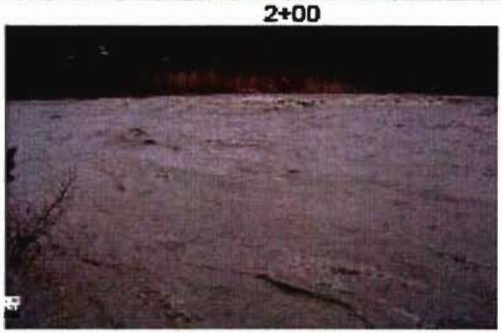

4+00

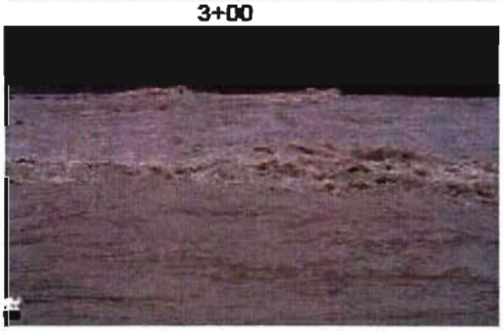

5+00

6+00

7+00

Water Level 6.99
by Cross Section

Appendix VI

Froude Number by Water Level Cross Sections

Cross Section by Water Level Photos

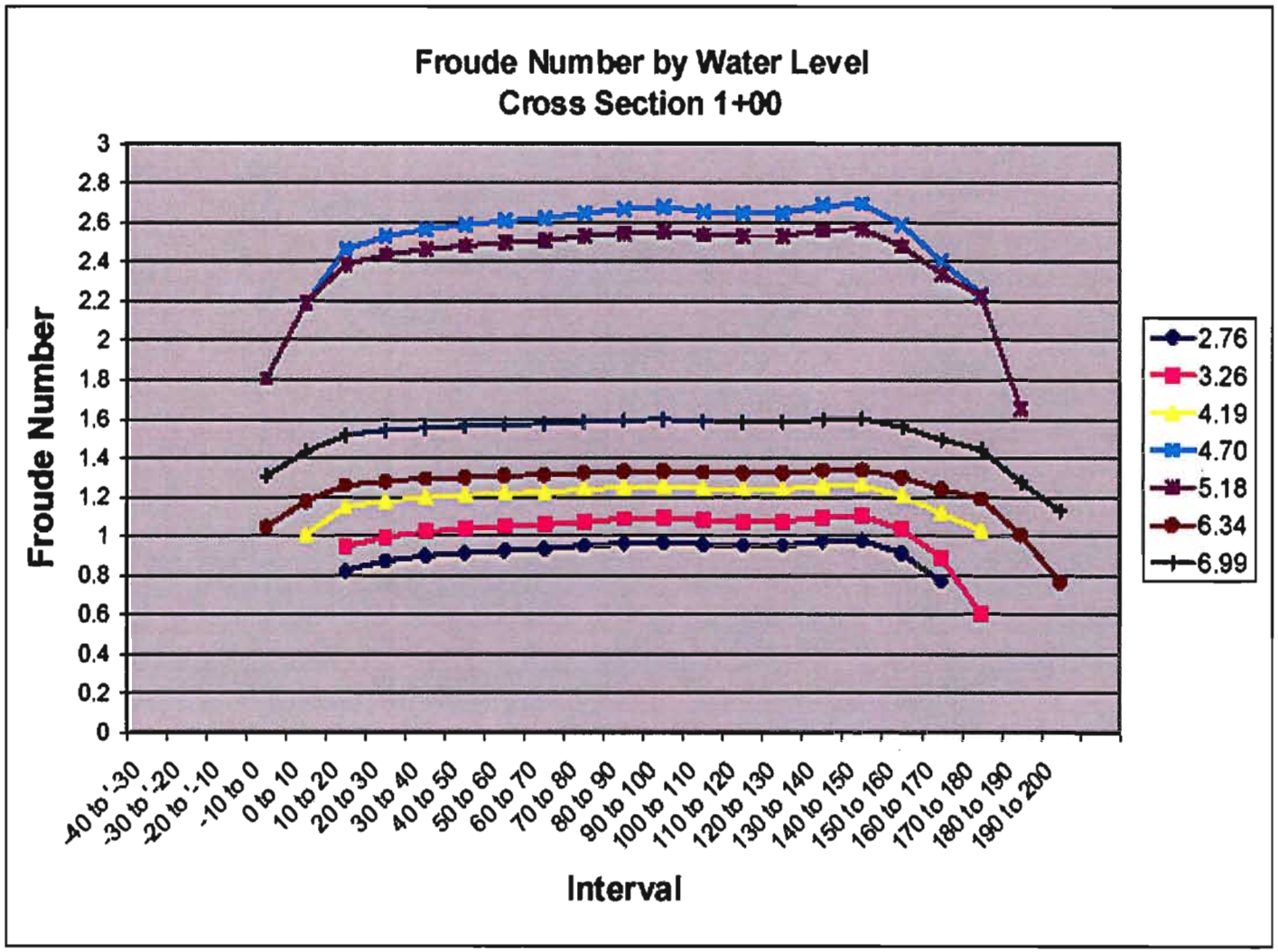
Froude Number by Water Level
Cross Section 1+00
Froude Number
3
2.8
2.6
2.4
2.2
2
1.8
1.6
1.4
1.2
1
0.8
0.6
0.4
0.2
0
-40 to -30
-30 to -20
-20 to -10
-10 to 0
0 to 10
10 to 20
20 to 30
30 to 40
40 to 50
50 to 60
60 to 70
70 to 80
80 to 90
90 to 100
100 to 110
110 to 120
120 to 130
130 to 140
140 to 150
150 to 160
160 to 170
170 to 180
180 to 190
190 to 200
Interval
2.76
3.26
4.19
4.70
5.18
6.34
6.99

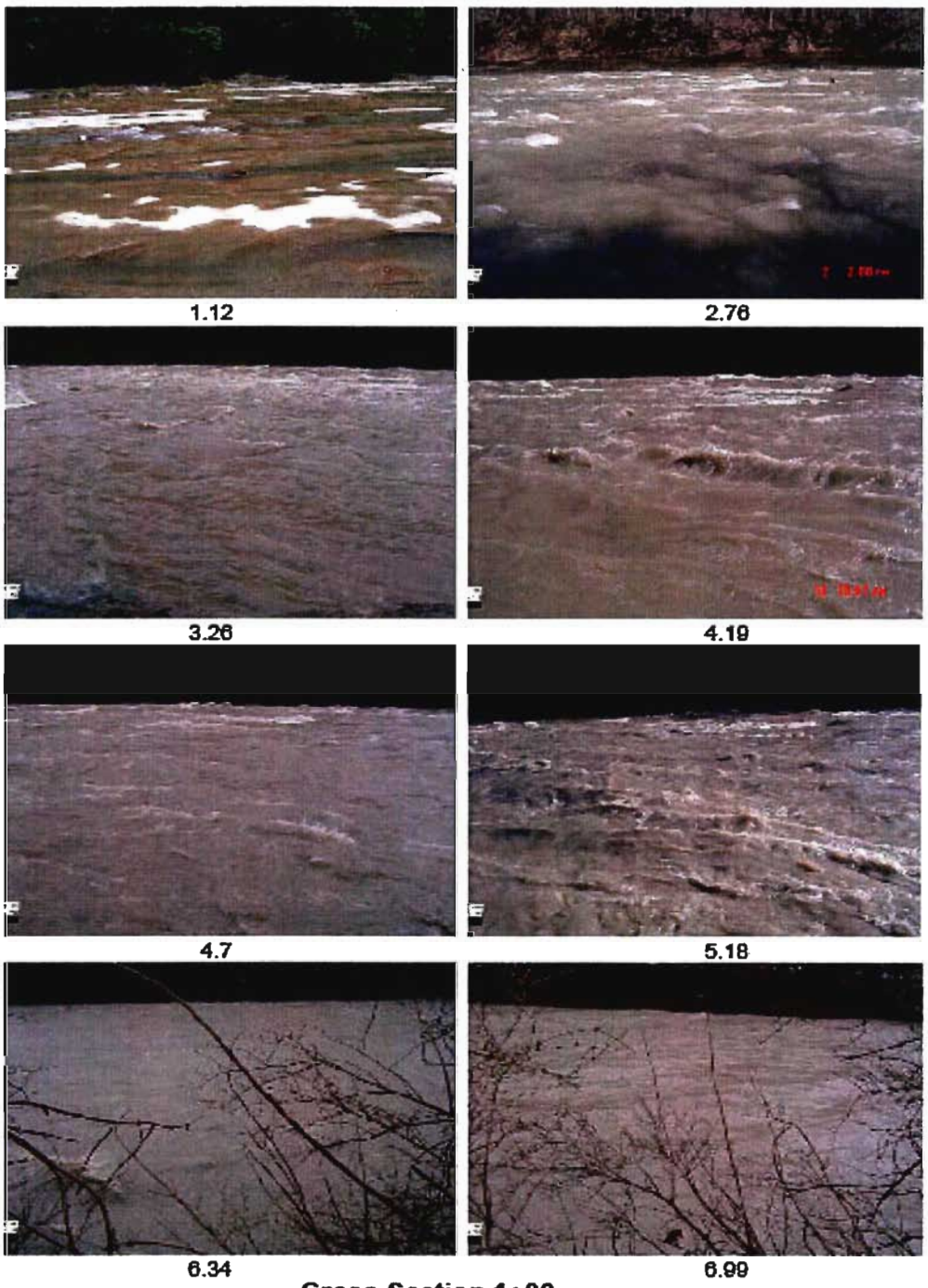

Cross Section 1+00
by Water Level

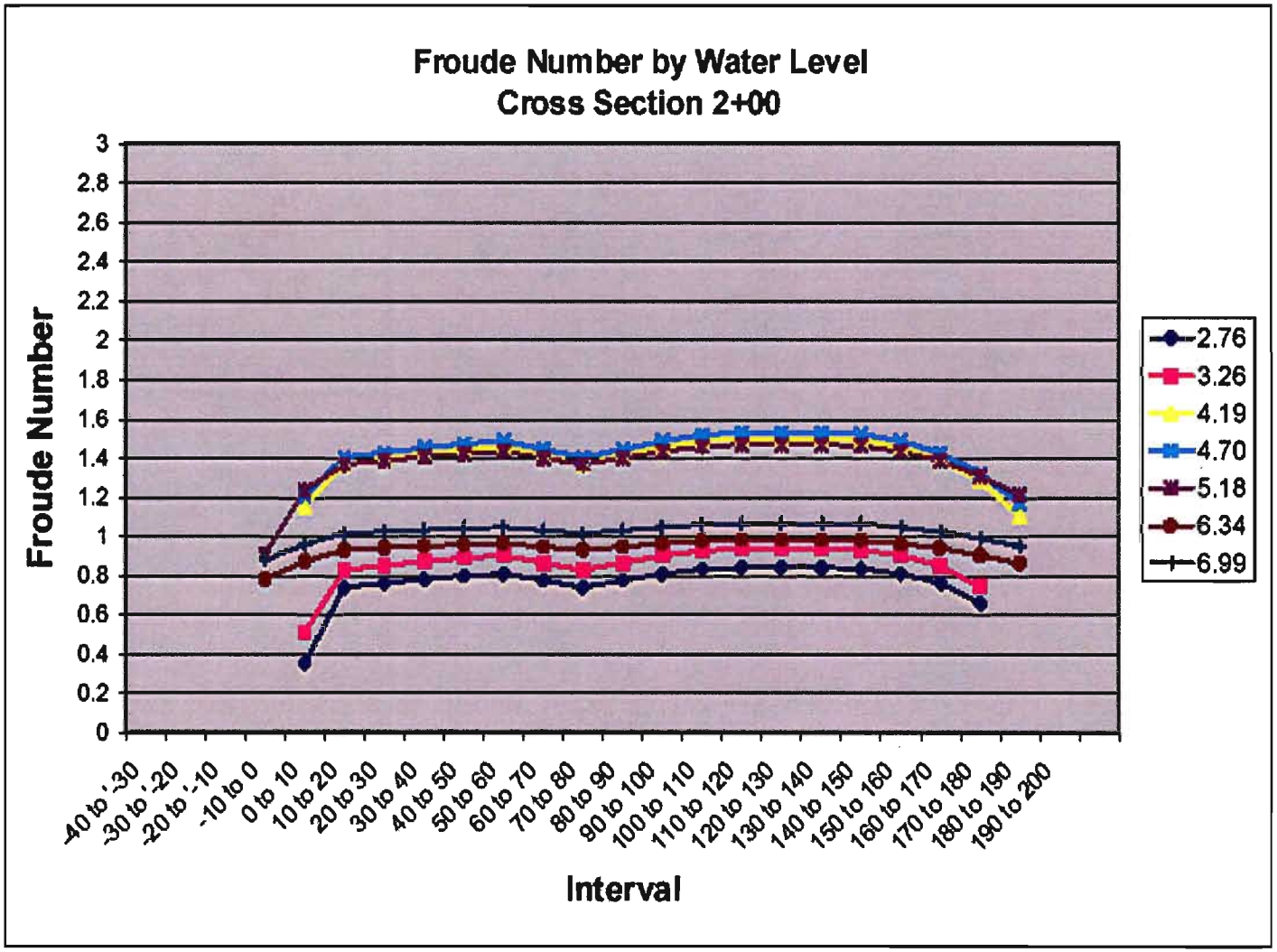
Froude Number by Water Level
Cross Section 2+00
Froude Number
3
2.8
2.6
2.4
2.2
2
1.8
1.6
1.4
1.2
1
0.8
0.6
0.4
0.2
0
-40 to -30
-30 to -20
-20 to -10
-10 to 0
0 to 10
10 to 20
20 to 30
30 to 40
40 to 50
50 to 60
60 to 70
70 to 80
80 to 90
90 to 100
100 to 110
110 to 120
120 to 130
130 to 140
140 to 150
150 to 160
160 to 170
170 to 180
180 to 190
190 to 200
Interval
2.76
3.26
4.19
4.70
5.18
6.34
6.99

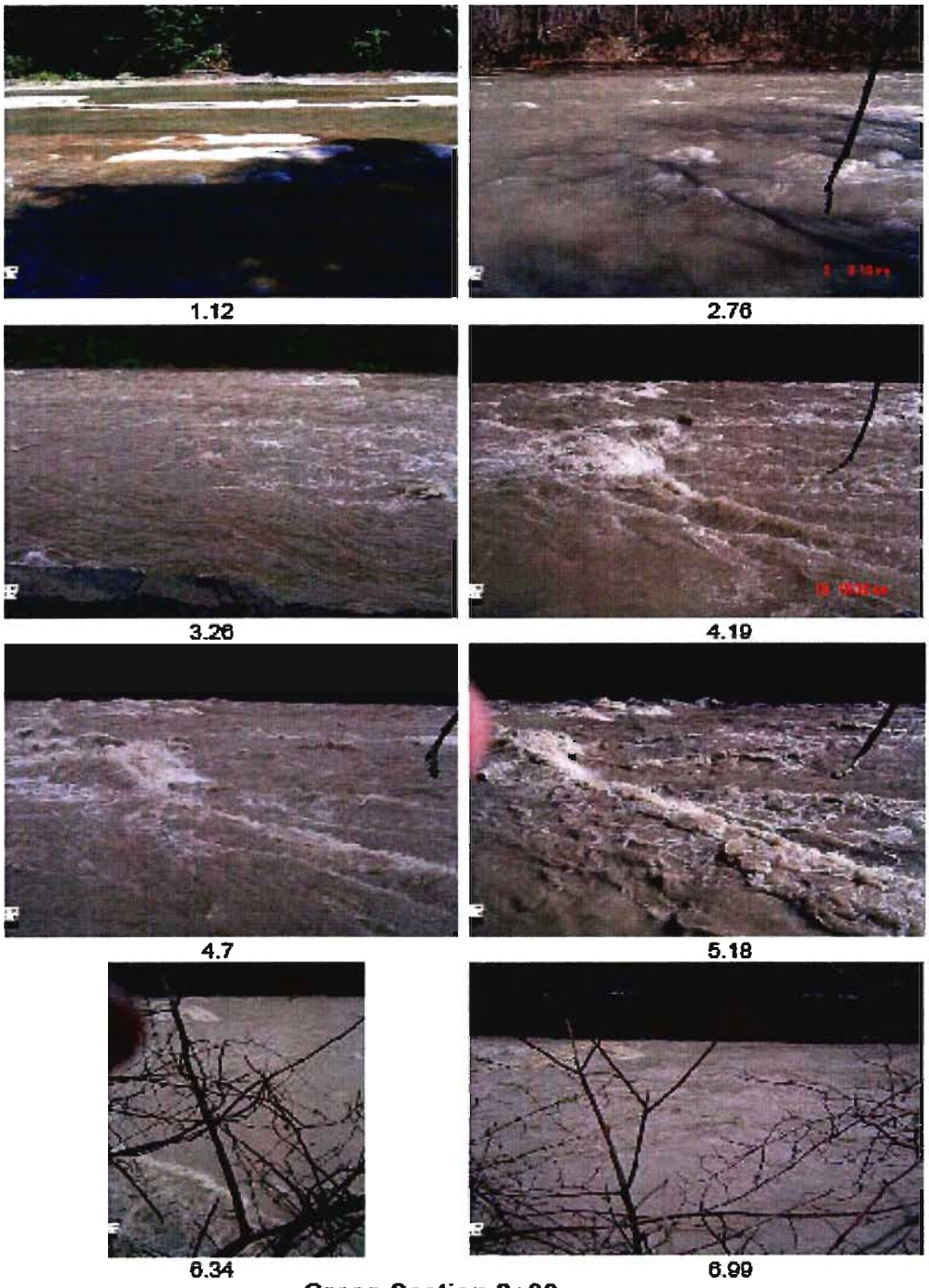

Cross Section 2+00
by Water Level

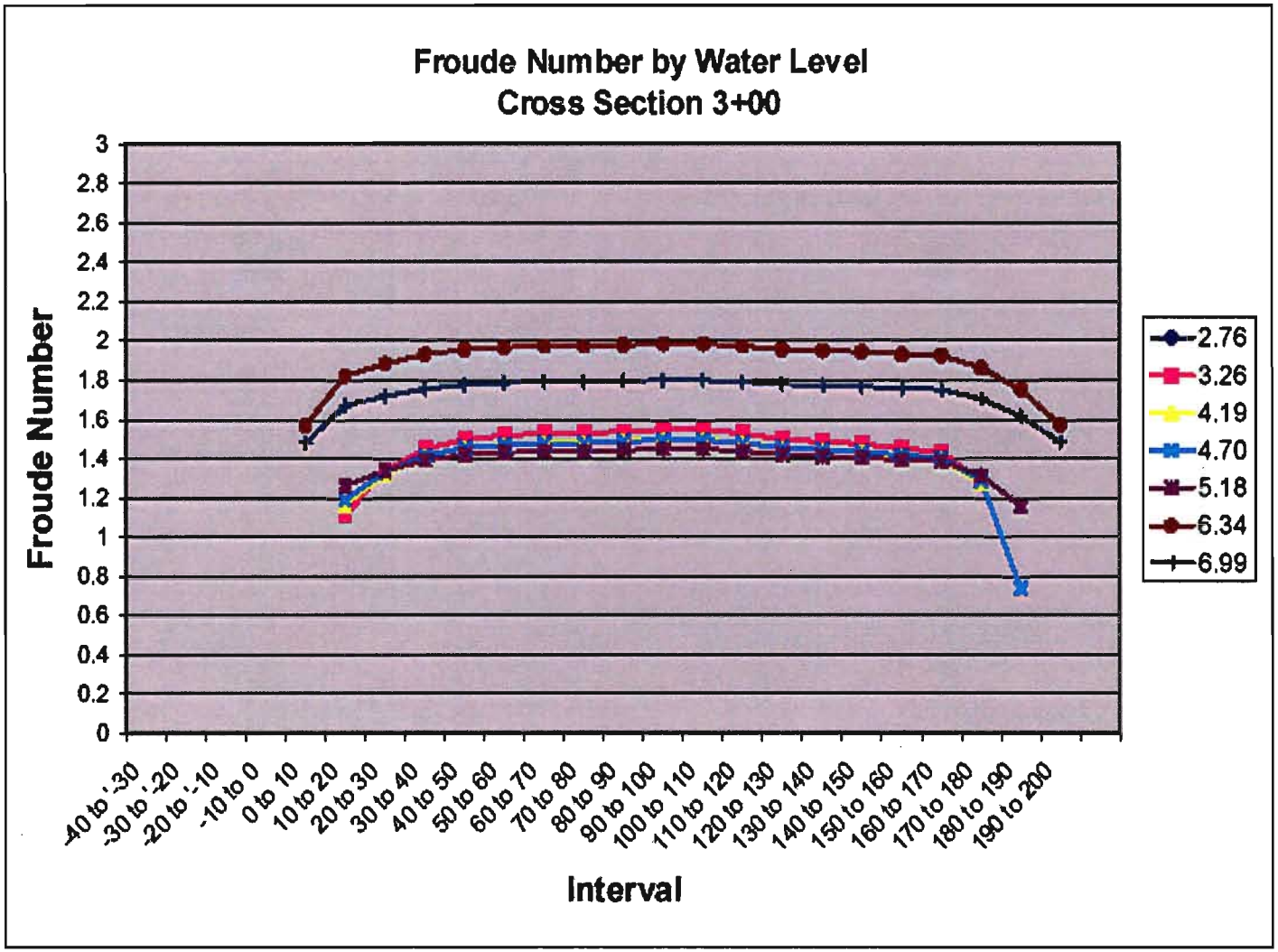
Froude Number by Water Level
Cross Section 3+00
Froude Number
3
2.8
2.6
2.4
2.2
2
1.8
1.6
1.4
1.2
1
0.8
0.6
0.4
0.2
0
-40 to -30
-30 to -20
-20 to -10
-10 to 0
0 to 10
10 to 20
20 to 30
30 to 40
40 to 50
50 to 60
60 to 70
70 to 80
80 to 90
90 to 100
100 to 110
110 to 120
120 to 130
130 to 140
140 to 150
150 to 160
160 to 170
170 to 180
180 to 190
190 to 200
Interval
2.76
3.26
4.19
4.70
5.18
6.34
6.99

1.12

2.76

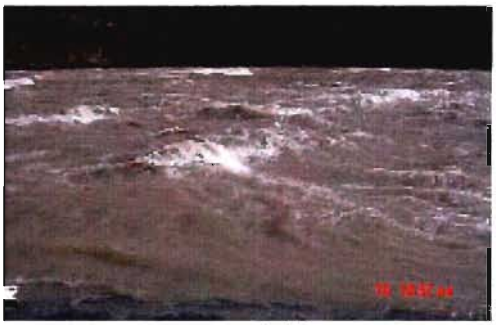

3.26

4.19

4.7

5.18

6.34

6.99

Cross Section 3+00
by Water Level

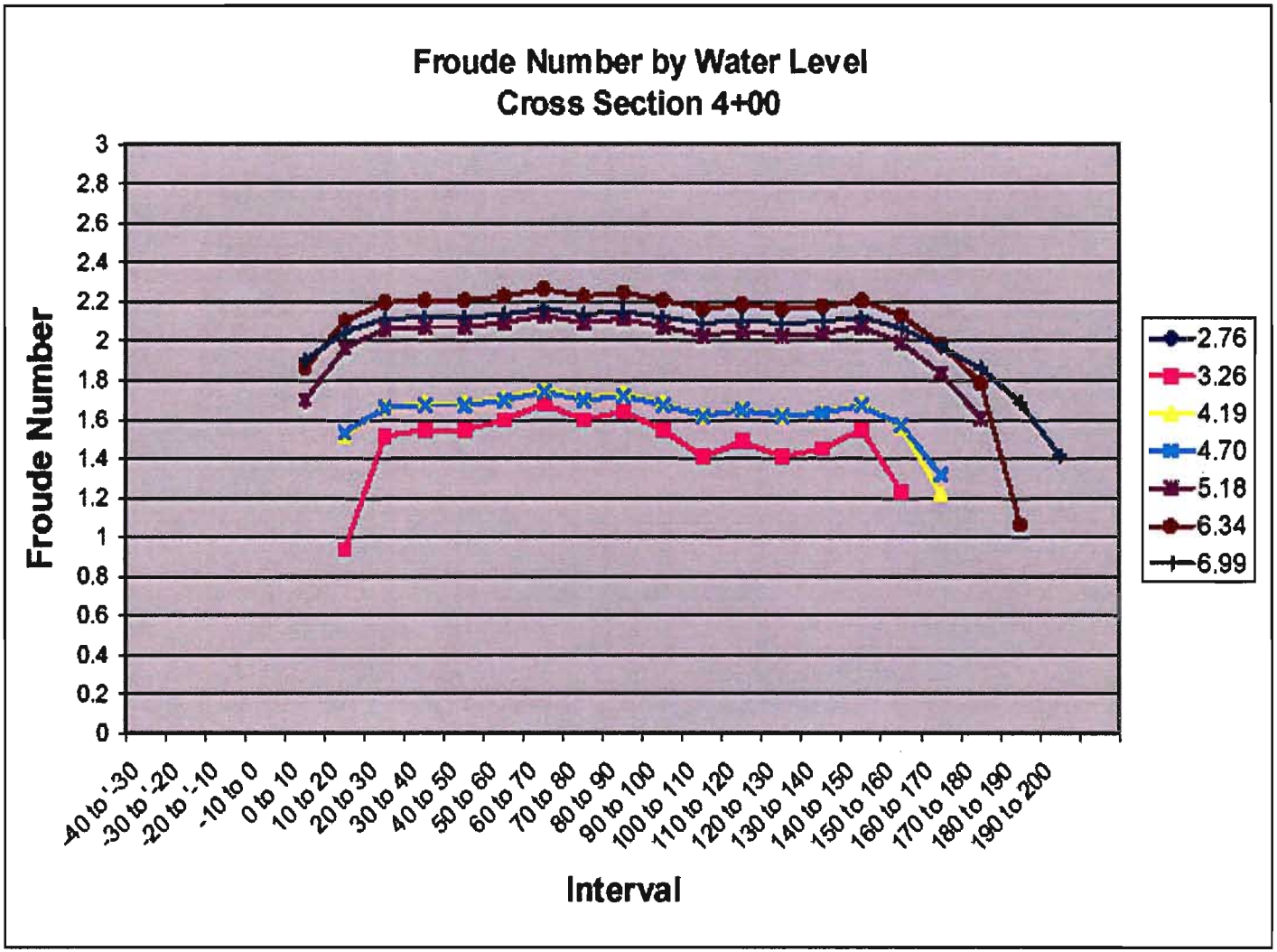
Froude Number by Water Level
Cross Section 4+00
Froude Number
3
2.8
2.6
2.4
2.2
2
1.8
1.6
1.4
1.2
1
0.8
0.6
0.4
0.2
0
-40 to -30
-30 to -20
-20 to -10
-10 to 0
0 to 10
10 to 20
20 to 30
30 to 40
40 to 50
50 to 60
60 to 70
70 to 80
80 to 90
90 to 100
100 to 110
110 to 120
120 to 130
130 to 140
140 to 150
150 to 160
160 to 170
170 to 180
180 to 190
190 to 200
Interval
2.76
3.26
4.19
4.70
5.18
6.34
6.99

1.12

2.76

3.26

4.19

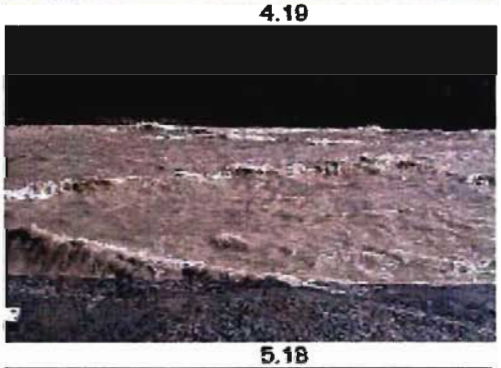

4.7

5.18

6.34

6.99

Cross Section 4+00
by Water Level

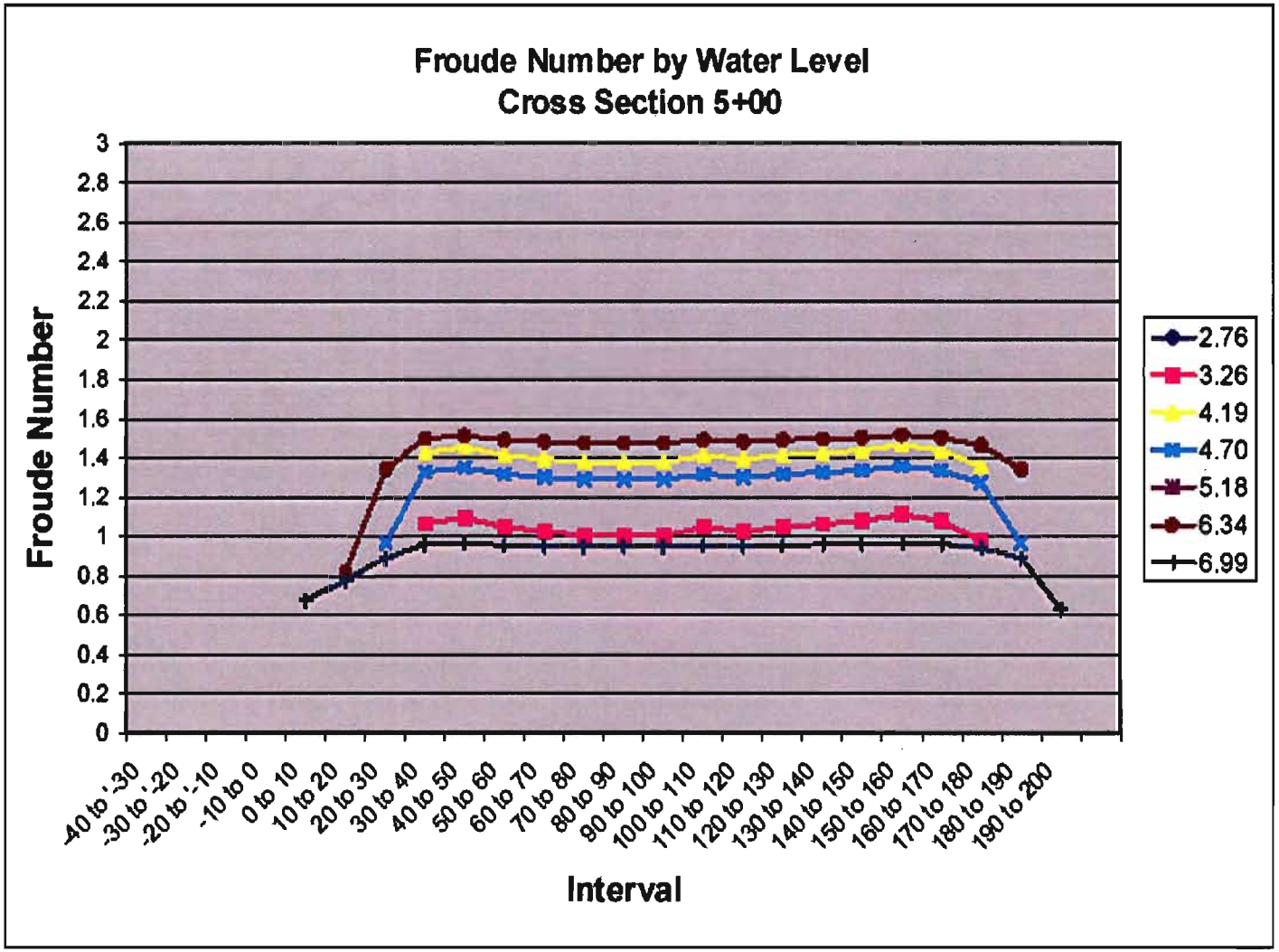
Froude Number by Water Level
Cross Section 5+00
Froude Number
3
2.8
2.6
2.4
2.2
2
1.8
1.6
1.4
1.2
1
0.8
0.6
0.4
0.2
0
-40 to -30
-30 to -20
-20 to -10
-10 to 0
0 to 10
10 to 20
20 to 30
30 to 40
40 to 50
50 to 60
60 to 70
70 to 80
80 to 90
90 to 100
100 to 110
110 to 120
120 to 130
130 to 140
140 to 150
150 to 160
160 to 170
170 to 180
180 to 190
190 to 200
Interval
2.76
3.26
4.19
4.70
5.18
6.34
6.99

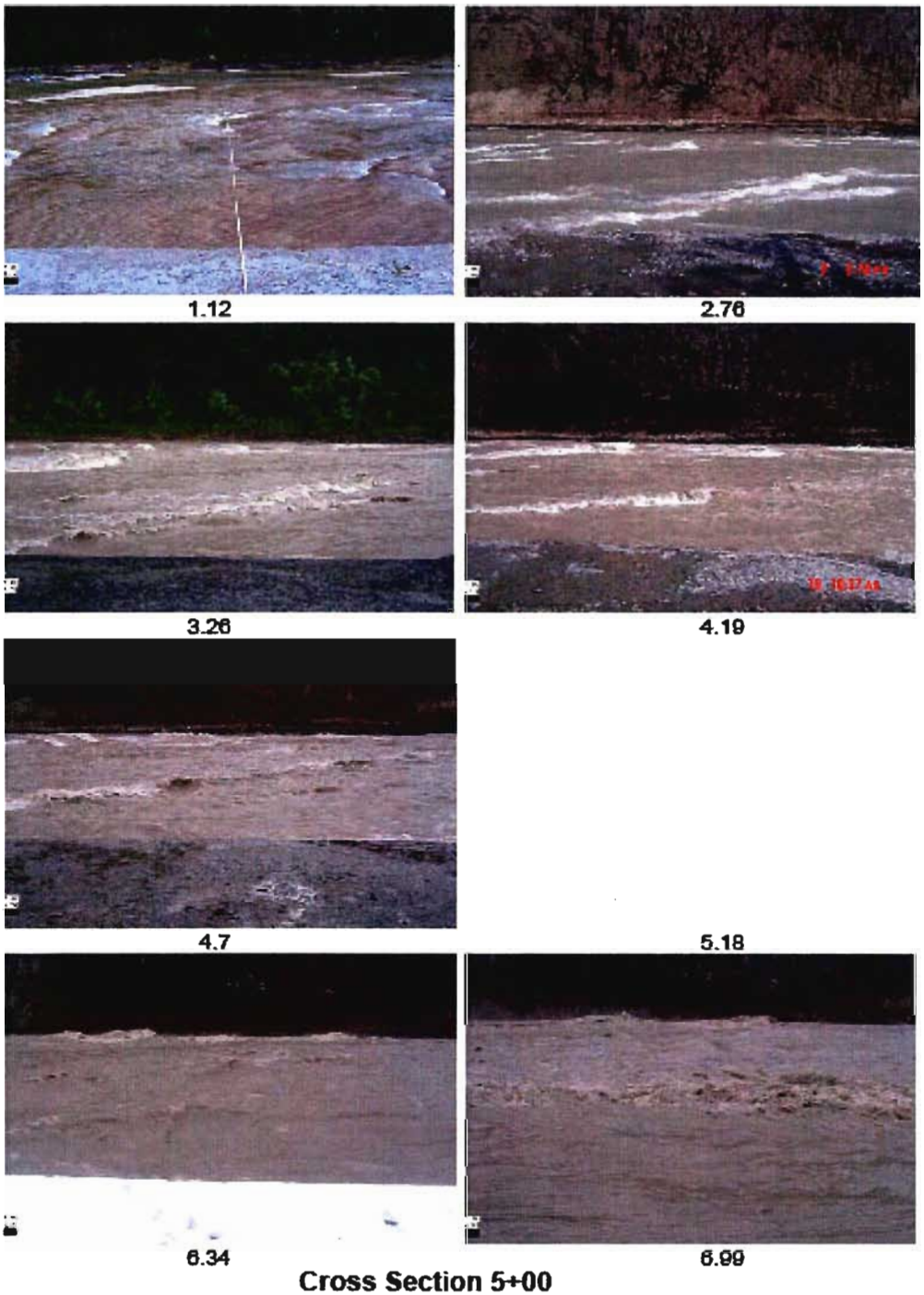

Cross Section 5+00
by Water Level

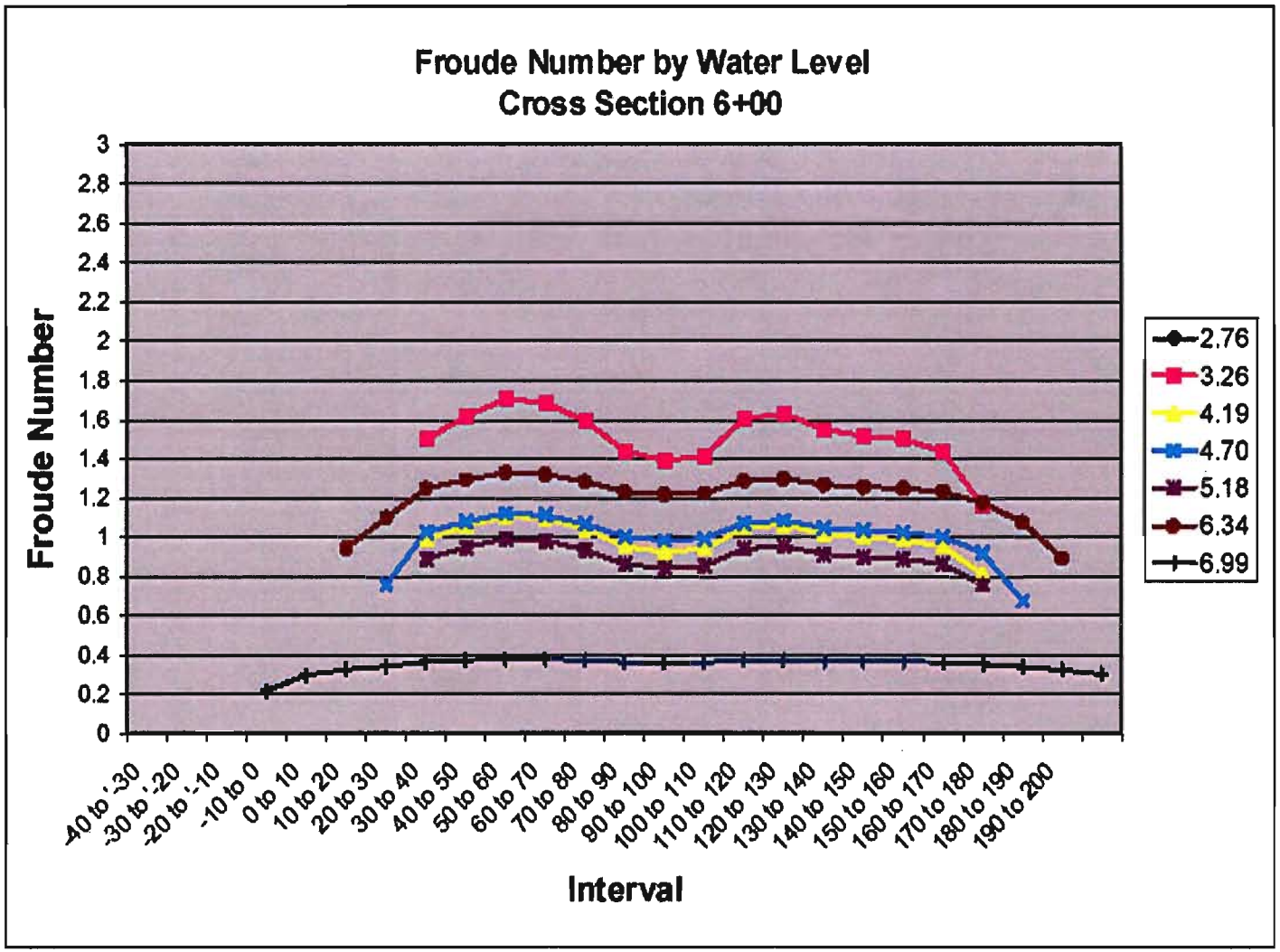
Froude Number by Water Level
Cross Section 6+00
Froude Number
3
2.8
2.6
2.4
2.2
2
1.8
1.6
1.4
1.2
1
0.8
0.6
0.4
0.2
0
-40 to -30
-30 to -20
-20 to -10
-10 to 0
0 to 10
10 to 20
20 to 30
30 to 40
40 to 50
50 to 60
60 to 70
70 to 80
80 to 90
90 to 100
100 to 110
110 to 120
120 to 130
130 to 140
140 to 150
150 to 160
160 to 170
170 to 180
180 to 190
190 to 200
Interval
2.76
3.26
4.19
4.70
5.18
6.34
6.99

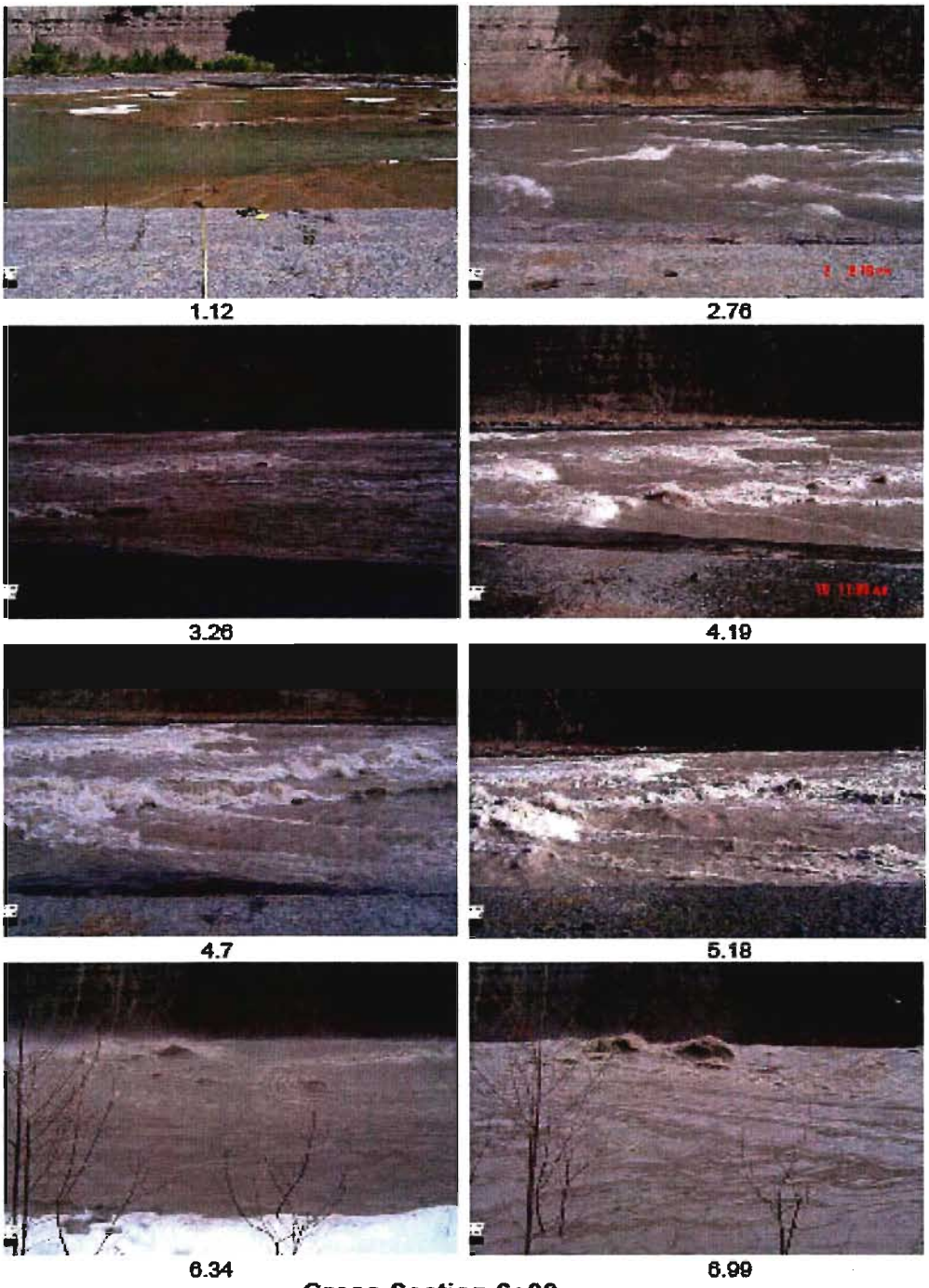

Cross Section 6+00
by Water Level

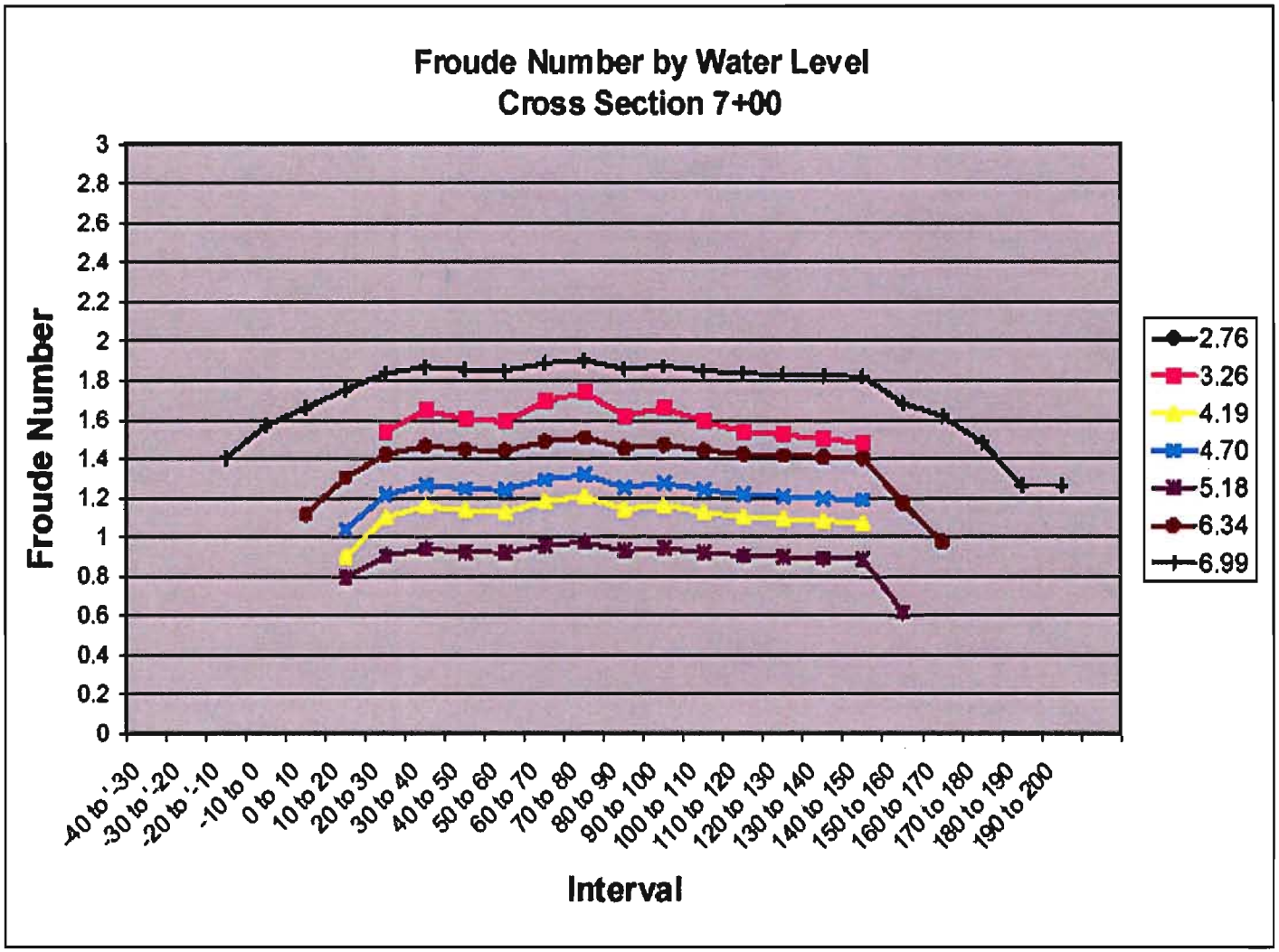
Froude Number by Water Level
Cross Section 7+00
Froude Number
3
2.8
2.6
2.4
2.2
2
1.8
1.6
1.4
1.2
1
0.8
0.6
0.4
0.2
0
-40 to -30
-30 to -20
-20 to -10
-10 to 0
0 to 10
10 to 20
20 to 30
30 to 40
40 to 50
50 to 60
60 to 70
70 to 80
80 to 90
90 to 100
100 to 110
110 to 120
120 to 130
130 to 140
140 to 150
150 to 160
160 to 170
170 to 180
180 to 190
190 to 200
Interval
2.76
3.26
4.19
4.70
5.18
6.34
6.99

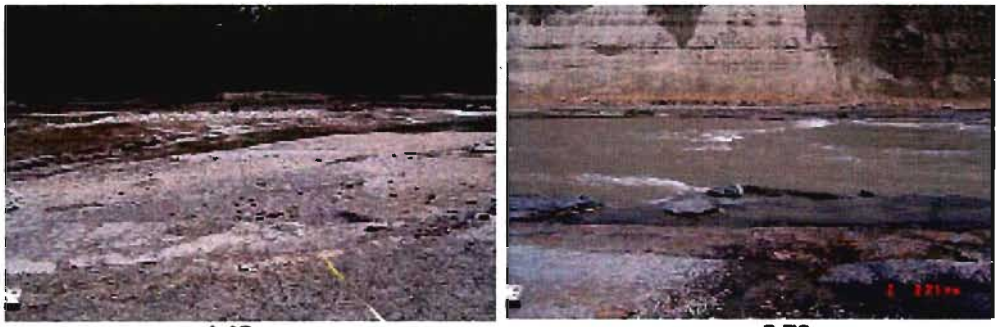

1.12

2.76

3.26

4.19

4.7

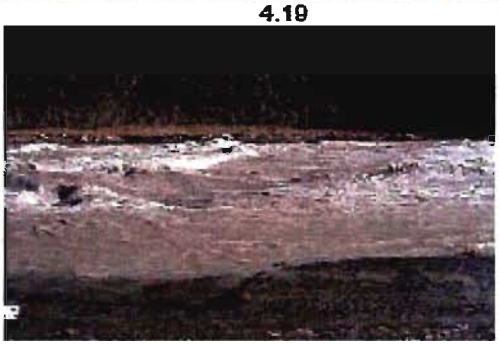

5.18

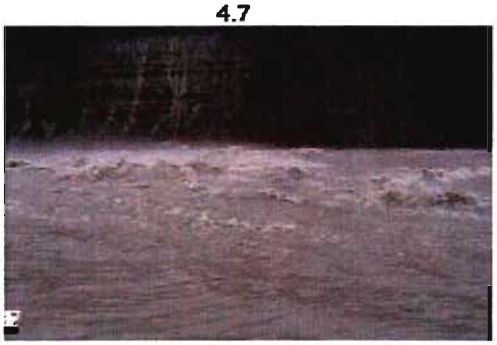

6.34

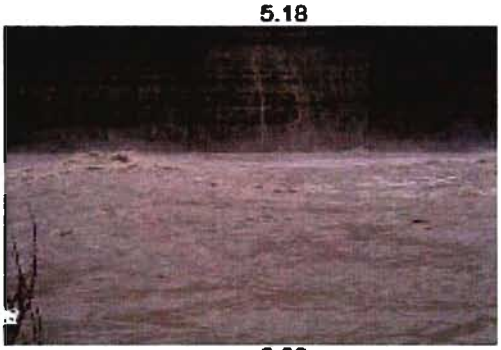

6.99

Cross Section 7+00
by Water Level

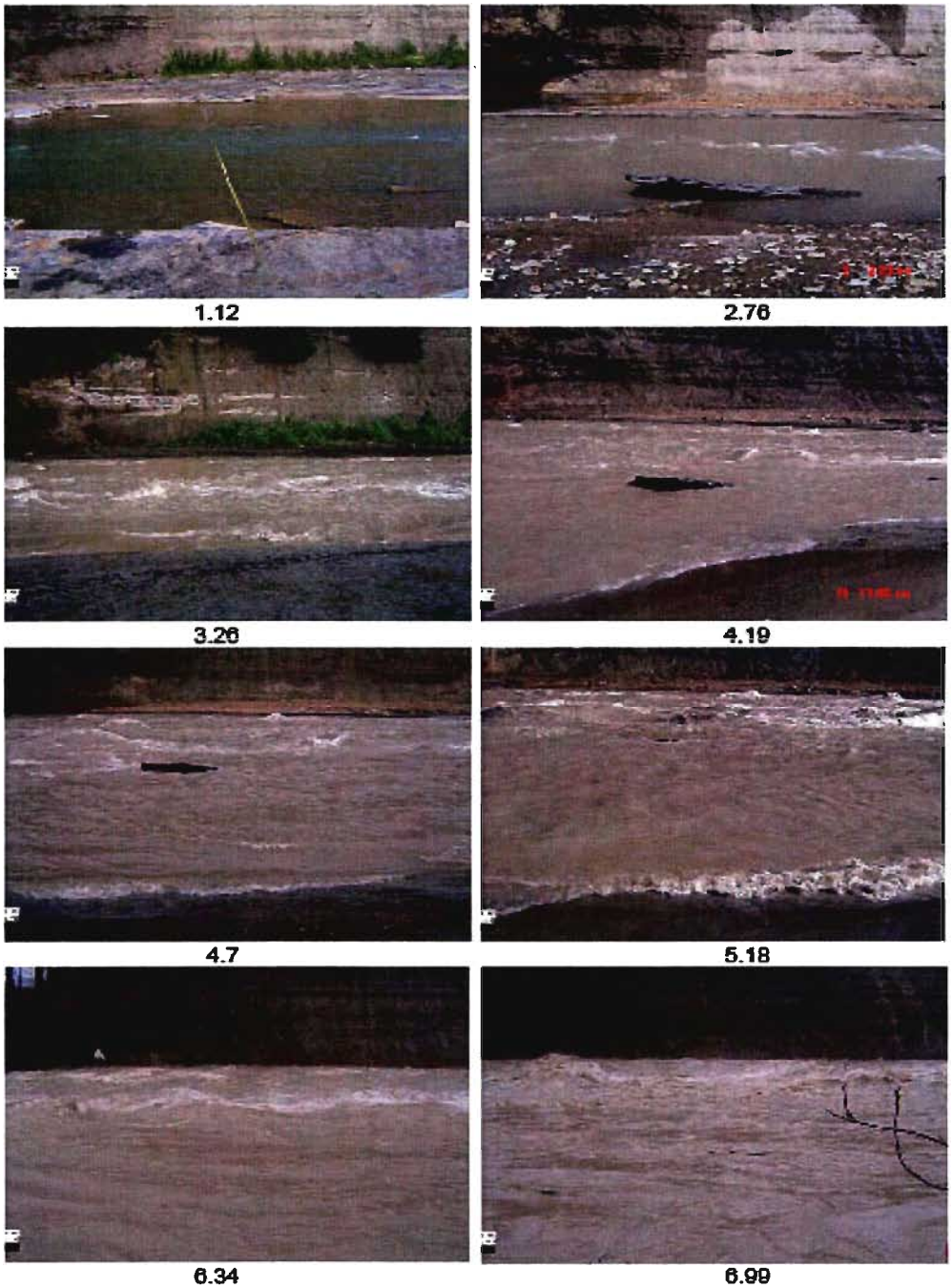

Cross Section 8+00
by Water Level